Bruton´s tyrosine kinase-mediated NLRP3 phosphorylation promotes inflammasome activation

Dissertation

der Mathematisch-Naturwissenschaftlichen Fakultät
der Eberhard Karls Universität Tübingen
zur Erlangung des Grades eines
Doktors der Naturwissenschaften

(Dr. rer. nat.)

Vorgelegt von
Bittner, Zsófia Ágnes
aus Budapest/Ungarn

Tübingen, 2019

Gedruckt mit Genehmigung der Mathematisch-Naturwissenschaftlichen Fakultät der Eberhard Karls Universität Tübingen.

Tag der mündlichen Qualifikation:	12.02.2020
Dekan:	Prof. Dr. Wolfgang Rosenstiel
1. Berichterstatter:	Prof. Alexander N.R. Weber
2. Berichterstatter:	Prof. Hans-Georg Rammensee

DANKSAGUNG

Ich möchte mich in erster Linie bei Professor Weber für das reizvolle Projekt, die begleitende Betreuung und die schöne Arbeitsatmosphäre bedanken.

Darüber hinaus bin ich der ganzen Arbeitsgruppe Weber, insbesondere Xiao Liu, Franziska Herster, Austin Chang, Yamel Cardona Gloria und Sabine Dickhöfer für die Hilfe im Labor und den Spaß in der Freizeit dankbar.

Professor Rammensee bin ich für die großartige Leitung des Tübinger Immunologischen Instituts zur Dankbarkeit verpflichtet.

Abschließend möchte ich mich bei meiner Familie bedanken: Ohne ihr Rückgrat hätte ich das Studium und darauffolgend die Promotion nicht vollenden können.

SUMMARY

The NLRP3 inflammasome is a potent pro-inflammatory machinery that assembles upon danger sensing of the cell and leads to pro-inflammatory cytokine maturation and release such as IL-1β and IL-18, as well as to a pro-inflammatory form of cell death: pyroptosis. Its activity is regulated on multiple levels: via NLRP3 interaction partners, NLRP3 post-translational modifications, and subcellular localization.

In this study we aimed to elucidate the molecular mechanisms by which the previously identified NLRP3 regulator, Bruton´s tyrosine kinase (BTK), controls NLRP3 inflammasome function. It had been published that human and murine cells lacking intact BTK expression produce reduced amounts of IL-1β, and the FDA-approved BTK kinase inhibitor ibrutinib also blocked NLRP3 inflammasome activity. We thus hypothesized that BTK´s kinase function is relevant in NLRP3 inflammasome regulation. We observed that NLRP3 and BTK interacted and were tyrosine phosphorylated upon inflammasome activation in primary human and murine macrophages, and NLRP3 tyrosine phosphorylation was dependent on BTK´s kinase activity. We established that BTK directly phosphorylates NLRP3 and identified the tyrosine residues that are modified by BTK: Y136/Y140/Y143/Y168. We noticed that the residues Y136/Y140/Y143 are located in the recently identified polybasic region, which serves trans-Golgi network phospholipid binding and pre-activation of NLRP3. We speculated that the negative charge introduced by the phosphorylation of the polybasic region might weaken trans-Golgi network binding of NLRP3 and facilitate NLRP3 inflammasome assembly in the cytosol. Phosphomimetic polybasic constructs indeed showed reduced binding to phospholipid covered agarose beads. Furthermore, we observed diminished NLRP3 and ASC oligomerization when cells lacked BTK or were treated with ibrutinib. Finally, *Nlrp3* KO immortalized macrophages produced lower amounts of IL-1β when reconstituted with Y>F phosphoacceptor deficient human NLRP3, displaying functional relevance of the phosphorylations carried out by BTK.

Together, we showed that BTK represents a druggable regulator of the NLRP3 inflammasome that combines scaffold functions, post-translational modification, and cellular localization control to promote NLRP3 inflammasome assembly and activation.

ZUSAMMENFASSUNG

Das NLPR3 Inflammasom ist eine wirkungsvolle proinflammatorische Maschinerie, welche bei „Zellgefährdungsstimuli“ entsteht und Signalgebung auslöst. Am Ende der Signalkaskade wird Caspase-1 autokatalytisch aktiviert und schneidet pro-IL-1β und pro-IL-18 in deren aktive Formen. Zusätzlich stirbt die Zelle eines inflammatorischen Zelltods, genannt Pyroptose. Die Aktivität des NLRP3 Inflammasoms wird auf mehreren Ebenen reguliert: über Bindungspartner, mittels post-translationaler Modifikationen, sowie durch Lokalisation im Zytosol.

In dieser Studie haben wir angestrebt, die Mechanismen, über die Bruton´s Tyrosinkinase (BTK) NLRP3 reguliert, aufzuklären. Vorarbeiten haben gezeigt, dass die Präsenz einer intakten BTK die IL-1β Ausschüttung erhöht. Inhibierung von BTK mit dem FDA-genehmigten Kinaseinhibitor Ibrutinib blockierte die IL-1β Produktion. Wir stellten die Hypothese auf, dass die Kinaseaktivität von BTK in dem Regulationsmechanismus eine Rolle spielt. Wir haben festgestellt, dass NLRP3 und BTK interagierten und tyrosinphosphoryliert wurden, wenn man das NLRP3 Inflammasom in primären PBMCs oder BMDMs stimulierte. Daraufhin haben wir gezeigt, dass BTK NLRP3 phosphoryliert und haben die modifizierten Tyrosinreste identifiziert: Y136/Y140/Y143/Y168. Wir haben bemerkt, dass Y136/Y140/Y143 in der kürzlich beschriebenen polybasischen Region liegen, die für die Phospholipid-Bindung von NLRP3 am „trans-Golgi Network“ sorgt. Wir haben vermutet, dass Phosphorylierung dieser Region durch die zusätzliche negative Ladung zur Lösung von NLRP3 vom Golgi führt. Tatsächlich haben „phosphomimetische“ NLRP3 Konstrukte (Y>E) weniger an Phospholipid-beschichteten Agarosebeads gebunden, als WT Konstrukte. Zusätzlich haben *Btk* KO Zellen und ibrutinib-behandelte Immunzellen weniger NLRP3 Oligomere im Zytosol gebildet. Außerdem haben mit NLRP3 Y>F rekonstituierte Makrophagen weniger IL-1β produziert, als mit WT NLRP3 rekonstituierten Zellen, was einen klaren Hinweis auf die funktionelle Rolle der Phosphostellen darstellt.

In dieser Arbeit haben wir gezeigt, dass BTK NLRP3 auf mehreren Ebenen steuert: über direkte Bindung, posttranslationale Modifikationen und zytosolische Lokalisation.

TABLE OF CONTENTS

LIST OF FIGURES AND TABLES

ABBREVIATIONS

For chemical elements, physical quantities, and amino acids (AA) common abbreviations were used.

AIM2	Absent in melanoma 2
APC	Antigen-presenting cell
ARIH2	Ariadne RBR E3 Ubiquitin Protein Ligase 2
ASC	Apoptosis-associated speck-like protein containing a CARD
ATG16L1	Autophagy related 16 like 1
BLNK	B cell linker
BMDM	Bone-marrow derived macrophages
BRCC3	BRCA1/BRCA2-Containing Complex Subunit 3
BRET	Bioluminescence resonance energy transfer
cAMP	Cyclic adenosine monophosphate
cGAS	Cyclic GMP-AMP synthase
CARD	Caspase activation and recruitment domain
CD	Cluster of differentiation
CINCA	Chronic infantile neurological, cutaneous, and articular syndrome
CLL	Chronic lymphocytic leukemia
DAG	Diacylglycerine
ddH_2O	Double-distilled H_2O
DMEM	Dulbecco's Modified Eagle's Medium
DNA	Deoxyribonucleic acid
ER	Endoplasmic reticulum
FADD	Fas-associated protein with death domain
FBXL2	F-box and leucine rich repeat protein 2
FBXO3	F-box protein 3
FCAS	Familial cold autoinflammatory syndrome
FDA	Food and Drug administration
FIIND	Function to find domain
FL	Full-length
GAPDH	Glyceraldehyde 3-phosphate dehydrogenase
HA	Hemagglutinin
HBS	HEPES buffered saline
HEK	Human embryonic kidney
HEPES	4-(2-hydroxyethyl)-1-piperazineethanesulfonic acid
HIN-200	Hematopoietic interferon-inducible nuclear proteins with a 200-amino-acid repeat
HMGB1	High-Mobility-Group-Protein B1
IFN	Interferon
IKKε	IκB kinase-ε
IP	Immunoprecipitation
IP_3	Inositol trisphosphate
IRAK	Interleukin (IL)-1 receptor-associated kinase
ITAM/ITIM	Immunoreceptor tyrosine-based activation/inhibition motif
JNK	c-Jun N-terminal kinase
KO	Knock out
LPS	Lipopolysaccharide

LTA	Lipoteichoic acid
MAV	Mitochondrial antiviral-signaling protein
MCL	Mantle cell lymphoma
MHC	Major histocompatibility complex
min	Minute
MOPS	3-(*N*-morpholino)propanesulfonic acid
mRNA	Messenger ribonucleic acid
MW	Molecular weight
MWS	Muckle-Wells syndrome
MyD88	Myeloid differentiation primary response 88
Nek7	NIMA Related Kinase 7
NEMO	NF-kappa-B essential modulator
NF-κB	Nuclear factor 'kappa-light-chain-enhancer' of activated B-cells
NLRP3	NACHT, LRR and PYD domains-containing protein 3
NOD2	Nucleotide-binding oligomerization domain-containing protein 2
NOMID	Neonatal-Onset Multisystem Inflammatory Disease
NP-40	Nonyl phenoxypolyethoxylethanol
O.n.	Over-night
PAGE	Polyacrylamide gel electrophoresis
PBMC	Peripheral blood mononuclear cells
PH	Pleckstrin homology
PI4P	Phosphatidylinositol-4-phosphate
PIP_2	Phosphatidylinositol 4,5-bisphosphate
PKC	Protein kinase C
PP2A	Protein phosphatase 2
PTPN22	Protein tyrosine phosphatase, non-receptor type 22
PYD	Pyrin domain
RIG-I	Retinoic acid inducible gene I
RIPA	Radioimmunoprecipitation assay buffer
RIPK1	Receptor-interacting serine/threonine-protein kinase 1
ROS	Reactive oxygen species
RT	Room temperature
SCAP	SREBP cleavage-activating protein
SGT1	Suppressor of G2 allele of SKP1
SH	Src homology
SN	Supernatant
SREBP	Sterol regulatory element binding proteins
STING	Stimulator of interferon genes
TBK1	TANK-binding kinase-1
TBS(-T)	Tris-buffered saline (with Tween-20)
TH	Tec homology
TNFα	Tumor necrosis factor α
TXNIP	Thioredoxin interacting protein
VRAC	Volume-regulated anion channel
WCL	Whole cell lysate
WM	Waldenström's macroglobulinemia
WT	Wild type

1. INTRODUCTION

1.1. Overview of the immune system

Most biological entities possess the capability to combat danger that threatens their homeostasis. The defense mechanisms of more complex organisms are strictly organized, regulated, and described as a so-called "immune system" (Chaplin 2010). Although several molecules of the immune system are highly conserved, the responsiveness and mode of action varies on a large scale between species. In general, the vertebrate immune system is divided into two parts, based on their reaction time and specificity, namely the innate immune system and the adaptive immune system, which perfectly harmonize and complement each other in function (Charles Alderson Janeway et al. 2001).

The innate immune system reacts to a group of crude ligands, whereas the adaptive immune system detects highly specific sequences (such as peptides and epitopes), and its ligand specificity is unique for every individual (Akira, Uematsu, and Takeuchi 2006). While activation and effector responses of the innate immune system are rapid, expansion of the adaptive immune reaction takes up to days; however, the reaction will form an immunological memory that enables the adaptive immune system to act faster in case of recurrent infections (Chaplin 2010). The adaptive immune system relies on the innate immune system for its activation, as innate immune mechanisms and cells detect pathogens, and subsequently alarm (e.g. via pro-inflammatory cytokines) and instruct (via professional antigen presentation) adaptive immune cells. These two arms of immunity, even though often described and considered separately, are tightly connected, protect the host in synergy and do not operate entirely separately (Chaplin 2010). The respective functions and their cooperation are briefly outlined here, followed by a review of inflammation as a pivotal process that connects both arms of the immune system.

1.1.1. Components of the innate immune system

Innate immune defenses comprise the various barriers of the body (e.g. physical such as the skin or chemical, such as enzymes or low pH in the stomach), humoral components (e.g. the complement system, acute phase proteins), cells of the hematopoietic myeloid lineage (e.g. macrophages, polymorphonuclear cells, dendritic cells), certain lymphoid cells (e.g. NK cells

and other innate lymphocytes) and even contributions by non-hematopoietic immune cells (e.g. keratinocytes, mucosal epithelial cells) (Chaplin 2010).

1.1.2. Innate immune mechanisms

The effector functions of innate immune components are multifarious and take place in several tissue compartments. Firstly, the invader is facing the physical barriers of the body. Each surface (skin, gut) is additionally covered by humoral elements of the innate immune system that constantly protect the host, such as antimicrobial peptides, soluble receptors, and complement components. These molecules participate in both marking and direct killing of pathogens (Shishido et al. 2012). For instance, lysozymes hydrolyze peptidoglycans of the bacterial cell wall (Ragland and Criss 2017), complement factors opsonize pathogens (Mayilyan et al. 2008), and the antimicrobial peptide LL37 can form pores in the lipid membrane of certain microbes leading to the destruction of the bacterial cell (Xhindoli et al. 2016). Furthermore, soluble receptors (e.g. mannose-binding lectin) sense and decorate the pathogen and can then activate the complement system (Fujita, Matsushita, and Endo 2004). Pathogens may be eliminated directly via complement-induced membrane attack formation, or indirectly, via facilitated phagocytosis of "opsonized" microbes.

Phagocytosis is the main route for elimination of pathogens and removal of cell debris. Although almost every cell performs phagocytosis, innate immune cells are professional phagocytes. Neutrophils efficiently screen the blood stream for pathogens that they take up via Fcγ receptor- or complement factor-mediated phagocytosis. These cells are also the first ones in the tissue at the site of infection (Mócsai 2013). Monocytes and macrophages perform phagocytosis besides Fcγ receptor (in combination with antibodies)- or complement factor recognition, also via scavenger receptor and mannose receptor engagement (Aderem and Underhill 1999). Phagocytosed material is fused with the lysosome resulting in phagolysosome in which the phagocytosed material is degraded. Apart from the destruction of microbial invaders, phagocytosis opens the possibility for antigen processing and presentation to adaptive immune cells (M et al. 2003). In addition to phagocytosis, another effector mechanism employed by NK cells is the killing of infected cells via perforin and Granzyme B. Perforin released from NK cells forms pores on the target cells, which enables the uptake of Granzyme B that cleaves caspase-3, leading to apoptosis of the target cell (Trapani and Smyth 2002).

Upon innate immune system activation, cells release cytokines that serve immunomodulatory functions, and chemokines that facilitate immune cell migration. Type I cytokines (e.g. TNFα, IL-1β, IFN-γ) fuel cellular responses, whereas type II cytokines (e.g. IL-2, IL-4, IL-10) predominantly modulate adaptive humoral immune reactions. Type I cytokines trigger an inflammatory condition which entails the production of chemokines that attract further innate and adaptive immune cells to the inflamed area (Altan-Bonnet and Mukherjee 2019).

1.1.3. The adaptive immune system

The adaptive immune system is composed of specific hematopoietic cells from the lymphoid lineage, e.g. T cells and B cells (Chaplin 2010). In contrast to the relatively "spontaneous" activation of the innate immune system by MAMPs or DAMPs, activation of the adaptive immune system is more complex and dependent on many factors, such as other immune cells, cytokines, and licensing. Adaptive immune cells recognize highly specific and unique sequences and are able to distinguish between ligands that differ in minute details e.g. a single amino acid (Hemmer et al. 2000; Vivier and Malissen 2005). The vast repertoire of receptors required to enable such specific recognition is achieved via gene rearrangement. Therefore, adaptive immune cells need to undergo a strictly regulated maturation process to filter potentially autoimmune or non-reactive cells. At the same time, the fact that an individual receptor is cognate to, initially, one single cell, makes clonal expansion an essential requirement (Chaplin 2010). The mechanisms governing T and B lymphocyte receptor diversification, recognition and clonal expansion are briefly detailed in the following section.

1.1.3.1. T cells

After T-cell receptor rearrangement, T cells undergo positive and negative selection in the thymus to obtain a population whose T cell co-receptors recognize MHC molecules, but their T cell receptors (TCR) do not bind presented self-MHC peptides too strongly (Klein et al. 2014). There are two major types of T cells, based on their co-receptor expression: CD8+ T cells and CD4+ cells. CD8 is a glycoprotein that assists the recognition of peptides presented on MHC class I molecules. Cells, that present non-self-peptides on their MHC class I molecules are usually infected (e.g. by viruses) or cancer cells. Recognition of a peptide on MHC class I in the presence of specific cytokines (e.g. IL-2) leads to activation of the

CD8+ T cells and subsequent killing of the target cell via perforin/granzyme release or via receptor-mediated cell death (Fas receptor engagement). Hence CD8 T cells have been called cytotoxic T lymphocytes (CTLs) (Van Den Broek, Borghans, and Van Wijk 2018).

Although there are also cytotoxic CD4+ cells, most CD4+ T cells are so-called helper cells, i.e. they support the activation of other innate and adaptive immune cells. The glycoprotein CD4 facilitates the recognition of peptides presented on MHC class II molecules. Only professional antigen presenting cells (e.g. dendritic cells of the innate immune system or B cells of the adaptive immune system) phagocytose intruders, mainly bacteria or parasites, and present peptides on MHC class II molecules (Roche and Furuta 2015). CD4+ T cells are activated upon TCR-MHC class II engagement in the presence of co-stimulatory signals mediated by CD28 (T cells) and CD80 (APC) interaction. CD4+ T cells then start to produce IL-2 that stimulates them in an autocrine way and leads to their clonal expansion and maturation. The cytokine combination IL-2 and IFNγ stimulation leads to Th1, whereas IL-2 and IL-4 leads to Th2 polarization of the CD4+ T cells. Th1 cells further release IL-2 and IFNγ that trigger activation of innate immune cells (e.g. macrophages leading to inflammation) and promotes cytotoxic responses via NK cells and CTLs; Th2 cells release predominantly IL-4 that promotes B cell activation and wound repair via anti-inflammatory M2 macrophage polarization (Romagnani 2000; Gieseck, Wilson, and Wynn 2018).

1.1.3.2. B cells

B lymphocytes have two primary functions: they are professional APCs, as mentioned above, and furthermore they produce antibodies. Similar to T cells, B cells also undergo positive and negative selection, clonal selection and expansion, but in the bone-marrow and specialized non-thymic lymphoid organs (Chaplin 2010). Mature naïve B cells reside in the lymph nodes and the spleen and screen the environment with their B cell receptors (BCR) for antigens. Antigen binding of the BCR triggers a downstream signaling cascade involving several kinases (e.g. Syk and Bruton´s tyrosine kinase, see 1.5.2), which culminates in the proliferation of the B cell and presentation of the antigen on MHC class II molecules (Woyach, Johnson, and Byrd 2012). Th2 cells that recognize the peptides presented on MHC class II molecules of the B cells, as described above, release IL-4, and additionally upregulate the co-stimulatory receptor CD40L that binds to CD40 on the B cells. IL-4 together with the co-stimulatory signal provokes BCR class switching (change of the antibody type) and

formation of plasma cells (antibody-producing activated B cells), and memory B cells. Antibodies are secreted BCRs specific for the certain antigen that initiated activation of the B cell (Stavnezer, Guikema, and Schrader 2008). They bind and opsonize persisting antigens, so professional phagocytes, mostly innate immune cells, can be activated via their Fc receptors, provoke inflammation, and eliminate the pathogen. Antibodies can also trigger the activation of the classical complement pathway (L. L. Lu et al. 2018). This way B cells build a bridge between the non-specific activation of the innate immune system and the highly specific adaptive immune response. Production of specific antibodies upon a primary infection might take up to several days (Klimpel 1996). The antibodies thus enable a second wave of innate immune activation apart from the initial reaction immediately upon infection, and further fuel inflammation and pathogen clearance.

1.2. Inflammation

Inflammation is a state in which the immune system is stimulated by either microbes or tissue damage (i.e. sterile inflammation) ("A Current View on Inflammation" 2017). It serves the protection of the host from invaders, as well as tissue repair. It can be local or systemic, evoked by foreign or self-derived stimuli, is under tight regulation, and, if not tightly controlled or switched off, acute inflammation can turn into chronic inflammation and severe diseases such as rheumatic diseases, chronic inflammatory bowel disease, or Alzheimer´s disease (L. Chen et al. 2018; Khor, Gardet, and Xavier 2011). In the last few years, inflammation as a research topic has gained much interested and many diverse topics were studied regarding their relationship with inflammation: diet, microbiota, aging, neurodegenerative diseases, senescence, etc.

Inflammation is tissue-specific and has multiple components and counterparts. Tissue hormones, such as serotonin, histamine, and leukotrienes are main inflammatory mediators produced by tissue cells (e.g. endothelium), innate immune cells, and platelets. These inflammatory mediators have several routes of action: they lead to vasodilatation that enables extravasation of immune cells into the damaged tissue (Abdulkhaleq et al. 2018). Vasodilatation also underlies redness and edema of the inflamed area. Furthermore, they lead to platelet aggregation, pain in the inflamed tissue, and elevated body temperature.

Besides the above-mentioned amines and enzymes, pro-inflammatory cytokines are the other major group that contributes to inflammation. Pro-inflammatory cytokines (IL-1β, IL-18, TNFα, IL-6, IL-12) are mainly released by innate immune cells (predominantly

macrophages) and hold potent immune-activating properties (J. M. Zhang and An 2007). They stimulate both innate and adaptive immune cells, sustain a positive inflammatory feedback loop, and contribute to pain sensation. Furthermore, they induce production of acute-phase proteins in the liver (e.g. fibrinogen, MBL, complement components) that further fuel inflammation (Abdulkhaleq et al. 2018). Inflammation is multi-layered and inhomogeneous; therefore, it is challenging to study and interpret generalized models. Nevertheless, as inflammation is inevitable for maintaining homeostasis, and has been brought into connection with a multitude of diseases (see above), it is crucial to gain deeper understanding in the molecular events contributing to an inflammatory state.

1.3. Pattern recognition receptors

An important common feature of innate immune (and some adaptive) cells is the capability to respond to sensed danger or pathogens immediately through their special receptors. These are germline-encoded, and unlike TCR or BCR, lack genetic refinement to increase diversity (Chaplin 2010). Instead of sensing a wide variety of microbe-derived ligands, innate immune receptors use the strategy to recognize conserved regions of the microbial molecules, often intrinsic to their life cycle and ubiquitously found in multiple microbes, e.g. cell wall components. These "patterns" have been called "microbe-associated molecular patterns, MAMPs". Hence, they were termed "pattern recognition receptors, PRRs" by Charles Janeway (C. A. Janeway 1989). As far as the pathogens do not mutate their characteristic patterns, the innate immune system will serve as an effective and indispensable "first line of defense" against invaders. In addition to MAMPs, PRRs have been shown to sense endogenous universal indicators of cellular stress or damage, i.e. endogenous danger. Hence the term damage-associated molecular patterns, DAMPs, has been coined to describe PRR agonists such as HMGB1 (Roh and Sohn 2018).

The PRRs are divided into four subgroups based on their protein architecture: Toll-like receptors (TLRs), Nod-like receptors (NLR), RIG-I-like receptors and C-type lectin receptors (CLRs) (Takeuchi and Akira 2010). These will be further discussed in the following sections.

1.3.1. Toll-like receptors

The Toll gene was first discovered by Christiane Nüsslein-Volhard in Tübingen, as a receptor in dorsal-ventral polarity during development in *Drosophila* (Anderson, Bokla, and Nüsslein-Volhard 1985; Anderson, Jürgens, and Nüsslein-Volhard 1985). The importance of the TLRs emerged upon the characterization of an additional function of the Toll protein, namely in the anti-fungal immunity of the fruit fly (Lemaitre et al. 1996). Today, ten human TLRs are recognized (TLR1-10) that may be expressed on the cytoplasm or in endosomes and that function as homo- or heterodimers (see table 3.1.) (Kawai and Akira 2011). TLRs sense their ligands (see table 1.1.) via a leucine-rich-repeat region on the ectodomain and transfer the signal intracellularly through a cytoplasmic Toll/interleukin-1 receptor (TIR) domain. Engagement of TLRs leads to downstream signaling cascade utilizing the adaptor MyD88 (except for TLR3 that uses TRIF), signaling mediators (e.g.IRAKs, NEMO) resulting in the activation of transcriptional factors (e.g. NF-κB or IRF) and pro-inflammatory cytokine or type 1 interferon production (Barton and Medzhitov 2003; Kawai and Akira 2008).

Table 1.1. List of human TLRs, activating ligands and adaptor proteins.

TLR	Dimer formation	Activating ligands	TIR-containing adaptor
1	2	Lipopeptides	MyD88
2	1,6	Lipopeptides	MyD88/Mal, TRAM/TRIF
3		dsRNA	TRIF
4	2	LPS	MyD88/Mal
5		Flagellin (Flag)	MyD88
6	2,1	Lipopeptides	MyD88/Mal
7		ssRNA	MyD88/Mal
8		ssRNA	MyD88/Mal
9		CpG DNA	MyD88/Mal
10		Unknown	

1.3.2. C-type lectin receptors

C-type lectin receptors recognize carbohydrates via carbohydrate-recognition domains in a calcium-dependent manner. Nevertheless, the outcome of carbohydrate binding to distinct CLRs varies from phagocytosis to activating or inhibitory immune modulation, dependent on the ligand and the downstream signaling motif (ITAM vs. ITIM) of the receptor (Hoving, Wilson, and Brown 2014). CLR-mediated responses were first brought into connection with anti-fungal immunity, however the role of CLRs in bacteria and virus sensing is emerging (del Fresno et al. 2018).

1.3.3. RIG-I like and NLR receptors

Unlike TLRs and CLRs, that are transmembrane PRRs, NLRs and RIG-I like receptors are located in the cytosol. Generally, sensing DAMPs by these receptors leads in many cases to the formation of a multiprotein complex incorporating ASC and caspase-1, called the inflammasome; resulting in catalytic activation of the proinflammatory cytokines pro-IL-1β and pro-IL-18 (Broz and Dixit 2016); or alternatively (in case of RIG-I) to an antiviral state elicited by type I IFNs (Poeck et al. 2010).

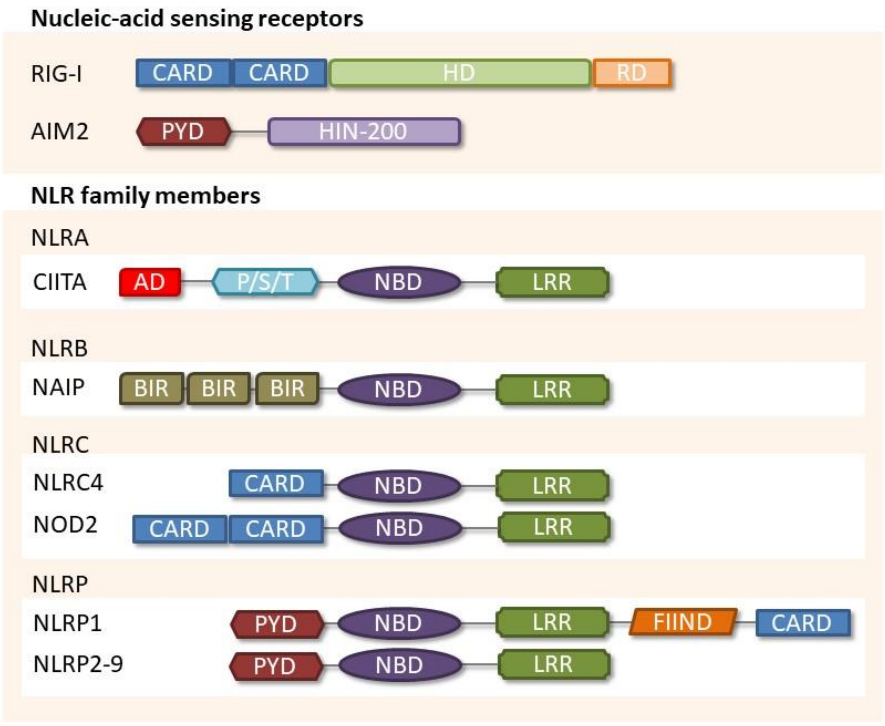

Figure 1.1. Scheme of the described nucleid-acid sensing receptors and NLR structures.

1.3.3.1. RIG-I signaling

RIG-I sensor molecules are expressed in most cells of the human body. Once RIG-I senses its PAMP, which is viral RNA, a conformational change takes place leaving the CARD domain of RIG-I accessible for homologous interaction with the CARD domain of MAV, thereby translocating to the mitochondria. MAV transmits downstream signaling via TBK1 and IKKε, which in turn activates NF-κB and IRF3 activation and transcription of pro-inflammatory cytokines as well as type I IFNs. Additionally to RIG-I, the helicases LGP2 and MDA-5 also react analogously to foreign cytosolic RNA (Loo and Gale 2011).

1.3.3.2. The AIM2 inflammasome

AIM2, besides cGAS, is a fundamental DNA sensor that reacts upon detection of foreign DNA as well as self-DNA located in the cytoplasm. AIM2 detects DNA with its HIN-200 domain (C-terminal), whereupon the N-terminal PYD binds to the PYD of ASC. ASC then forms a platform for pro-caspase-1 oligomerization and autocatalytic activation. Active caspase-1 further cleaves pro-IL-1β and pro-IL-18 to mature cytokines that are released by the cell. The molecule IFI16 also contains a HIN-200 domain and belongs to the AIM2 inflammasome family (Latz, Xiao, and Stutz 2013; Man, Karki, and Kanneganti 2016).

1.3.3.3. The NLR inflammasomes

Common features of the NLR receptors are C-terminal LRR domains, and a nucleotide-binding intermediate domain (NACHT). The N-terminal effector domain varies between the NLR proteins, with it possibly being an acidic transactivation domain (NLRA), a BIR domain (NLRB), a CARD (NLRCs), a PYD (NLRPs), or the unknown X domain of NLRX1 (Yeretssian 2012). Even though 22 human NLRs have been identified, and they all oligomerize upon activation, not all of them were shown to form an inflammasome, and the functional mechanisms of inflammasome formation have only been studied in detail for a few of them (A. Lu and Wu 2015). In the next paragraphs, the activation of some exemplary NLRs that form inflammasome will be described.

In 2002, NLRP1 was the first NLR demonstrated to be able to trigger inflammasome formation (Martinon, Burns, and Tschopp 2002). On the C terminus, the last LRR domain of NLRP1 is linked to a FIIND domain that is connected to a CARD domain. The CARD domain of NLRP1 binds directly, without utilizing an adaptor protein, to the CARD domain of capsase-1 and activates it (Chavarría-Smith and Vance 2015). NLRP1 reacts in vitro to the peptidoglycan component muramyl dipeptide and *in vivo* to anthrax toxin (Faustin et al. 2007; Moayeri, Sastalla, and Leppla 2012). Colchicine, a toxic alkaloid that inhibits microtubule polymerization is used to prevent NLRP1 inflammasome activation by bacterial toxins (Heilig and Broz 2018).

NLRP6 is primarily expressed in intestinal mucosa cells, signals via ASC and caspase-1, and is crucial for elimination of intracellular bacteria, as it is activated by bacterial components (e.g. lipoteichoic acid) sensed in the cytosol (Hara et al. 2018). NLRP6 contributes to anti- as well as pro-inflammatory signaling and its activity contributes to the maintenance of a healthy microbiota. Consequently, NLRP6 deficiency might lead to disbalance in the bacterial population of the gut microbiota and eventually to colitis (Levy et al. 2017).

A further antibacterial inflammasome forming NLR is NLRC4. NLRC4 functions as an adapter protein between the receptor NAIP, that recognizes flagellin or type III secretion system proteins, and the downstream effector caspase-1 (Zhao et al. 2011). Upon signaling, NLRC4 binds NAIP via NACHT and LRR homotypic interactions and caspase-1 via CARD-CARD interplay. Thereby caspase-1 is activated and the common inflammasome downstream events (pro-IL-1β and pro-IL-18 cleavage, and IL-1β and IL-18 release) occur. As recently described (Y. Li et al. 2018), the adaptor proteins ASC and NLRC4 utilize their CARD domains in a unified way to form platforms for caspase-1 oligomerization and activation. Miss-sense mutation in the *Nlrc4* gene is associated with increased IL-1β production in familial cold autoinflammatory syndrome (Kitamura et al. 2014).

NOD2, an additional member of the NLRC family, likewise detects conserved bacterial components (e.g. muramyl peptide) in the cytosol (Laman et al. 2016). Consequent to ligand binding, NOD2 oligomerizes and utilizes RIP2 (via CARD-CARD interaction) for further downstream signaling. RIP2 activates the transcription factor NFκ-B that induces proinflammatory gene expression. Via its CARD domain, NOD2 also binds and triggers caspase-1 directly, leading to cleavage of the transcribed proinflammatory cytokines pro-IL-1β and pro-IL-18 (Negroni et al. 2018).

Besides inflammasome activation, NOD2 was identified to be responsible for autophagy initiation, as it binds and activates the autophagy-inducing protein ATG16L1 (Negroni et al. 2018).

1.3.3.4. Pyroptosis

The type of cell death accompanying inflammasome activation has not been well understood, even though it had been frequently observed and measured. The gasdermin family member gasdermin-D (GSDMD) was recently brought into connection with a novel type of proinflammatory programmed cell death taking place in connection with inflammasome activation: pyroptosis. Upon inflammasome signaling, caspases (caspase-1, caspase-4, caspase-5, caspase-11) are activated, which not only cleave proinflammatory cytokines, but also GSDMD. The N-terminal fragment of GSDMD forms pores in the cell membrane, which leads to disintegration of the cell and cell death (J. Shi, Gao, and Shao 2017). Surprisingly, cleavage of GSDMD by caspase-3 leads to an N-terminal peptide that is unable to form cytotoxic pores (Rogers et al. 2017). The pores formed by cleaved GSDMD also serve the release of the mature cytokines IL-1β and IL-18 (Man, Karki, and Kanneganti 2017).

1.4. NLRP3 inflammasome

NLRP3 belongs to the PYD containing NLR family; is expressed in myeloid cells, keratinocytes, and to some extent in lymphoid cells; and represents the probably most broadly studied NLR (Latz, Xiao, and Stutz 2013). One of the reasons for the high interest in understanding how NLRP3 functions as a receptor and how the NLRP3 inflammasome assembles might be the wide range of seemingly unrelated DAMPs that NLRP3 senses; the extent of downstream signaling upon NLRP3 engagement; and the diverse set of diseases that are either associated with genetic NLRP3 mutation or correlate with NLRP3 hyperactivity. In the next section, the structure, activation, regulation, and consequences of dysregulation of the NLRP3 inflammasome will be discussed.

1.4.1. The structure of NLRP3

NLRP3 consists of an N-terminal PYD (10 kDa) that is connected to the NACHT domain (40 kDa) via a 127 amino acid long linker. The NACHT domain is further divided into the functional subunits NBD, helical domain 1 (HD1), winged helix domain (WHD) and helical domain 2 (HD2) (Sharif et al. 2019). The NACHT domain is followed by a linker region (206 amino acids) that binds to the first of nine LRR domains (21 amino acids each, connected by 9 amino acid linkers, ca 40 kDa in total). According to the most widely accepted insights, the LRR domain is supposed to be responsible for ligand recognition, the NACHT domain for homotypic oligomerization of NLRP3 and the PYD for interaction with the adaptor molecule ASC. Nevertheless, a recent publication stated that NLRP3 lacking the LRR domain was just as sensitive to activation as FL NLRP3, whereas NLRP3 lacking the PYD was auto-active, suggesting an auto-inhibitory role of the PYD (Hafner-Bratkovič et al. 2018).

As NLRP3 senses a broad array of distinct activating signals, solving its structure and the structural changes it undergoes upon activation would help enormously to elucidate the mechanisms behind its function as a receptor. Unfortunately, the crystal structure of full-length NLRP3 has not been solved yet. Moreover, the crystal structure of the inactivate NLRP3 monomer would have to be complemented by the structure of the activated NLRP3 oligomer, (better yet in complex with ASC), as predictions suggest strong structural differences between the inactive and the active NLRP3 conformation.

There are, however, several publications describing the crystal and cryo-EM structure of the NLRC family members NLRC4 (in monomeric inactive form as well as in complex with NAIP) (Zhao et al. 2011; Diebolder et al. 2015), and NOD2 (Maekawa et al. 2016). Even though the N-terminal domain differs between the NLRC family (N-terminal CARD) and the NLRP family (N-terminal PYD), structural homology modelling gave us first insights to the organization of NLRP3, at least that of the NACHT and LRR domains. The models can be further refined by the incorporation of the available crystal structure of NLRP3´s PYD (Bae and Park 2011). Most recently, cryo-EM data of NLRP3 in dimer with NEK7 revealed the actual structure of NLRP3 NACHT and LRR domains, which showed the typical "earring shape" that is consistent with the models based on NLRC4 (Sharif et al. 2019). The cryo-EM structure exposed a comparable NBD/HD1/WHD part of the NACHT domain to that of the inactive NLRC4, whereas the structures of the NACHT subunit HD2 as well as the LRR domain are shifting between the structures of established NLRs.

1.4.2. Molecular mechanism of NLRP3 inflammasome assembly

The earliest model of NLRP3 inflammasome assembly was established before the first available NLR crystal structures, based on the formation of the apoptosome and domain similarities between NLRs and the apoptosome forming sensor proteins (e.g. CED-4, Apaf-1) (Zou et al. 1999). The structure of the apoptosome sensor protein oligomers showed a "disc" or "donut"-like shape formed by eight NACHT domains, building an interface for caspase catalytic activation (Qiao et al. 2013). It is now known that unlike in case of the apoptosome, caspase activation takes place on NLRP3 inflammasome-forming ASC filaments.

In steady state, NLRP3 is monomeric and in an inactive conformational state. In this form, based on the NLRC4 structure, the LRR domain is lying close to the NBD/HD1/WHD subunits of the NACHT domain. Upon ligand sensing (most probably indirectly), NLRP3 undergoes conformational change and unfolds, separating the LRR from the NACHT domain (Elliott and Sutterwala 2015). Consequent to opening of NLRP3, the NACHT domain becomes accessible for homotypic interaction and formation of the "donut-like" oligomer, composed of 11 or 12 NLRP3 molecules, upon which ASC filaments form (Sharif et al. 2019). Basic criterion of NLRP3 oligomerization and ASC adherence is ATP binding by the NACHT domain NBD region Walker A motif, and ATP hydrolysis by the NBD region Walker B motif; with ATP binding being upstream of hydrolysis (Jiang et al. 2017).

Centre of the inflammasome signalling are the homotypic PYD/PYD interactions, first between NLRP3 and ASC and then between ASC and ASC. ASC PYD binds NLRP3 PYD with higher affinity than ASC PYD, enabling the downstream signaling originated from NLRP3 (Oroz et al. 2016). ASC filaments then undergo prion-like polymerization arising from NLRP3, which then form a platform for caspase-1 binding via CARD-CARD interactions, resulting in a star-shaped macromolecular complex. Caspase-1 molecules thereby come to close proximity with each other, leading to dimerization, conformational change, autocatalytic cleavage and activation of caspase-1 (A. Lu and Wu 2015).

1.4.3. Canonical NLRP3 inflammasome activation

Activation of the NLRP3 inflammasome the canonical way requires two steps: a first "priming" signal and a second "activation" signal. The second signal without the first signal is not sufficient for canonical inflammasome activation (Kelley et al. 2019).

One unique characteristic of NLRP3 within the NLRs is its relatively low expression in steady state of the cells (Latz, Xiao, and Stutz 2013). Originally, the priming step of inflammasome activation was seen to serves the upregulation of the expression of both NLRP3 and pro-IL-1β mRNA. It takes place upon engagement of a transmembrane PRR (e.g. TLR4) via PAMP recognition (e.g. LPS), leading to NF-κB activation and the above-mentioned transcriptional regulation of NLRP3 and pro-IL-1β (Latz, Xiao, and Stutz 2013). Nevertheless, novel functions of the priming step have been recently emerged that will be discussed in the next section.

The signals that act as the second, inflammasome activating events are very heterogenous and more debated in the field. The most accepted activation event is potassium efflux. It has been observed that many NLRP3 triggers (nigericin, crystals, ATP) (Y. Yang et al. 2019) commonly result in the reduction of intracellular potassium concentration which is the actual indirect DAMP of NLRP3 (Latz, Xiao, and Stutz 2013).

An additional, more debated ion-dependent NLRP3 trigger is calcium transfer between cell compartments. Massive calcium release from the ER destabilizes the mitochondria that results in ROS production and consequently in NLRP3 activation (Murakami et al. 2012). Studies both supporting and disproving this hypothesis have been published therefore more research is needed to resolve the role of calcium in NLRP3 signaling.

Disintegration of the cell membrane by nigericin or MSU not only leads to potassium efflux directly, but also to sodium diffusion into the cell. The increased ion load in the cell results in swelling and decrease in relative potassium concentration, which again triggers NLRP3 inflammasome activation, with sodium being an ancillary catalyst (Schorn et al. 2011).

Chloride efflux through chloride channels (e.g. VRAC) upon decrease of extracellular chloride concentrations was also reported to be involved in NLRP3 inflammasome activation (Schorn et al. 2011; Compan, Baroja-Mazo, López-Castejón, et al. 2012).

A further “danger” signal that NLRP3 reacts upon is ROS production by the mitochondria (Zhou et al. 2011). ROS was shown to be generated in several situations consequent to NLRP3 inflammasome activation, such as fatty acid uptake (with high-fat-diet), mitochondrial stress, and imiquimod-treatment. On the other hand, some studies reported mitochondria-dependent activation of the NLRP3 inflammasome that was nevertheless free of ROS generation (Wen et al. 2011; Bauernfeind et al. 2011). Thus, the part ROS plays in NLRP3 signaling still needs to be further clarified.

The cell´s outer membrane is not the only membrane whose disbalance or damage provides the second signal for NLRP3 activation. Lysosomal rupture was also proven to induce NLRP3 inflammasome assembly (Halle et al. 2008). Aβ was the first substance that was shown to induce lysosomal damage further leading to NLRP3 activation. Since then, several other compounds (e.g. silica crystals, aluminum salts, cholesterol crystals) were demonstrated to provoke NLRP3 signaling consequent to phagocytosis, lysosomal burst, and cathepsin B release (Hornung et al. 2008).

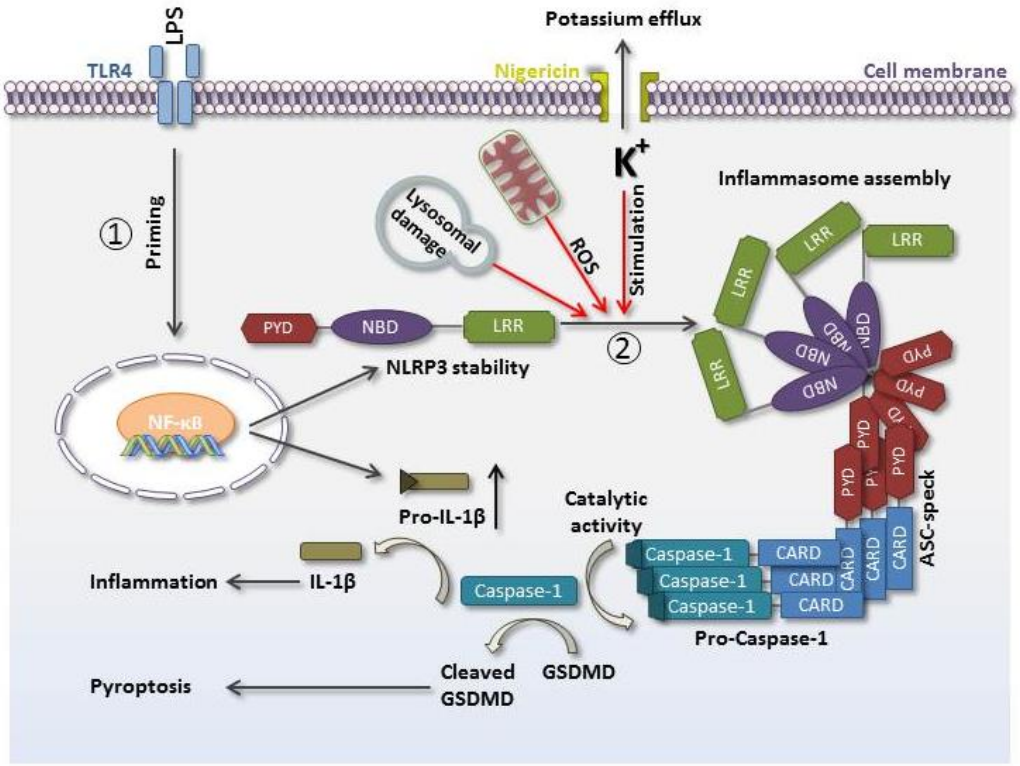

Figure 1.2. Scheme of the canonical inflammasome activation.

Upon the priming step, NLRP3 and pro-IL-1β are transcribed, and NLRP3 protein is stabilized and protected against degradation. The second, stimulating signal, such as potassium efflux, ROS, or lysosomal damage leads to inflammasome assembly.

1.4.4. Noncanonical NLRP3 activation

Even though both canonical and noncanonical inflammasome activation result in caspase activation and pyroptosis, the signaling mechanisms are quite distinct. While the canonical inflammasome pathway takes place in two steps (priming and activation) and is mediated by caspase-1 activation, the effector function is fulfilled by caspase-4/5 (caspase-11 in the

mouse) upon noncanonical inflammasome induction (Kayagaki et al. 2015; Baker et al. 2015). Technically speaking, the noncanonical inflammasome can serve as an upstream event of the canonical NLRP3 inflammasome. While extracellular LPS stimulation of the cell primes the canonical inflammasome via TLR4 engagement; intracellular LTA and intracellular LPS trigger formation of the noncanonical inflammasome (NLRP6 and NLRP3) (Kayagaki et al. 2013). Lipid A in LPS is a direct ligand of caspase 4/5, which is recognized by the CARD domain. Caspase-4/5 oligomerize upon lipid A sensing and become active via autocatalytic cleavage. Instead of pro-IL-1β, caspase-4/5 cleaves GSDMD that leads to pore-formation on the cell membrane and to pyroptosis (see section 1.3.3.4.). Potassium efflux through the pyroptotic pores triggers the NLRP3 inflammasome as a second signal, and the canonical NLRP3 inflammasome signaling runs through, resulting in the release of the proinflammatory cytokines.

1.4.5. The alternative NLRP3 pathway

It has been observed that a long priming step (over 12 hours) alone is able to trigger NLRP3 activity in human and porcine monocytes, but not in murine cells (Gaidt et al. 2016). The signaling originates from TLR4 engagement via LPS binding. TLR4 then utilizes the adaptor molecule TRIF to mediate downstream signaling. Further downstream molecules include RIPK1, FADD, and caspase-8. Caspase-8 finally induces NLRP3 inflammasome formation in an unidentified way (Y. Yang et al. 2019). There might be additional intermediary molecules (e.g. Nek7). Even though the alternative inflammasome pathway results in NLRP3 activation, and ASC and caspase-1 are involved, it is free from pyroptosis. Therefore, the release route of IL-1β and IL-18 also remains unknown (Gaidt et al. 2016).

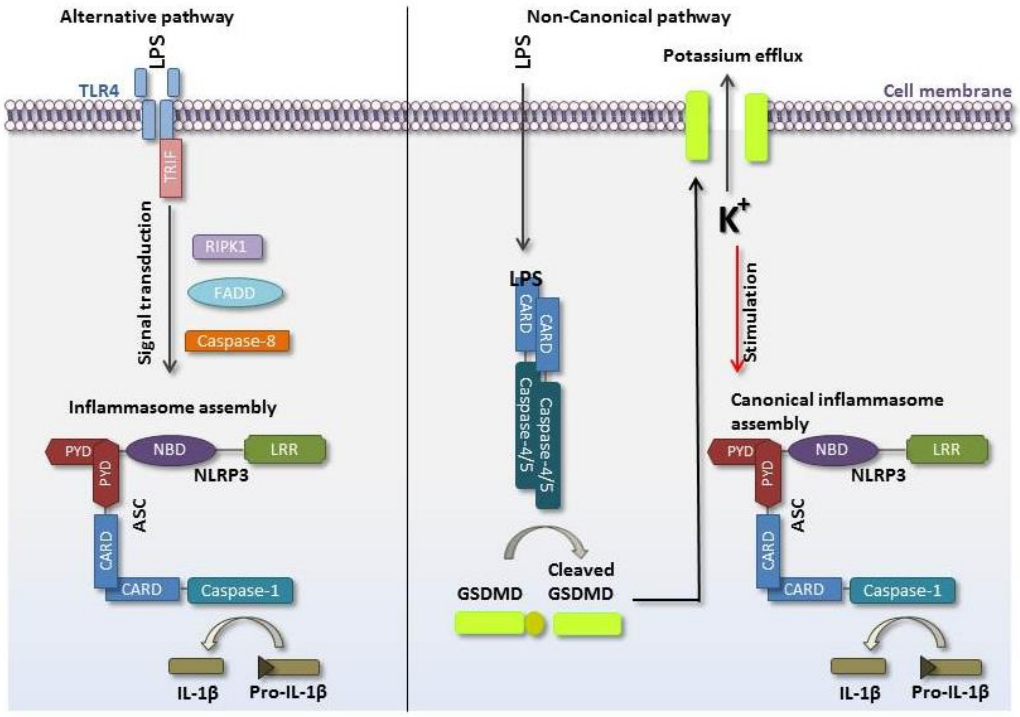

Figure 1.3. Scheme of the alternative and non-canonical inflammasome activation.

In the alternative pathway, extracellular LPS recognition leads to inflammasome activation via a signal cascade. In case of the non-canonical activation, caspase4/5 recognizes intracellular LPS which leads to potassium efflux and thereupon NLRP3 inflammasome assembly. Figure modified from (Y. He, Hara, and Núñez 2016).

1.4.6. Cell organelle localization of NLRP3

Multiprotein complexes are often organized on cell organelles. It is therefore not surprising that NLRP3 was reported to bind to several cellular compartments at distinct activation stages.

Upon nigericin treatment, both NLRP3 and ASC translocated to mitochondrial and endoplasmic reticulum markers in THP1 cells (Menu et al. 2012). Defective mitochondrial functions, e.g. evoked by voltage-dependent anion channel inhibition, reduced ROS release and NLRP3 activity (Hamilton and Anand 2019). Furthermore, it was observed that the negative regulator SHP targets NLRP3 at the mitochondria (C. S. Yang et al. 2015). On the other hand, mitochondrial localization of NLRP3 could not be detected in mouse macrophages (Wang et al. 2013). Similar to RIG-I recruitment, MAVS might play a role in NLRP3 mitochondrial binding, or alternatively cardiolipin, when present on the mitochondrial outer membrane (Hamilton and Anand 2019; Iyer et al. 2013). How NLRP3 is transported to

the mitochondria is not fully understood yet. A recent study reported that NLRP3 is guided along the microtubules by MARK4 to the mitochondria, where inflammasome assembly takes place, restricting inflammasome formation to one location in the cell (X. Li et al. 2017). These observations connect the known NLRP3 triggers e.g. cell damage, ROS, and mitochondrial DNA, often linked to loss of mitochondrial integrity, with NLRP3 localization at the mitochondria, which would be consequentially favorable for the cell. Nevertheless, the chronology of cell damage and mitochondrial localization, as well as the factors that support NLRP3 translocation remain largely unknown.

Besides direct mitochondria binding, NLRP3 was also shown to interact with the mitochondria mediated by the ER. Disbalance in ER function leads to stress of the cell and to NLRP3 activation. One of these mechanisms could be traced back to the unfolded-protein response sensor IRE1α (Bronner et al. 2015). Upon ER disfunction, the activated IRE1α induced ROS production by the mitochondria which led to NLRP3 mitochondria translocation and downstream activation. IRE1α inhibition and thus IL-1β reduction was shown to have beneficial effects in hypoxic-ischemic brain injury, atherosclerosis, and liver injury.

A further link between the ER, the mitochondria and NLRP3 is calcium. The ER is responsible for calcium homeostasis. Thus, ER disfunction leads to calcium disbalance, mitochondrial damage and NLRP3 inflammasome activation (Murakami et al. 2012; Lee et al. 2012).

Besides calcium, the ER regulates cholesterol trafficking as well. Cholesterol crystals, (as described in 1.4.3.) can also trigger the NLRP3 inflammasome. Furthermore, NLRP3 can be activated cholesterol-dependently, however indirectly, by the cholesterol derivate 25-HC, which causes potassium efflux. It was shown that a reduction in cholesterol levels suppress NLRP3 activity (Jang et al. 2016; de la Roche et al. 2018).

In addition to the mitochondria and the ER, the role of the Golgi network in NLRP3 inflammasome activation and assembly has been progressively studied in the last years. The importance of the Golgi in NLRP3 regulation was first recognized in 2017 (Z. Zhang et al. 2017). Then, it was shown that increased DAG levels upon NLRP3 inflammasome stimulation leads to translocation of NLRP3 to the MAMs at the Golgi network. Simultaneously, DAG also recruits PKD, which phoshorylates NLRP3 and mediates its release from the Golgi (Z. Zhang et al. 2017), see 1.4.7. This study was followed up with a recent publication showing that ionic forces recruit NLRP3 to the trans-Golgi network (TGN), whereby TGN serves as a scaffold for NLRP3 oligomerization (J. Chen and Chen 2018). It

was demonstrated that NLRP3 binds via its positively charged polybasic region located in the PYD-NACHT linker to the negatively charged phospholipids, namely PtdIns4P, at the TGN. On the TGN membrane NLRP3 forms oligomers smaller in size than the ones found in complex with ASC-specks. Nonetheless, how these NLRP3 puncta are released from the TGN to form the NLRP3 inflammasome in the cytosol was not discussed in this work.

A third study connected the role of ER, mitochondria, and Golgi in NLRP3 inflammasome activation, namely via the molecules SREBP and SCAP. Independently of NLRP3 signalling, the protein complex SREBP-SCAP translocate to the Golgi from the ER to prompt cholesterol synthesis. Additionally, NLRP3 is transported with the SREBP-SCAP proteins to the Golgi in murine macrophages. NLRP3 was also in complex with SCAP at the mitochondria prior to translocation to the Golgi (Guo et al. 2018).

Additionally to diverse cytosolic localization of NLRP3, NLRP3 was shown to be located in the nucleus in Th2 cells and function as a transcription factor, together with IRF4, promoting Th2 differentiation and activity (Bruchard et al. 2015).

1.4.7. Posttranslational regulation of NLRP3

Apart from the transcriptional regulation of NLRP3 during the priming step, post-translational modifications along both first and second signals are crucial for positive as well as negative regulation of NLRP3.

NLRP3 is ubiquitinated at all domains and rapidly degraded without inflammasome stimulation, keeping its expression basal. The deubiquitinase BRCC3 was identified to deubiquitinate the LRR domain of NLRP3, thus licencing its activation upon stimulation (Py et al. 2013). The ubiquitinated residues, however, were not determined. The ubiquitin ligase MARCH7 was shown to ubiquitinate the LRR of NLRP3 that is bound to cAMP leading to NLRP3 downregulation. cAMP labeling of NLRP3 is induced by dopamine receptor signaling, which plays a role in neuroprotection by preventing inflammation in the brain (Yan et al. 2015). The ubiquitin ligase TRIM31, when expressed in parallel with NLRP3, ubiquitinates NLRP3 PYD upon priming, resulting in proteosomal degradation (H. Song et al. 2016). Nonetheless, activating ubiquitination during the priming step has also been described. The ubiquitinase Pellino2 was reported to support inflammasome activation by LPS-mediated ubiquitination of NLRP3 (Humphries et al. 2018). Furthermore, Pellino2 also ubiquitinates and disrupts IRAK1/NLRP3 interaction that would inhibit NLRP3 activation. On the other

hand, during priming FBXL2 ubiquitinates NLRP3 at Lys689, which determines degradation of NLRP3 (Han et al. 2015). This process is counteracted by the LPS-induced activation of FBXO3, which ubiquitinates and downregulates FBXL2, resulting in the maintenance of the newly transcribed NLRP3 simultaneous to priming. Again, a further ubiquitination event, namely via ARIH2 at the NACHT domain of NLRP3, inhibits NLRP3 assembly (Kawashima et al. 2017).

As described above, several inflammasome promoting and suppressing ubiquitination steps have been described, however independently and observed in different contexts. It is therefore challenging to form a working hypothesis incorporating all the described ubiquitination events in a chronological and logical manner.

In addition to ubiquitination, phosphorylation of NLRP3 plays a substantial role in its regulation. Unlike NLRP3 ubiquitination, most of the reported NLRP3 phosphorylation events occur during the second, activating signal, with the exception of one: Phosphorylation of NLRP3 Ser194 during the priming process serves for NLRP3 deubiquitination, preserving NLRP3 intact for inflammasome activation (N. Song et al. 2017).

cAMP not only binds to NLRP3 directly, as described above, but higher cAMP concentrations in the cytosol activate PKA, which in turn phosphorylates the NLRP3 NACHT domain at residue S295. This phosphorylation event is a signal for ubiquitin ligases to ubiquitinate NLRP3 which leads to NLRP3 elimination (Guo et al. 2016).Very interestingly, one year after this study had been published, a remarkably different effect of phospho-Ser295 was reported: Phosphorylation of Ser295 by PKD facilitates release of NLRP3 from the Golgi and promotes NLRP3 inflammasome assembly. Authors of this publication argue that phosphorylation of Ser295 by PKA inhibits Golgi binding of NLRP3 in the first place, whereas phosphorylation of Golgi-bound NLRP3 by PKD leads to NLRP3 inflammasome formation (Z. Zhang et al. 2017). Phosphorylated Ser5 inhibits NLRP3-ASC PYD/PYD interactions. The kinase executing this phosphorylation is unknown, however, the phosphatase responsible for the reversing dephosphorylation of Ser5 could be identified, namely PP2A (Stutz et al. 2017). PP2A thus acts as an inflammasome activator. Another NLRP3 activating phosphatase is PTPN22, which removes the NLRP3 inflammasome assembly-blocking phosphorylation from Tyr891 (kinase not identified yet) (Spalinger et al. 2017).

Alkylation of NLRP3, possibly at the NBD, inhibits ATP binding, which, as mentioned above, is critical for NLRP3- self and ASC interaction. Alkylation of NLRP3 thus reduces

NLRP3 activation. Furthermore, it has been reported that alkylated NLRP3 shows increased ubiquitination tendency and thus elevated degradation (Shim et al. 2017).

Nitric oxide was reported to inhibit IL-1β release in macrophages (Mao et al. 2013).This effect was tracked back to S-nitrosylation of an NLRP3 cystein residue (Mishra et al. 2013). Nonetheless, the nitrosylated cysteine residue has not been determined yet.

An uncommon form of post-translational modification, namely sumoylation was recently shown to prohibit NLRP3 activation. The SUMO E3 ligase MAPL performs sumoylation of several lysine residues of NLRP3, which is reversed by the proteases SENP6 and 7 upon signal two of NLRP3 activation. Targeting SENP6 and 7 might be a potential NLRP3 inhibition strategy (Barry et al. 2018).

The complexity and plurality of the NLRP3-modificating posttranslational events represent the significance of the meticulously controlled NLRP3 inflammasome assembly that still requires further research efforts to fully understand and elucidate.

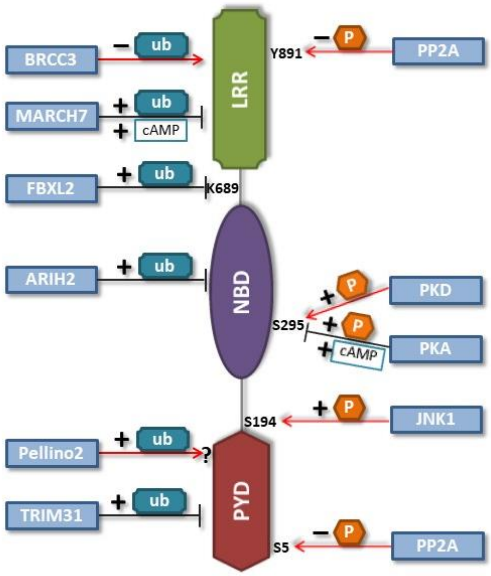

Figure 1.4. Schematic illustration of NLRP3 post-translational modifications.

Several molecules modulate both positively and negatively NLRP3 activity via post-translational modifications. Red arrows represent activation, whereas black lines stand for inhibition. Ub: ubiquitination, P: phosphorylation. Figure modified from (Y. Yang et al. 2019).

1.4.8. Regulation of NLRP3 by interaction partners

Apart from post-translational modifications, NLRP3 is regulated via several interaction partners. Hsp90, together with SGT1, was shown to stabilize NLRP3 in an inactive monomeric state, prohibiting auto-reactivity (Mayor et al. 2007). The ROS sensor TRX disengages from TXNIP upon oxidation, whereupon TXNIP binds to NLRP3 leading to its activation (X. Ye et al. 2017; L. Li et al. 2019). Another inflammasome activation promoting molecule was reported to be GBP5, by binding to the PYD and facilitating ASC-speck formation (Shenoy et al. 2012).

The serin/threonine kinase Nek7 was identified by two research groups in parallel to be a positive regulator of the NLRP3 inflammasome, but not other NLRs (H. Shi et al. 2016; Y. He et al. 2016). Nek7 governs NLRP3 activity to multiple second signals, however, the exact molecular mechanisms have not been deciphered yet. Even though Nek7 binds NLRP3 NACHT and LRR domains with its catalytic domain, the kinase activity of Nek7 seems to be dispensable for inflammasome regulation (Y. He et al. 2016). It could be shown that Nek7 promotes NLRP3 oligomerization, ASC-speck formation and downstream NLRP3 signaling, therefore scaffold functions of Nek7 can be hypothesized.

Furthermore, the Ito and Weber labs recognized Bruton´s tyrosine kinase (BTK) as a novel positive regulator of NLRP3 (Ito et al. 2015; Liu et al. 2017). This topic will be further discussed in section 1.5.5.

1.4.9. NLRP3 associated diseases

Elevated IL-1β levels and uncontrolled inflammation could be traced back to increased NLRP3 activity in several diseases (Mangan et al. 2018). These could be triggered by gain-of-function *Nlrp3* mutations or NLRP3 hyperactivity independently of a genetic mutation.

1.4.9.1. Cryopyrin-associated periodic syndromes (CAPS)

One underlying reason for stringent NLRP3 signaling is a group of mutations in the CIAS1 gene, coding for NLRP3, leading to signal-insensitive auto-active NLRP3. These CIAS1 mutations led to the discovery of NLRP3, originally termed as CIAS. The autoinflammatory

diseases elicited from CIAS1 mutations, CAPS, as the name suggests, are associated with periodic inflammatory flairs, with unknown triggers in most cases. Dependent on the severity, CAPS are divided into three groups: the mildest form FCAS, the moderate MWS, and the severe CINCA or NOMID. The symptoms vary from fever, urticaria (FCAS); renal amyloidosis (MWS); to arthropathy, and central nervous system disturbance leading to hearing loss or aseptic meningitis (CINCA) (Booshehri and Hoffman 2019).

Over 90 mutations of NLRP3 have been shown to cause a spectrum of different CAPS manifestations: CAPS mutations are often located in the third exon of NLRP3 and code for altered amino acids in the PYD-NACHT linker, the NACHT domain and the LRR domain (Goldbach-Mansky 2011). The underlying mechanism by which these mutations lead to auto-active NLRP3 is not unified; dependent on the location, they could alter ATP binding (Walker A motif) or hydrolysis (Walker B motif); or lead to structural changes causing enhanced oligomerization tendency. As the exact process of structural changes that NLRP3 undergoes upon activation is not fully understood yet, it is difficult to predict the functional effects of a single CAPS mutation. Furthermore, mutations might interrupt the binding of negative regulators to NLRP3 or promote the interaction with positive regulators.

1.4.9.2. NLRP3 related metabolic diseases

Metabolic disorders such as overweight and type 2 diabetes mellitus have also been linked to NLRP3 disfunction in a mutation-independent manner. The NLRP3 inflammasome components NLRP3, ASC and caspase-1 have been found in increased amounts in adipose tissue (Unamuno et al. 2019). In adipose tissues, the AMPK levels decrease, which leads to reduced mitochondrial autophagy, mitochondrial disfunction and ROS production that triggers NLRP3 activation; which further fuels immune cell infiltration and inflammation (Steinberg and Schertzer 2014). NLRP3-mediated IL-1β leads to insulin resistance directly via downregulation if the insulin-receptor substrate 1, and indirectly via induction of TNFα production, another insulin-resistance mediator (Jager et al. 2007). Indeed, loss of NLRP3 activity in adipose mice reversed insulin resistance and improved glucose uptake. Western diet was shown to influence trained innate immunity in an NLRP3-dependent manner, leading to chronic inflammation (Christ et al. 2018).

In the western world, since infections do not represent a life threat and life expectancy prolonged, cardiovascular diseases became prominent and provoked more attention in the research field. Western diet does not only trigger metabolic inflammation but also inflammation of the cardiovascular system leading to atherosclerosis, which underlies most cardiovascular diseases. Increased amounts of cholesterol, typical for atherosclerosis, triggers NLRP3 inflammasome activation via previously described routes (see 1.4.3) and fuels inflammation contributing to atherosclerosis pathogenesis. Targeting NLRP3 in atherosclerosis could be a potential treatment strategy in cardiovascular pathologies (Karasawa and Takahashi 2017).

Recently, inflammation of the central nervous system observed in Alzheimer´s and Parkinson´s diseases has also been linked to NLRP3 activity (Heneka et al. 2013; Dolgin 2019). Amyloid-β peptides, present in the brain plaques of Alzheimer´s disease, can serve as first and second signal in the microglia and trigger NLRP3 inflammasome activation. NLRP3 knock-out mice showed less severe disease development compared to NLRP3 WT mice (Heneka et al. 2013). Similarly to amyloid-β, α-synuclein aggregates in the Lewy bodies of Parkinson´s disease patient´s brains triggers the NLRP3 inflammasome of the microglia and contributes to disease progression (Gordon et al. 2018). Uptake of α-synuclein is mediated by CD36. Fyn kinase prompts NFκB activation via PKCδ activation, serving the priming of NLRP3, and furthermore it promotes ROS production by the mitochondria which delivers the second signal for inflammasome activation (Panicker et al. 2019). In both Alzheimer´s and Parkinson´s diseases, NLRP3 inhibition shows promising results in disease amelioration in mouse models.

Table 1.2. List of NLRP3 assosiated diseases and treatment options. Figure modified from (Mangan et al. 2018)**.**

Disease	Improved in Nlrp3 KO?	NLRP3 inhibitors that improve the condition (used in models)
Alzheimer´s disease	Yes	Fenamate, MCC950
Atherosclerosis	Yes	MCC950
Asthma	Yes	MCC950
Cryopyrin-associated periodic syndromes	Yes	MCC950 OLT177 CY-09
Gout	Yes	B-hydroxybutyrate (BHB) Quercetin
Inflammatory bowel disease	Yes	MCC950 INF39
Myokardial infarction	Yes	MCC950
Obesity-induced inflammation or insulin resistance	Yes	CY-09
Stroke	Yes	Ibrutinib MCC950

1.4.10. NLRP3 inflammasome targeting strategies

To date, treatment options considered for NLRP3-associated inflammatory diseases are targeting alarmins released upon NLRP3 activation, primarily IL-1β, or the IL-1 receptor (IL-1R) (Mangan et al. 2018).

The most significant compound is the monoclonal antibody canakinumab, developed by the company Novartis that neutralizes IL-1β by binding, and blocks IL-1β/IL-1 receptor interactions. It is applied in rheumatoid arthritis and CAPS; and is in clinical trial for further inflammatory disorders (e.g. gout) (Hoy 2015). Canakinumab is administered every 8 weeks via subcutaneous injections. Alternatively, the recombinant protein rilonacept can be administered for CAPS treatment. Rilonacept mimics the ectodomains of the IL-1 receptor and binds both IL-1β and IL-1α, thereby suppressing their function (Hoffman, Yasothan, and Kirkpatrick 2008). Rilonacept is injected weekly subcutaneously.

A different strategy represents the protein anakinra. The IL-1 receptor antagonist anakinra blocks the receptor and prohibits downstream signaling. It is applied in rheumatoid arthritis, and CAPS (Cavalli and Dinarello 2018). It is administered daily, subcutaneously.

The treatment possibilities available to date are limited and wearing for the patient. They are administered via injections, which may lead to local reactions at the site of administration and is more painful than taking medicine orally.

Due to these shortcomings, recent research, including the work in this project, has focused on targeting NLRP3 either directly or at the level of direct interactors. The main aim is inhibition of NLRP3 itself, as targeting NLRP3 would hinder the originator of the inflammatory cascade instead of suppressing the general mediator at the end of the signal pathway (IL-1β/IL-1 receptor in case of the current strategies). Furthermore, NLRP3 activation also leads to the inflammatory cell death proptosis, as well as IL-18 release, which are not inhibited using the current treatment options.

MCC950 is a small molecule developed and described in 2015 (Coll et al. 2015). Even though it proved to be a very potent and specific inhibitor of NLRP3 (both canonical and non-canonical pathways), and was widely distributed in in vitro and *in vivo* NLRP3 inflammasome research, the inhibitory mechanism of MCC950 was to some extent elucidated as recent as 2019, and is still not entirely understood. It could be shown that MCC950 binds to the Walker B motif of NLRP3, thereby inhibiting ATP hydrolysis and oligomerization of NLRP3 (Coll et al. 2019). An independent study showed in parallel that MCC950 indeed binds residues of the Walker B motif; and claimed that NLRP3-MCC950 interaction stabilizes the inactive closed conformation of NLRP3 (Tapia-Abellán et al. 2019). Even though MCC950 restricts NLRP3 activity upon oral administration in mice, the application is humans is not foreseen yet.

Recently, Tranilast, a tryptophan metabolite analogue, used for the treatment of allergy, was recognized to inhibit NLRP3. Tranilast interacts with the NACHT domain of NLRP3 and prohibits NLRP3 homotypic interactions and downstream signaling (Huang et al. 2018). It also showed protective effects in several NLRP3-driven inflammatory mouse models: gout, type 2 diabetes and CAPS. Being an FDA approved inhibitor it is promising to be able to apply Tranilast in NLRP3-associated inflammatory diseases, once further studies prove its effectiveness.

Another small molecule, CY-09, applied for the inhibition of CFTR, was shown to bind to the Walker A motif of NLRP3 and inhibit downstream signaling (Jiang et al. 2017). CY-09 showed NLRP3 inhibitory effects in mouse models and is being tested for human administration against NLRP3-driven inflammatory conditions.

The active β-sulfonyl nitrile, OLT1177, is in clinical testing for application in gouty arthritis. In the meantime, it was identified as an NLRP3 inhibitor (Marchetti et al. 2017). Similarly to CY-09, OLT1177 directly associates with NLRP3 and prevents ATP hydrolysis. It was shown to be effective in CAPS monocytes and was well tolerated in clinical trials.

Previously, oridonin, a herbal derivate, was brought into connection with anti-inflammatory activities via NLRP3 inhibition (H. He et al. 2018). Recently the molecular mechanisms could be deciphered: it binds the residue C279 in the NACHT domain covalently and prohibits NLRP3/Nek7 interaction. Thereby NLRP3 signaling is disturbed.

Even though the above-mentioned compounds may be promising as direct and specific NLRP3 inhibitors, more research is needed for the certainty of the effectiveness of these molecules in NLRP3 inflammasome restriction in humans.

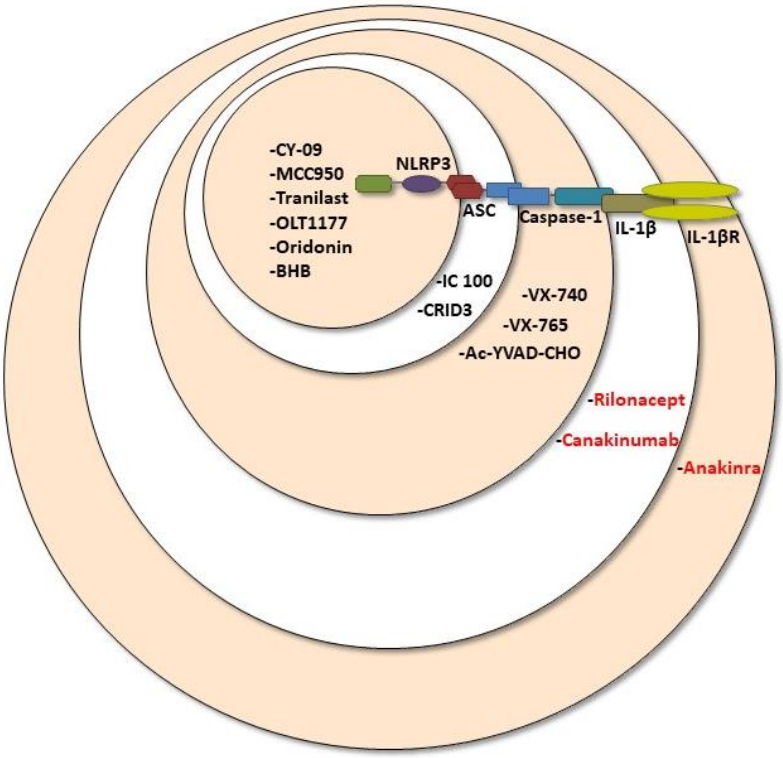

Figure 1.5. Schematic illustration of the inhibitors that might be applicable in NLRP3 inflammasome restriction.

Each circle represents a molecule-associated level of NLRP3 inflammasome assembly that could be targeted via multiple molecules. FDA-approved drugs are written in red. (Mangan et al. 2018), ZyVersa Therapeutics, (Coll and O'Neill 2011).

1.5. Bruton´s tyrosine kinase (BTK)

Bruton´s tyrosine kinase is a non-receptor tyrosine kinase predominantly expressed in B cells and myeloid cells (Mano 1999). In 1952, the pediatrician Bruton characterized a disease with periodic bacterial infections in male children caused by the lack of antibodies (BRUTON 1952). He successfully treated the patients with IgG administration (Ponader and Burger 2014). This condition was later brought into connection with mutations in the *BTK* gene, leading to dysfunctional BTK and an arrest in B cell maturation (see 1.5.2) (Vetrie et al. 1993). As BTK is encoded on the X chromosome, therefore the disease evocated by dysfunctional BTK was termed X-linked agammaglobulinemia (XLA) or Bruton´s agammaglobulinemia after its discoverer. Since then, the role of BTK in B cells has been extensively studied and its relevance gained even more attention after it had been identified as a potential target in B cell malignancies; and BTK inhibitors were established as a treatment in B cell lymphomas. Recently, the function of BTK in myeloid cells has also been researched.

1.5.1. The structure of BTK

The TEC family member BTK (besides TEC, ITK, BMX, RLK) is composed of five domains: an N-terminal PH domain followed by a TEC-homology domain (TH), two Src-homology domains SH2 and SH3, and a C-terminal kinase domain with catalytic activity (Mano 1999). The PH domain serves binding to membrane phospholipids of BTK. The TH domain of BTK is involved in the binding of BTK SH3 domain, thereby facilitating BTK/BTK interactions. The SH2 domain serves the recruitment of BTK to BLNK. The C-terminal domain holds effector functions. K430R mutation in the kinase domain leads to a catalytically dead BTK. The mutation R28C in the PH domain disrupts BTK´s ability to bind to membrane phospholipids, whereas the mutation E41K leads to increased phospholipid binding affinity (Z. Li et al. 1997).

Table 1.3. List of BTK mutations and functional defects.

Mutation site	Domain	Functional defect
R28C	PH	Membrane association impaired (Xid)
E41K	PH	Constitutively active
Y223F	SH3	Autophosphorylation impaired
K430R	Kinase	Kinase dead (KD)
Y551F	Kinase	Upstream phosphorylation impaired

1.5.2. BTK in B cell receptor signaling

Upon ligand binding, the cytosolic ITAM motif of the BCR is phosphorylated by the tyrosine kinases Syk and Lyn. Consequent to phosphorylation of the ITAM motif, recruitment of BLNK to the BCR is initiated, and BLNK and Syk interplay via SH2 homotypic interaction (Merolle et al. 2018). BLNK is then phosphorylated by Syk and functions as a scaffold protein for further recruitment of BTK and PLCγ2 via SH2 engagement. In parallel, CD19 associates with the BCR and Lyn phosphorylates the cytosolic CD19 to initiate PI3K binding via its SH2 domain (Merolle et al. 2018). PI3K then phosphorylates phosphatidylinositol 4,5 biphosphate (PIP_2) to phosphatidylinositol 3,4,5 triphosphate (PIP_3) at the plasma membrane, to which BTK and PLCγ2 are recruited via their PH domain. This interaction serves signal amplification and sustenance. BTK is activated via the phosphorylation of Y551 by Syk, whereupon the residue Y223 is auto-phosphorylated. Both BTK and Syk initiate downstream signaling by phosphorylating PLCγ2. PLCγ2 breaks down PIP_2 to DAG and IP_3. IP_3 serves for the increase of cytosolic Ca^{2+} concentrations, which results in both NFAT activation, a transcription factor of several genes, as well as PKC activation, which culminates NF-κB activation and proliferation resulting in survival of the B cell (Merolle et al. 2018).

1.5.3. BTK in innate immune signaling

The role of BTK in innate immune cell signaling became evident upon the observations that *Xid* mice (R28C mutation leading to impaired PIP3 binding and function of BTK, see above) were susceptible to multiple infections that pointed toward additional innate immune defects besides insufficient B cell maturation and antibody production (B. Ye et al. 2019; Weber et al.

2017). These observations indicated the function of BTK in TLR signaling that were experimentally confirmed. BTK transmits TLR signaling via connecting the adaptor molecule MyD88 with Mal, possibly by phosphorylating Mal (Gray et al. 2006). Besides TLR, BTK is involved in the TREM-1 receptor signaling as well as STING activation (Ormsby et al. 2011; Stadler et al. 2017). Furthermore, BTK was found to be fundamental in phagocytosis (Jongstra-Bilen et al. 2008; Weber et al. 2017). Nevertheless, immunosuppressive roles of BTK have also been observed in primary human innate cells manifesting in BTK-dependent decrease of cytokine release upon TLR engagement (Weber et al. 2017).

In mice, BTK dysfunction led to a decreased monocyte count yet increased granulocyte numbers, however, the granulocytes were immature (Melcher et al. 2008; Fiedler et al. 2011). Neutropenia has also been frequently observed in XLA patients. Additionally, increased ROS production was detected by XLA neutrophils, indicating a role of BTK in ROS repression (Honda et al. 2012). Furthermore, XLA patients showed longer coagulation times, and BTK was shown to be involved in GPVI signaling in platelets, which is crucial for blood coagulation (Rigg et al. 2016). In tumor macrophages, BTK activity led to tumor growth (Ping et al. 2017).

Taken together, BTK holds manifold functions in innate immune cells, and researchers have just recently begun to reveal the connections between the distinct cell types and the roles that BTK plays in their function.

1.5.4. BTK in B cell malignancies and BTK inhibition

As BTK is essential for B cell survival and maturation, B cells strongly rely on BTK-mediated signaling for propagation in the majority of B cell malignancies. BTK serves the constitutive signal transduction in the mature CLL B cells (Pal Singh, Dammeijer, and Hendriks 2018). In MCL B cells, increased phosphorylation of BTK Y233 has been detected, and BTK´s role in the retention of malignant B cells in the lymph nodes has been implied (Cinar et al. 2013). In Waldenström´s Macroglobulinemia, the oncogenic MyD88 L265P variant showed increased binding to phosphorylated BTK (G. Yang et al. 2013). Furthermore, BTK was shown to significantly contribute to tumor progression in follicular lymphoma, multiple myeloma, and marginal zone lymphoma (Pal Singh, Dammeijer, and Hendriks 2018). Consequent to these observations, BTK inhibition as strategy for B cell malignancy treatment has crystallized towards the early 2000s.

The small molecule ibrutinib binds covalently to the sulphur atom present in the C481 residue of BTK´s kinase domain and blocks the enzymatic function of BTK (Davids and Brown 2014). The phosphorylation of Y551 by Syk is not influenced by ibrutinib. *In vivo*, ibrutinib was first verified in mice and dogs in 2010 (Honigberg et al. 2010) and shortly thereafter in humans in 2013, whereupon it was approved by the FDA for therapy in CLL, MCL and WM (Advani et al. 2013). Ibrutinib is in Phase II studies for the application in additional B cell malignancies, such as FL and MCL (Kuo et al. 2017; Dreyling et al. 2016). Ibrutinib is applied orally.

Ibrutinib does not lead to tumor lysis syndrome, therefore a cytotoxic effect of BTK inhibition on B cells can possibly be precluded. It can be hypothesized that ibrutinib blocks integrin-dependent B cell accumulation in the lymph nodes, thus mobilized B cells die by "neglect" (Burger and Wiestner 2018; Pal Singh, Dammeijer, and Hendriks 2018). Ibrutinib holds no curative capacity, it is usually a life-long treatment (Pal Singh, Dammeijer, and Hendriks 2018). During the long therapy course, BTK often gains mutations that lead to ibrutinib resistance, such as C481S, and T316A (Woyach et al. 2014; Pal Singh, Dammeijer, and Hendriks 2018). Side-effects of ibrutinib include prolonged bleeding time due to low platelet counts, neutropenia, and therefore susceptibility to infections. Nevertheless, the side-effects rarely lead to therapy abortion. Ibrutinib is not highly specific to BTK, it inhibits other TEC-family kinases, as well as EGFR and JAK3 (Pal Singh, Dammeijer, and Hendriks 2018). Thus, more selective inhibitors are being developed, such as acalabrutinib (currently in phase III trial), BGB-3111, and Ono/GS-4059 (Pal Singh, Dammeijer, and Hendriks 2018). Ibrutinib is often applied in combination with chemotherapy, as circulating malignant B cells become available for cytotoxic agents. Furthermore, ibrutinib is also used for the treatment of chronic of graft vs. host disease after bone-marrow transplantation (Miklos et al. 2017).

1.5.5. BTK and the NLRP3 inflammasome

BTK was recently identified as a novel NLRP3 regulator by Ito et al. and the Weber group (Ito et al. 2015; Liu et al. 2017). It has been shown that BTK is rapidly (within minutes) phosphorylated upon nigericin treatment. Furthermore, BTK was shown to interact with the LRR and NACHT domains of NLRP3 in overexpression systems, and furthermore BTK binding to ASC was detected. BTK deficient human PBMCs (isolated from XLA patients) released reduced amounts of IL-1β, although TNFα production was not affected.

Similarly, murine BMDMs from *Btk* KO or Xid mice secreted decreased IL-1β. *In vivo*, ibrutinib treatment diminished brain damage in a brain ischemia model in mice.

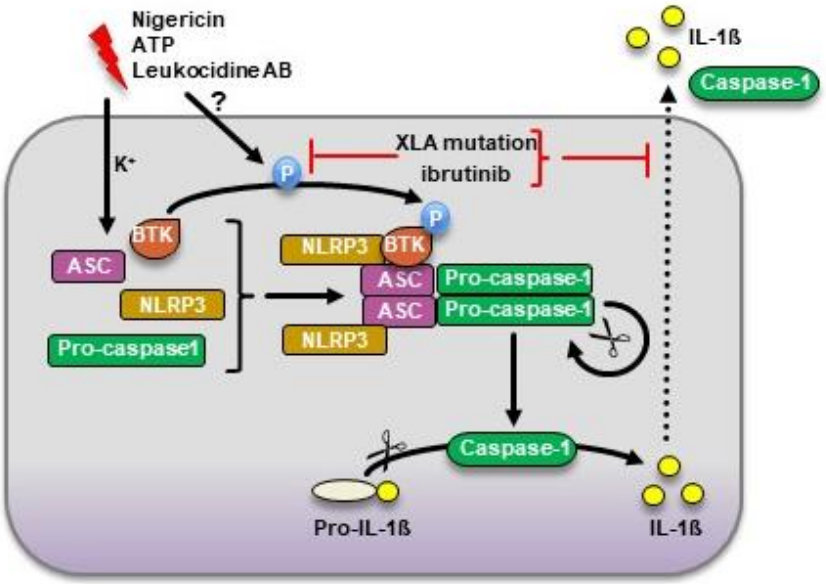

Figure 1.6. Graphical abstract of BTK´s role in NLRP3 inflammasome activation.

It was previously shown that BTK interacts with NLRP3 and ASC, and genetic ablation or inhibition of BTK´s kinase activity impaired IL-1β production. Figure modified from (Liu et al. 2017).

1.6. Aim of the study

As described above, BTK was validated as a positive regulator of the NLRP3 inflammasome in human and murine monocytes and macrophages (Ito et al. 2015; Liu et al. 2017). However, the exact regulatory mechanism remained elusive. Even though BTK was found to be phosphorylated upon nigericin treatment, which would imply induction of its enzymatic activity, the role of BTK as a kinase was not elucidated and scaffold functions in NLRP3 activation were hypothesized.

In this work, the molecular mechanisms by which BTK regulates the NLRP3 inflammasome were studied:

1) Is NLRP3 a direct substrate of BTK?
2) If NLRP3 proves to be a substrate of BTK, which tyrosine residue is modified?
3) What are the mechanistic consequences of tyrosine phosphorylation of NLRP3 in terms of inflammasome activation?

These questions were addressed using multiple cell-based, *in vitro*, and biochemical approaches.

2. METHODS

2.1. Chemicals and reagents

Table 2.1. List of chemicals and reagents.

Reagent	Company	Product nr
Acalabrutinib	Selleckchem	S8116
AceGlow™ substrate	Peqlab	730-1511
Agar-Agar	Roth	22662
Ampicillin sodium salt	Sigma	A9518
Ampuwa	Fresenius Kabi	1833
ATP	Sigma	A6419-1G
Bovine serum albumin (BSA)	Biomol	01400.100
$CaCl_2 \cdot 2H_2O$	AppliChem	A3587
Chloroform	Sigma Aldrich	288306
DMEM	Sigma-Aldrich	D5796
Dimethyl sulfoxide (DMSO)	Sigma-Aldrich	D2650
Disuccinimidyl suberate (DSS)	ThermoFisher	21555
Ethylenediaminetetraacetic acid (EDTA) pH=8	ThermoFisher	15575020
Fetal calv serum (FCS)	TH-Geyer	11682258
Ficoll/Biocoll	Biochrom	ab211650
Glycerol	AppliChem	A2926
HEPES	Roth	6763.2
Ibrutinib	Selleckchem	S2680
Kanamycin disulfate salt	Sigma	K1876
KCl	Roth	6781.1
λ-Phosphatase	NEB	P0753S
LB-Broth	Sigma	L3022
L-Glutamine	Gibco	25030081
LDS sample buffer	Invitrogen	NP0008
LPS-EK	InvivoGen	Tlrl-peklps
MCC950	Cayman Chemicals	Cay17510-1
Methanol	VWR	20847.307
$MgCl_2$	Roth	A537.1
Milk powder	Roth	T145.3
Native running buffer	Invitrogen	LC2673
Native sample buffer	Novex (LifeTechnologies)	LC2673
Nigericin	Invivogen	tlrl-nig
Nitrocellulose membrane	GE Healthcare	15259794
NP-40	Sigma-Aldrich	I8896
PageRulerTM protein marker	ThermoFisher	26616
Phosphate buffered saline (PBS)	Thermo Fisher	14190-169
PhosStop	Roche	04906 837 001
Precast Gels (NuPage Bis-tris 4-12%)	Invitrogen	NP0329BOX
Precast Gels (NuPage Tris-acetate 3-8%)	Invitrogen	EA03752BOX
Protease Inhibitor	Roche	4693159001
Reducing Agent	Invitrogen	NP0009
Running Buffer	Thermo Fisher	NP0001
RNase/DNase free water	Thermo Fisher	10977049
RPMI	Sigma-Aldrich	R8758
Sodium dodecyl sulfate (SDS)	Applichem	A7249,1000

Sodium chloride	VWR	27810.295
Sodium-deoxycholate	Sigma-Aldrich	D6750
Sodium phosphate dibasic dihydrate	Sigma-Aldrich	30412
Sucrose	Sigma-Aldrich	16104
Transfer buffer	Thermo Fisher	NP0006
Triton X-100	AppliChem	A1388
Tris-HCl	Sigma-Aldrich	T5941
Trizima® Base, ≥ 99,9%	Sigma-Aldrich	1002210470
Trypan Blue Solution	Sigma-Aldrich	T8154
Trypsin	ThermoFisher	25300096
Tween® 20	Sigma-Aldrich	P7949

All chemicals were of purity ≥ 98% unless stated otherwise.

2.2. Materials

Table 2.2. List of materials.

Equipment	Company	Product nr
Agar plates	Greiner	632161
Cell scraper	Corning Incorporated	3010
Cell strainer	Greiner	542040
ELISA (human IL-1β)	Biolegend	437004
ELISA (murine IL-1 β)	R&D Technologies	DY401-05
ELISA (human TNFα)	Biolegend	430204
ELISA (murine TNFα)	Biolegend	430904
Eppendorf cups	Greiner	616201
Falcon tubes (15 ml)	Greiner	188271
Falcon tubes (50 ml)	Greiner	227261
Needles (27 G)	BD	305136
Pasteur pipette	VWR	414004-616
Revolve Microscope	ECHO	FJSD2001
U-bottom 96 well plates	Greiner	650101
V-bottom 96 well plates	Greiner	651101
½ Area flat bottom ELISA plates	Greiner	675061
6-well plates	Greiner	657160
24-well plates	Greiner	662160
6 cml cell-culture dishes	Greiner	628160
10 cm cell-culture dishes	Greiner	664160
10 ml syringes	BD	305959

2.3. Mice

Mice (*Btk* KO, C57BL6 Btk^{tm1wk}, *NLRP3* KO (Jackson stock No: 021302), and wild type C57BL/6J (Jackson) were maintained in a pathogen-free environment with regular hygene monitoring, according to the institutional guidelines of the Immunology Department in Tübingen. Mice were sacrificed using CO_2 followed by cervical dislocation.

2.4. Human blood sampling

This study was approved by the local ethics committees. Subjects were informed and provided a written agreement prior their contribution to the study. XLA patient samples were provided by the Center for Immunodeficiency at Freiburg University Hospital. Blood from age- and sex-matched healthy donors was drawn at the Immunology Department in Tübingen by physicians. CAPS patient samples were collected at the Pediatrics Department of the University Hospital in Tübingen.

2.5. Software

Table 2.3. List of software.

Software	Version
Compass for SW	
Fusion SL	
Geneious	6.1.
GraphPad Prism	8
Mendeley	
Microsoft Office	365
Pymol	2.3.1.

2.6. Primers and plasmids

Table 2.4. List of mutagenesis primers. All primers were synthetized by Biomers.

Mutation	Plasmid ID	Backbone	Primer ID	Primer sequence
Y84F	pZsB035	pTP074	AWm591NLRP3Y84Ffwd	GATCAACAGGAGAGACCTTTTTGAGAAAGCAAAAAGAGATGAGCC
			AWm592NLRP3Y84Frvs	GGCTCATCTCTTTTTGCTTTCTCAAAAAGGTCTCTCCTGTTGATC
Y123F	pZsB036	pTP074	AWm593NLRP3Y123Ffwd	GGAGTGGATGGGTTTACTGGAGTTCCTTTCGAGAATCTC
			AWm594NLRP3Y123Frvs	GAGATTCTCGAAAGGAACTCCAGTAAACCCATCCACTCC
Y136F	pZsB037	pTP074	AWm595NLRP3Y136Ffwd	GAAGAAAGATTTCCGTAAGAAGTACAGAAAGTACGTGAGAAGC
			AWm596NLRP3Y136Frvs	GCTTCTCACGTACTTTCTGTACTTCTTACGGAAATCTTTCTTC
Y140F	pZsB038	pTP074	AWm597NLRP3Y140Ffwd	CCGTAAGAAGTTCAGAAAGTACGTGAGAAGCAGATTCCAG
			AWm598NLRP3Y140Frev	CTGGAATCTGCTTCTCACGTACTTTCTGAACTTCTTACGG
Y143F	pZsB039	pTP074	AWm599NLRP3Y143Ffwd	CCGTAAGAAGTACAGAAAGTTCGTGAGAAGCAGATTCCAG
			AWm600NLRP3Y143Frev	CTGGAATCTGCTTCTCACGAACTTTCTGTACTTCTTACGG
Y168F	pZsB040	pTP074	AWm601NLRP3Y168Ffwd	GCCTCAACAAACGCTTCACACGACTGCGTCTCATCAAGG
			AWm602NLRP3Y168Frev	CCTTGATGAGACGCAGTCGTGTGAAGCGTTTGTTGAGGC
Y140FY143F	pZsB041	pTP074	AWm603NLRP3Y140FY143Ffwd	CCGTAAGAAGTTCAGAAAGTTCGTGAGAAGCAGATTCCAGTGC
			AWm604NLRP3Y140FY143Frev	GCACTGGAATCTGCTTCTCACGAACTTTCTGAACTTCTTACGG

Mutation	Plasmid ID	Backbone	Primer ID	Primer sequence
Y136FY140FY143F	pZsB054	pTP074	AWm607NLRP3Y136FY140FY143Ffwd	GAAGAAAGATTTCCGTAAGAAGTTCAGAAAGTTCGTGAGAAGCAGATTCC
			AWm608NLRP3Y136FY140FY143Frev	GGAATCTGCTTCTCACGAACTTTCTGAACTTCTTACGGAAATCTTTCTTC
Y249F	pZsB024	pTP074	AWm573NLRP3Y249Ffwd	GGCATCGGGGACACTCTTCCAAGACAGGTTTGAC
			AWm574NLRP3Y249Frvs	GTCAAACCTGTCTTGGAAGAGTGTCCCCGATGCC
Y258F	pZsB025	pTP074	AWm577NLRPY258Ffwd	CCAAGACAGGTTTGACTATCTGTTCTTTATCCACTGTCGGG
			AWm578NLRP3Y258Frvs	CCCGACAGTGGATAAAGAACAGATAGTCAAACCTGTCTTGG
Y381F	pZsB026	pTP074	AWm579NLRP3Y381Ffwd	GGCCAAAAGGAAAGAGTTCTTCTTCAAGTACTTCTCTGATGAGGCCC
			AWm580NLRP3Y381Frvs	GGGCCTCATCAGAGAAGTACTTGAAGAAGAACTCTTTCCTTTTGGCC
Y385F	pZsB030	pTP074	AWm581NLRP3Y385Ffwd	GGCCAAAAGGAAAGAGTACTTCTTCAAGTTCTTCTCTGATGAGGCCC
			AWm581NLRP3Y385Ffwd	GGGCCTCATCAGAGAAGAACTTGAAGAAGTACTCTTTCCTTTTGGCC
Y443F	pZsB018	pTP074	AWm567NLRP3Y443Ffwd	CCACCACCGCGGTGTTCGTCTTCTTCCTTTCC
			AWm568NLRP3Y443Frvs	GGAAAGGAAGAAGACGAACACCGCGGTGGTGG
Y518F	pZsB027	pTP074	AWm587NLRP3Y518Ffwd	GGAAGTGGACTGCGAGAAGTTCTTCAGCTTCATCCACATG
			AWm588NLRp3Y518Frvs	CATGTGGATGAAGCTGAAGAACTTCTCGCAGTCCACTTCC
Y533F	pZsB028	pTP074	AWm583NLRP4Y533Ffwd	CCAGGAGTTCTTTGCCGCCATGTTCTACCTGCTGGAAGAGG
			AWm584NLRP3Y533Frvs	CCTCTTCCAGCAGGTAGAACATGGCGGCAAAGAACTCCTGG
Y534F	pZsB029	pTP074	AWm585NLRP3Y534Ffwd	CCAGGAGTTCTTTGCCGCCATGTACTTCCTGCTGGAAGAGG
			AWm586NLRP3Y534Frvs	CCTCTTCCAGCAGGAAGTACATGGCGGCAAAGAACTCCTGG

Table 2.5. Table of additional plasmids.

Insert	Plasmid ID	Features	Gateway compatible
hBTK WT	pOW166	N-terminal Flag-tag	No
hBTK R28C	pOW167	N-terminal Flag-tag	No
hBTK E41K	pOW168	N-terminal Flag-tag	No
hBTK Y223F	pOW169	N-terminal Flag-tag	No
hBTK K430R	pOW170	N-terminal Flag-tag	No
hBTK Y551F	pOW171	N-terminal Flag-tag	No
hPYD	pEx342	N-terminal Flag-tag	No
hlinkerNACHT (AA80-536)	pEx434	N-terminal Flag-tag	No
hLRR (AA537-991)	pEx344	N-terminal Flag-tag	No
hNLRP3	pTP074	N-terminal HA tag	Yes
hLinker (AA80-220) WT	pZsB048	C-terminal HA tag, C-terminal m-Citrine	Yes
hLinker (AA80-220) Y136EY140EY143EY168E	pZsB049	C-terminal HA tag, C-terminal m-Citrine	Yes
hLinker (AA80-220) Y136FY140FY143FY168F	pZsB050	C-terminal HA tag, C-terminal m-Citrine	Yes
mPolybasicRegion (AA127-146) WT	pZsB074	N-terminal Flag tag C-terminal GFP	Yes
mPolybasicRegion (AA127-146) Y>E	pZsB075	N-terminal Flag tag C-terminal GFP	Yes
mPolybasicRegion (AA127-146) Y>F	pZsB076	N-terminal Flag tag C-terminal GFP	Yes
mPolybasicRegion (AA127-146) K>A	pZsB077	N-terminal Flag tag C-terminal GFP	Yes

2.7. Antibodies

Table 2.6. List of antibodies for immunoblot.

Specificity	Species	Company	Product nr	Dissolvent (o.n. at 4°C)
ASC	Rabbit	CST	#67824	5% BSA in TBS-T
hBTK	Mouse	BD	611117	5% BSA in TBS-T
mBTK *	Rabbit	CST	#8547	5% BSA in TBS-T
mCaspase-1	Rabbit	CST	#3866	5% BSA in TBS-T
Citrate synthetase	Rabbit	GeneTex	GTX110624	5% BSA in TBS-T
Flag	Mouse	Sigma-Aldrich	F1804	5% milk in TBS-T
GAPDH	Mouse	Thermo-Fisher	#MA5-15378	5% BSA in TBS-T
HA	Rabbit	CST	#3724	5% BSA in TBS-T
hIL-1β	Mouse	R&D Systems	MAB601	5% milk in TBS-T
mIL-1 β	Mouse	CST	#12242	5% BSA in TBS-T
Isotype control *	Rabbit	CST	#3900	Only for IP
hNLRP3 *	Rabbit	CST	#15101	5% BSA in TBS-T
mNLRP3	Mouse	Adipogen	AG-20B-0014-C100	5% BSA in TBS-T
p-Y-Multimab 1000 *	Rabbit	CST	#8954	5% BSA in TBS-T

All antibodies for immunoblot (IB) were used in 1:1000 dilution. *: used for IP in 1:200.

Specificity	Species	Company	Product nr	Dissolvent (1h at RT)
Anti-Mouse IgG (H+L) HRP conjugate		Promega	W4021	5% milk in TBS-T
Anti-Rabbit IgG (H+L) HRP conjugate	Goat	Vector	PI-1000	5% milk in TBS-T
VeriBlot for IP Detection Reagent (HRP)		Abcam	Ab131366	5% milk in TBS-T

Secondary antibodies were used in 1:5000 dilution.

2.8. Peptides

Table 2.7. List of peptides.

Human tyrosine	Sequence	Modification	Manufacturer
Y84	AINRRDLYEKAKRDE	None	In house
Y123	EWMGLLEYLSRISIC	None	In house
Y136Y140Y143	ICKMKKDYRKKYRKY	None	In house
Y136Y140Y143	KKDYRKKYRKYVRSR	None	In house
Y136Y140Y143	YRKKYRKYVRSRFQC	None	In house
Y136	KKDYRKKFRKFVRSR	None	In house
Y140	ICKMKKDFRKKYRKF	None	In house
Y143	FRKKFRKYVRSRFQC	None	In house
Y168	SVSLNKRYTRLRLIK	None	In house
Y249	DWASGTLYQDRFDYL	None	In house
Y255	LYQDRFDYLFYIHCR	None	In house
Y258	DRFDYLFYIHCREVS	None	In house
Y381	SEAKRKEYFFKYFSD	None	In house
Y385	RKEYFFKYFSDEAQA	None	In house
Y443	SKTTTAVYVFFLSSL	None	In house
Y518	EVDCEKFYSFIHMTF	None	In house
Y533Y534	QEFFAAMYYLLEEEK	None	In house
Y136	KKDYRKKFRKFVRSR	Y140F, Y143F	In house
Y140	ICKMKKDFRKKYRKF	Y136F, Y143F	In house
Y143	FRKKFRKYVRSRFQC	Y136FY140F	In house
Y136Y140Y143	KKDFRKKFRKFVRSR	Y136FY140FY143F	In house
Y168	SVSLNKRFTRLRLIK	Y168F	In house

Murine tyrosine	Sequence	Modification	Manufacturer
Y132	ICKKKKDYCKMFRRH	Y136F	In house
Y136	KKDFCKMYRRHVRSR	Y132F	In house
Y144	RHVRSRFYSIKDRNA	None	In house
Y164	SVDLNSRYTQLQLVK	None	In house

2.9. Buffers and solutions

Table 2.8. List of buffers and solutions.

Buffer	Recipe
2 M $CaCl_2$	14.72 g $CaCl_2x2H_2O$
2x HBS	11.92 g HEPES 37.28 g KCl 9.01 g Glucose 14.61 g NaCl 3.56 g Na_2HPO_4
LB medium	20 mg/l LB Broth in ddH_2O
2x RIPA lysis buffer	2.4 g Trisma base pH 7.4 8.8 g NaCl 10 ml Triton-X-100 5 g Sodium deoxycholate 1 g SDS 100 ml Glycerol Fill up to 500 ml with ddH_2O
2x native RIPA lysis buffer	2.4 g Trisma base pH 7.4 8.8 g NaCl 10 ml Triton-X-100 5 g Sodium deoxycholate 100 ml Glycerol Fill up to 500 ml with ddH_2O
20x TBS	121 g Tris HCl 175.2 g NaCl Fill up to 1 L with ddH_2O
TBS-T	0.1% Tween-20 in TBS

2.10. Microbiological Methods

2.10.1. Gateway cloning

The Gateway cloning technology was developed by Invitrogen from the early 90s to establish an efficient system where inserts can easily be exchanged restriction/ligation-independently between expression vectors while making sure that the reading frame is sustained (ThermoFisher Scientific). It is composed of a pool of entry, donor, and expression vectors that carry so-called “att” sites. Specific restriction enzymes (BP and LR clonase) recognize att sites and exchange the att-flanked inserts between two backbones that take place in a reaction.

Principally, the following reactions can take place: first, a Gateway compatible plasmid is generated, in which the insert is flanked between attB1 (5´) and attB2 (3´) sites. Insert of this plasmid can be easily moved into a donor vector, carrying attP1 (5´) and attP2 (3´) sites, using the enzyme mix BP clonase. Upon “BP reaction”, the insert of the attB bearing plasmid is inserted between the att sites of the donor vector, while the donor attP sites are transformed into attL sites. The plasmid carrying the gene of interest flanked by attL sites is then called an

entry vector. To generate an expression vector, the entry vector can be further used in an "LR reaction" together with a destination vector (attR sites) and the LR clonase.

As a result of the LR reaction, the insert is added into the destination vector, whereupon the attR sites are transformed to attB sites, and the end-product is called an expression vector. During the LR reaction, the entry vector is turned into a donor vector, carrying attP sites.

All LR (ThermoFisher 11791020) and BP (ThermoFisher 11789020) reactions were conducted according to the manufacturer´s protocol.

2.10.2. Site-directed mutagenesis

To generate the Y to F mutants, site-directed mutagenesis was performed. Site-directed mutagenesis is a PCR reaction using primers that are mis-matched with the template DNA (see table 2.4.), resulting in the desired altered amino-acid at the site of the nucleotide mis-match. Site-directed mutagenesis reactions were conducted using the QuikChange II Site-Directed MutagenesisKit (#200524) from Agilent Technologies according to the manufacturer´s protocols. In brief, the following PCR reaction was pipetted:

5 µl of 10× reaction buffer
10 ng of dsDNA template
125 ng of oligonucleotide primer #1
125 ng of oligonucleotide primer #2
1 µl of dNTP mix

The reaction was filled up to 50 µl volume with dH_2O. Then, 1 µl of PfuUltra HF DNA polymerase (2.5 U/µl) was added and the following PCR protocol was set:

Table 2.9. Site-directed mutagenesis PCR reaction.

Segment	Cycles	Temperature	Time
1	1	95°C	30 s
2	18	95°C	30 s
		55°C	1 min
		68°C	9 min 30 s

The PCR reaction was followed by digestion of the original plasmid by addition of 1 µl *Dpn* I for 1 h at 37°C. The enzyme *Dpn* I digests only methylated DNA, such as the original plasmid

that was produced by bacteria (dam^+) and therefore methylated, and not the desired mutated PCR products.

After *Dpn* I digestion, the PCR products were transformed into XL-Gold ultracompetent cells (provided by the mutagenesis kit). The bacteria were used for plasmid production, and plasmid purification, see 2.11.1.

2.10.3. Bacteria transformation

Plasmid DNA was transformed into bacteria using heat-pulse technique. In brief, 45 µl of the bacteria strain was aliquoted to a pre-chilled 14 ml Falcon tube (#14-959-10B). 2 µl of plasmid DNA was added to the bacteria and incubated for 30 min on ice. The bacteria were then heat-pulsed in a water bath at 42°C for 30 s and immediately placed on ice for another 2 min Next, 250 µl culture media (LB or NZY^+ in case of XL-Gold cells) was added to the cells and the tubes were incubated at 37°C for 1 h. The cells were then plated on agar plates (15 g/l Agar-Agar in LB medium and incubated at 37°C over-night.

2.11. Molecular-biological Methods

2.11.1. Plasmid isolation

Plasmid isolation was conducted using 250 ml bacteria culture for midi or 5 ml bacteria culture for mini preparation using PureYield™ Plasmid midi (A2492) or miniprep (A1222) kits (Promega) according to the manufacturer´s instructions. The bacteria were cultured in LB medium supplemented with 0.1 % antibiotics and shaken at 125 rpm over night at 37°C. From the bacteria culture glycerol stock were prepared by adding 850 µl bacteria culture to 150 µl glycerol. Isolated plasmid concentration and purity was measured using NanoDrop from Thermo Scientific.

2.11.2. DNA sequencing

DNA sequencing was conducted by Eurofins (previously GATC). Samples were submitted as required (5 µl of 100 ng/µl plasmid DNA mixed with 5 µl of 5 nmol/µl primer for light run,

and 20 µl of 100 ng/µl plasmid DNA for supreme run). Plasmid maps and sequence alignments were analyzed using Geneious 6.1.

2.12. Cell culture

2.12.1. Culture of HEK293T cells

HEK293T cells were cultured in DMEM media supplemented with 10% FCS, 1% Pen/Strep and 1% L-Glutamine. Cells were detached using Trypsin and seeded in 10^5/ml concentration one day prior to the experiment.

2.12.2. Plasmid transfection

HEK293T cells were transfected using the calcium-phosphate precipitation method. Briefly, plasmids were diluted in ddH_2O to the desired concentration, together with $CaCl_2$ to a 0.12 M end-concentration. Then 2x HBS was added to the plasmids and incubated for 20 min on RT before adding the plasmid mix to the cells. The transfected cells were harvested 2 days after transfection.

2.12.3. BMDM generation and NLRP3 inflammasome activation

Mice were sacrificed and tibia and femur were separated and cleaned from muscle tissues using forceps and scissors. The ends of the bones were cut open and bone marrow cells were flushed out of the bones using a 27G needle, 10 ml syringe and RPMI media supplemented with 10% FCS. Cells were filtered through a cell strainer, centrifuged at 400 x g for 5 min, resuspended in RPMI media supplemented with 10% FCS, 10% murine GM-CSF, 1% pen/strep and 1% L-Gln to a concentration of 3 x 10^6/ml cells, and seeded in either 6-well plates (2 ml/well) or 10 cm agar plates (10 ml/plate). Fresh media was added to the cells every second to third day. On day 7, cells were washed once with cold PBS, incubated in fresh cold PBS for 10 min at 4°C, and carefully detached using the head of a plastic Pasteur pipette. Cells were then collected, counted, and re-seeded at 10^6/ml concentration in RPMI media supplemented with 10% FCS, 1% pen/strep and 1% L-Gln. The cells were stimulated immediately or the next day.

For IL-1β release, BMDMs were primed with 100 ng/ml LPS for 3 hours and treated with 5 µM nigericin for 2 hours (added directly or in 500 µl opti-MEM for protein precipitation). The supernatant was taken off for ELISA or protein precipitation, and cells were lysed in complete RIPA lysis buffer for intracellular IL-1β measurement via immunoblot.

For NLRP3 phosphorylation, cells (4-6 x 10^6) were primed with 100 ng/ml LPS for 3 hours and then stimulated with 5 µM nigericin added to the media for 5 min, 10 min, and 20 min. Cells were then washed once with ice-cold PBS and were lysed in RIPA buffer. Cleared lysates were used for further analysis.

2.12.4. PBMC culture and NLRP3 inflammasome activation

PBMCs were isolated from whole blood using Ficoll density gradient centrifugation. In short, whole blood was diluted 1:1 in PBS and 20 ml diluted blood was carefully loaded on 20 ml of Ficoll (1.077 g/ml) in a 50 ml Falcon tube. The tube was centrifuged at 500 g for 25 min without brake. The PBMC layer was carefully sucked up using a Pasteur pipette, cells were washed three times in PBS (645 x g for 8 min, 448 x g for 8 min, and 241 x g for 8 min), counted, and seeded in 10^6/ml concentration in full RPMI media (10% FCS, 1% pen/strep, 1% L-Gln). Cells were immediately stimulated.

For IL-1β release, PBMCs were primed with 10 ng/ml LPS for 3 h, and stimulated with 15 µM nigericin, (either added directly or by replacement of the media with 500 µl opti-MEM supplemented with nigericin for protein precipitation) for 1 h. For NLRP3 phosphorylation assessment, cells (8-10 x 10^6) were primed the same way and stimulated for 5 min, 10 min or 20 min with 15 µM nigericin. Cells were then washed once with PBS and lysed in RIPA lysis buffer.

2.13. Analytical Methods

2.13.1. SDS-PAGE and Immunoblot

1x LDS loading dye and 1x reducing agent were added to the cleared lysates and boiled for 5 min at 95°C. The samples were then shortly centrifuged and 15-20 µl of the lysates were loaded into individual wells of an SDS gel (precast NuPage 4-12% from Thermo Fisher) and

run with constant voltage (140V) for 1.5 h, using NuPage MOPS SDS running buffer. The proteins were then transferred to a pre-wet nitrocellulose membrane using semi-dry transfer method at 25 A for 47 min with NuPage transfer buffer and 20% methanol. The membrane was then blocked in 5% BSA or 5% milk in TBS-T (according to the diluent of the primary antibody) for 1 h at RT. The membrane was then incubated in 4 ml of primary antibody solution in a 50 ml Falcon at 4°C over-night. The next morning, the membrane was washed 3x5 min in TBS-T, and the secondary antibody in 5% milk in TBS-T was added for 1 h at RT. The membrane was finally washed 3x5 min in TBS-T and exposed using AceGlow™-Solution A and B (1:1) with the CCD camera FUSION SL. The bands were analysed and quantified using the program FUSION.

2.13.2. WES capillary electrophoresis

Lysates that were analyzed via conventional immunoblot were analyzed using the ProteinSimple WES machine. 3 µl of the lysates were pipetted into the WES Separation 12-230 kDa module (#SM-W004) together with the standard pack (PS-ST01-08) and run on the WES according to the manufacturer´s instructions. The results were analyzed using Compass for SW software.

2.13.3. Immunoprecipitation (IP) and Co-IP

Cleared lysates (750 µl from HEK293T cells, 250 µl from BMDMs and PBMCs) were supplemented with antibodies against endogenous proteins (p-Y 1:200, NLRP3 CST 1:200, see table 2.6.) and incubated over-night at 4°C while rotating. The next day, 20 µl/sample Dynabeads™ Protein G for Immunoprecipitation (#10003D) from Invitrogen were washed three times in 500 µl RIPA and added to the lysates for 1.5 h at 4°C with rotation. The protein-bound beads were washed 3x8 min in 500 µl RIPA and finally resuspended in 50 µl of IP sample buffer (2x LDS and 2x reducing agent), boiled for 7 min at 95°C to detach proteins from the beads, shortly centrifuged, and bead-free supernatant was loaded onto SDS gel for immunoblot analysis (see 2.13.1.).

In case of recombinant proteins, 30 µl/samplemagnetic-beads (Pierce™ Anti-HA Magnetic Beads, 88836; or Thermo Fisher; Anti-FLAG® M2 Magnetic Beads, M8823, Merck) were washed 3x with 500 µl RIPA buffer and added to 750 µl the cleared HEK293T cell lysates

(see above) for 3-4 h with rotation at 4°C. Beads were then washed 3 x 8 min in RIPA buffer and finally the beads were resuspended in 50 µl IP sample buffer, boiled for 7 min at 95°C, stored on -20°C or loaded immediately on the SDS gel.

2.13.4. Native PAGE

For native PAGE, cells were lysed in RIPA lysis buffer that did not contain SDS. Lysates were centrifuged at 2.300 x g for 10 min to pellet DNA. The supernatant was then centrifuged at 16.100 x g for 25 min and the pellet was resuspended in 1x NativePAGE sample buffer (Thermo Fisher, BN2003). The samples were loaded onto NuPage 3-8% Tris-Acetate gels (Thermo Fisher, EA0375BOX) without boiling and native PAGE was conducted using Tris-Glycine running buffer (Thermo Fisher, LC26754). The gel was soaked in 10% SDS solution for 10 min before performing semi-dry transfer and continuing with conventional immunoblot (2.13.1.).

2.13.5. Protein cross-linking for Co-IP

BMDMs were primed with 100 ng/µl LPS and treated with 60 µM ibrutinib and 15 µM nigericin. Cells were lysed in RIPA lysis buffer and pellets were cross-linked using DSS and analyzed as described in (Khare et al. 2016). Briefly, 4 x 10^6/ml mio BMDMs/condition were primed with 100 ng/ml LPS for 3 h and stimulated with 5 µM nigericin for 45 min Cells were then washed once with 2 ml PBS and lysed in 500 µl RIPA buffer. The lysate was then centrifuged at 2.300 x g for 10 min at 4°C. The supernatant was taken off and the pellet was resuspended in 500 µl PBS. 2 mM DSS was added to the supernatant and the resuspended pellet, which were incubated for 30 min at RT while rotating. The samples were then centrifuged at 2.300 x g for 10 min at 4°C. The pellets were quenched with 40 µl LDS sample buffer, boiled for 5 min at 95°C and analyzed via immunoblot.

2.13.6. Protein precipitation for immunoblot

500 µl opti-MEM supernatant of 10^6/ml stimulated cells was precipitated using methanol and chloroform. Briefly, 500 µl methanol and 125 µl chloroform was added to the supernatant

and vortexed for 15 s. The mixture was then centrifuged at 16.000x g for 3 min at 4°C. The protein layer at the methanol/chloroform interface was washed once with 500 µl methanol and centrifuged again as in the previous step. The protein pellet was then resuspended in 50 µl 1x LDS and 1x reducing agent loading buffer, boiled for 5 min at 95°C and analyzed via immunoblot.

2.13.7. Size-exclusion chromatography

BMDMs were stimulated and lysed in 50 mM Tris-HCl pH 7.4, 1% NP-40, and 150 mM NaCl. 100 µl cleared lysate was loaded on an equilibrated Superdex 200 Increase 10/300 GL (GE Healthcare) column and proteins were eluted using ÄKTA Purifier (GE Healthcare) and buffer containing 50 mM Tris-HCl pH 7.4 and 150 mM NaCl with 0.25 ml/min flow. 200 µl fractions were collected and analyzed via immunoblot.

2.13.8. Enzyme-linked immunosorbent assay (ELISA)

IL-1β and TNFα concentrations in supernatants were measured using sandwich ELISA kits, according to the manufacturer´s instructions.

2.13.9. *In vitro* kinase assay

For the verification that NLRP3 is a substrate of BTK, recombinant NLRP3 from Novus Biologicals **(**H00114548-P01) and BTK from Sino Biological (10578-H08B) or Abcam (ab205800) were incubate at 30°C for 3 hours using 1x CST kinase buffer (#9802) in the presence of 2 mM ATP. As a negative control, recombinant Posi-Tag Epitope Tag Protein (Biolegend, 931301) was used. Before- and after kinase assay-samples were boiled and analyzed via SDS PAGE and immunoblot.

To find the tyrosine residues phosphorylated by BTK, NLRP3 15mer synthetized peptides carrying a Y residue in the middle (see table 2.7.) were incubated with recombinant BTK (Sino Biologicals #10578-H08B) for 3 h in CST kinase buffer supplemented with 2 mM ATP. Next, the samples were boiled and anti-His magnetic beads (Dynabeads™ His-Tag Isolation and Pulldown, 10104D, Thermo Fisher) were added to deplete the samples of phosphorylated

BTK. The samples were cleared from the magnetic beads and the supernatants were manually spotted on a nitrocellulose membrane. The dried spots were stained using the Pierce reversible protein stain (24580) to visualize total peptide amounts. The membrane was then blocked with 5% BSA in TBS-T and conventional anti-phospho-Tyrosine primary and secondary antibody incubation steps followed.

2.13.10. Subcellular fractionation

BMDMs were homogenized using 10 ml syringe and 27 G x 19 mm needles in homogenization buffer (0.25 M sucrose, 10 mM Tris HCl (pH 7.5), 10 mM KCl, 1.5 mM $MgCl_2$, protease inhibitor and PhosStop). Homogenized cells were centrifuged at 1000 x g for 5 min to remove nucleus. The supernatant was centrifuged at 5000 x g for 10 min to obtain heavy membrane fraction (pellet, P5). The supernatant was centrifuged 100.000 x g for 20 min to separate light membrane fraction (P100) from the cytosol (S100). P5 and P100 were washed once with homogenization buffer and then used for sucrose gradient ultracentrifugation, separately. For sucrose gradient ultracentrifugation, a continuous 15-45% (w/w) sucrose gradient was prepared in 10 mM Tris-HCl (pH 7.5), 20 mM KCl, and 3 mM $MgCl_2$ using a Biocomp Gradient Station (Biocomp Instruments, Fredricton, NB, Canada). P5 or P100 was loaded on top of the gradient and centrifuged at 170.000 x g for 3 h. The gradient was fractionated into 12 fractions of 1.1 ml using the fraction collector module of a Biocomp Gradient Station. Protein content of each fraction was analyzed via immunoblot.

2.13.11. PI4P bead IP

HEK293T cells were transfected with HA-tagged human WT or Y>E PYD/NACHT linker (AA94-219). Cells were lysed in 500 µl RIPA and 45 µl PI4P (Echelon Biosciences, P-B004A) or same amount of control beads (Echelon Biosciences, P-B000) were added to cleared lysates and incubated for 1.5 h on 4°C while rotating. Beads were then washed 3 times with RIPA, boiled and bound proteins were analyzed via immunoblot. Alternatively, cells were transfected with WT, Y>E or K>A Flag-tagged murine polybasic region (AA127-146). PI4P beads or control beads were blocked in 2% BSA, 0.5% NP-40 and 200 µg/ml Flag peptide (Sigma-Aldrich, F3290) for 2 h on 4°C. Transfected cells were then lysed in 500 µl

RIPA and the expressed proteins were purified using Anti-FLAG® M2 Magnetic Beads (M8823, Merck). Beads were washed 3x with 500 µl RIPA and boiled to elute the purified polybasic region. Blocked PI4P beads or same amount of control beads were added to the eluted protein and incubated for 1.5 h on 4°C while rotating. Beads were then washed 3x8 min with 500 µl RIPA buffer, resuspended in IP LDS sample buffer, boiled, and bound protein was analyzed using immunoblot.

3. RESULTS

3.1. NLRP3 tyrosine phosphorylation is dependent on BTK kinase activity

In previous work of our group, IL-1β release from primary human and murine monocytes and macrophages was reduced when BTK was ablated, either genetically (e.g. XLA patient in human or *Btk* KO in mice); or by inhibition of BTK kinase activity by diverse kinase inhibitors (Liu et al. 2017). These results indicate that BTK, besides serving as a scaffold, might also regulate the NLRP3 inflammasome via its kinase effector function. To test this hypothesis, the dependency of NLRP3 tyrosine phosphorylation on BTK´s kinase activity was studied in primary cells and using HEK293T overexpression system.

3.1.1. IL-1β release is dependent on BTK in human and murine monocytes and macrophages

To repeat and confirm that IL-1β release is dependent on the presence and kinase activity of BTK (Liu et al. 2017), IL-1β concentrations were measured in the supernatant of LPS-primed and nigericin stimulated WT, ibrutinib-treated and *Btk* KO BMDMs as well as PBMCs isolated from healthy donors, ibrutinib-treated cancer patients or XLA patients (see figure 3.1.).

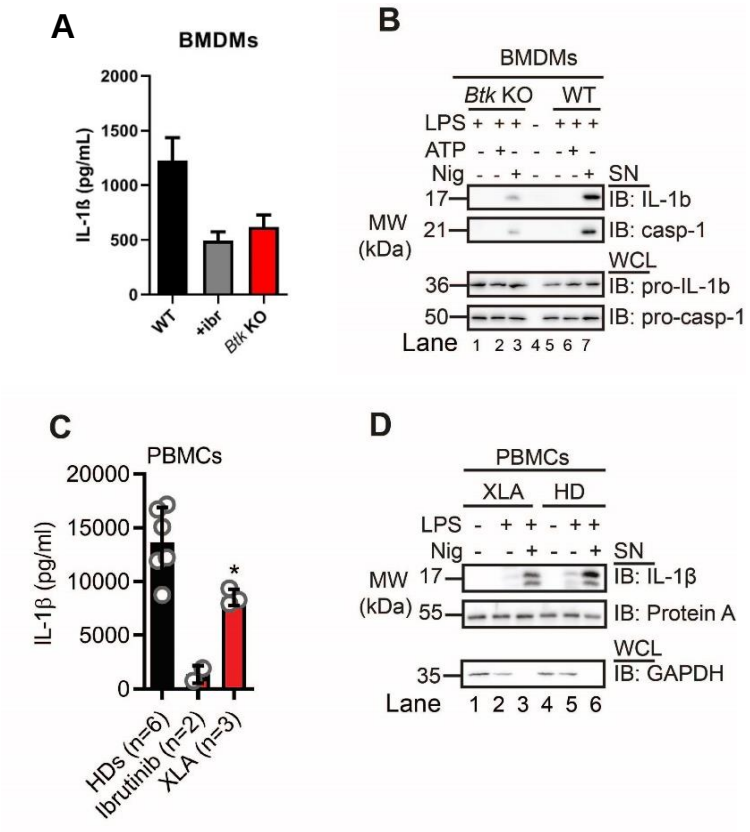

Figure 3.1. IL-1β release is dependent on BTK in primary human and murine monocytes and macrophages.

A) IL-1β ELISA from LPS-primed and ibrutinib- and nigericin treated WT BMDMs and LPS-primed and nigericin stimulated *Btk* KO BMDMs (n=2). The data were generated by Xiao Liu. B) Cleaved IL-1β and caspase-1 immunoblot of the precipitated SN and pro-IL-1β and pro-caspase-1 immunoblot of the WCL from LPS-primed and nigericin or ATP stimulated WT and *Btk* KO BMDMs (one representative of n=2). C) IL-1β ELISA from the SN of LPS-primed and nigericin treated healthy donor (HD, n=6), ibrutinib patient (n=2), and XLA patient (n=3) PBMCs. *: $p<0.05$ using one-way ANOVA with Dunnett correction (Alexander Weber). Experiments were conducted by Xiao Liu. D) Cleaved IL-1β immunoblot from the SN of LPS-primed and nigericin treated XLA and healthy PBMCs (one representative of n=2). Protein A in the SN serves as precipitation control, GAPDH in the WCL controls equal cell numbers between conditions.

In both murine and human system, genetic ablation of BTK or suppression of BTK kinase activity using inhibitors significantly reduced IL-1β release compared to healthy or untreated cells (see figure 3.1.). These results are in line with previously published observations (Ito et al. 2015; Liu et al. 2017) and indicated that BTK kinase activity might play a direct role in NLRP3 inflammasome activation.

3.1.2. NLRP3 and BTK interact in primary cells and *in vitro*

As a kinase-substrate relationship between BTK and NLRP3 was hypothesized, we expected at least temporary interaction between BTK and NLRP3 in primary cells. In previous studies, NLRP3 and BTK binding was briefly shown in BMDMs, as well as BMDMs, and mainly in the HEK293T overexpression system (Ito et al. 2015). We therefore aimed to further analyze the kinetics of NLRP3 and BTK interaction upon inflammasome activation in primary cells, using a co-immunoprecipitation approach and lysates from activated primary murine BMDMs and human PBMCs. As controls, isotype control antibodies of the IP antibodies and *Nlrp3* KO BMDMs were used. NLRP3 and BTK were shown to form stable interactions in primary cells (see figure 3.2. A) and B)), as BTK could be co-precipitated with NLRP3. The interaction was enhanced upon LPS priming of the cells. Nonetheless, LPS also augmented the expression of NLRP3 which might be the underlying reason for the increased BTK precipitation. Furthermore, BTK binding to NLRP3 was not compromised by ibrutinib treatment of the cells. The negative controls (isotype control and *Nlrp3* KO cells) showed only minimal signal, comparable to the background.

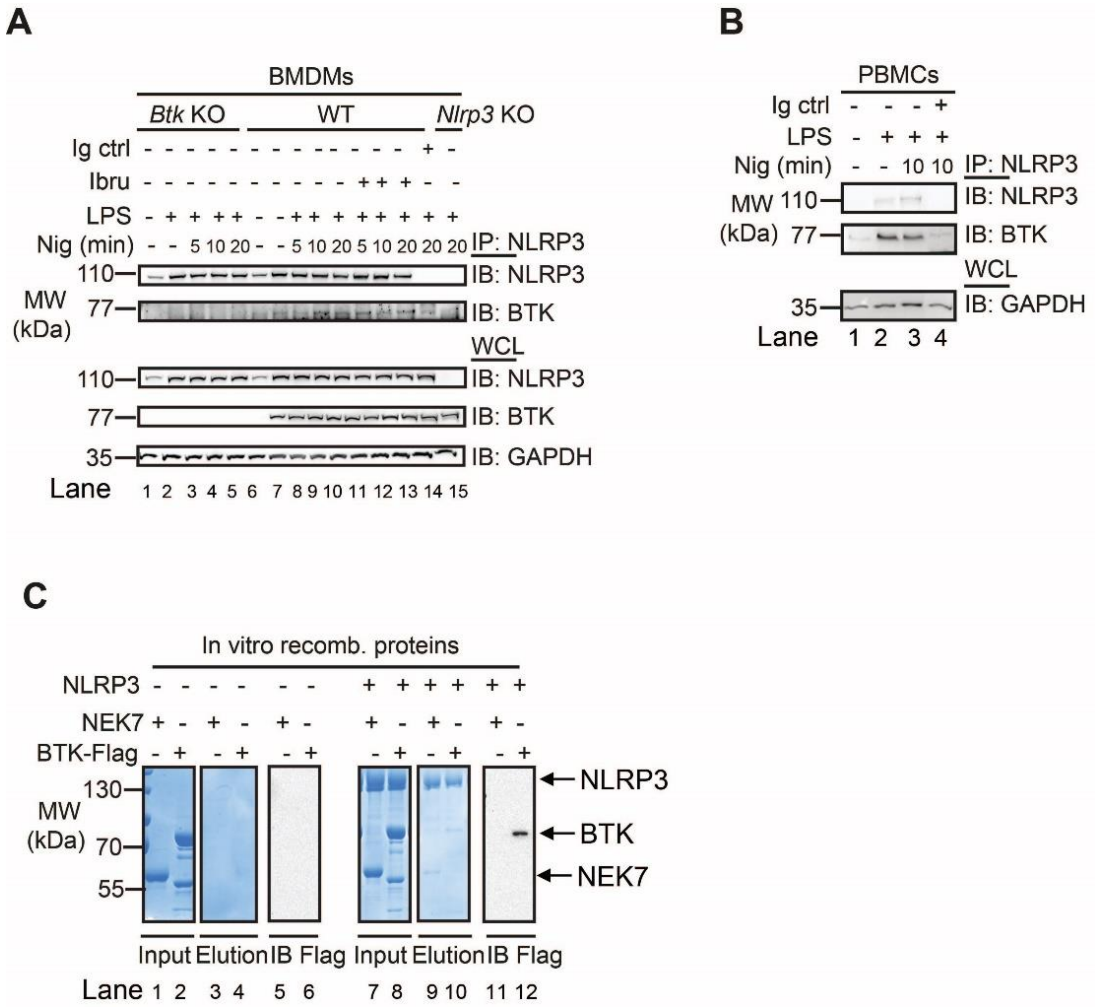

Figure 3.2. NLRP3 and BTK form stable complexes.

A) Co-immunoprecipitation using NLRP3 antibody or isotype control from WT, *Btk* KO and *Nlrp3* KO untreated, LPS-primed, ibrutinib-treated and for distinct time-points nigericin stimulated BMDMs (one representative of n=3, individual conditions indicated in the figure panel). B) Co-immunoprecipitation using NLRP3 antibody or isotype control antibody from untreated, LPS-primed and nigericin stimulated PBMCs, as indicated in the panel (one representative of n=2). C) *In vitro* interaction assay of purified Flag-tagged BTK or His-SUMO-tagged Nek7 (positive control) with MBP-tagged NLRP3 using amylose beads with affinity to MBP-NLRP3. Eluted proteins were analyzed with SDS-PAGE and immunoblot. Experiments (n=3) were conducted by Liudmila Andreeva.

Furthermore, purified recombinant NLRP3 and BTK were incubated *in vitro* and interaction was analyzed via affinity chromatography (see figure 3.2.C). BTK and NLRP3 interacted in a cell-free *in vitro* affinity purification assay as well.

These results indicate a significant role of BTK in NLRP3 inflammasome activation, as BTK and NLRP3 interaction stably manifested in primary cells upon NLRP3 inflammasome stimulation, as well as in *in vitro* interaction assays.

3.1.3. NLRP3 is rapidly tyrosine phosphorylated upon nigericin treatment

BTK is tyrosine-phosphorylated (Y551) within minutes upon nigericin treatment, as published previously (Liu et al. 2017). Tyrosine 551 phosphorylation is an upstream event of BTK catalytic function, thus, we were wondering whether NLRP3 tyrosine phosphorylation would coincide with BTK tyrosine phosphorylation, which would strongly indicate that NLRP3 tyrosine phosphorylation is dependent on BTK kinase activity. For this purpose, IP was performed using p-Y antibody, and the IP samples were analyzed for NLRP3 and BTK content.

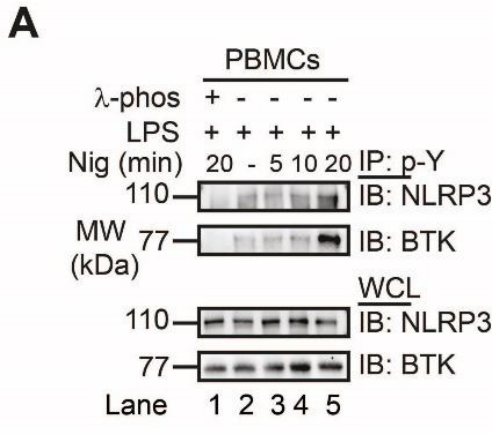

Figure 3.3. p-Y IP from human PBMCs.

A) p-Y IP from LPS-primed and for different time-point nigericin stimulated PBMCs (one representative of n=4). IP samples were analyzed for NLRP3 and BTK content. Comparable WCL samples control the protein input in each condition.

Both NLRP3 and BTK showed strong tyrosine phosphorylation upon LPS-priming and 20 min nigericin treatment in human PBMCs. λ-phosphatase treatment of the lysate (depletion of phospho-groups from all amino acids) abolished p-Y-NLRP3 and p-Y-BTK, confirming the specificity of the p-Y antibody to solely phosphorylated proteins. Tyrosine phosphorylation of NLRP3 mirrored the tyrosine phosphorylation of BTK.

These results strongly indicate that NLRP3 tyrosine phosphorylation is dependent on BTK kinase activity.

3.1.4. BTK deficiency coincides with reduced NLRP3 tyrosine phosphorylation

After having shown that BTK and NLRP3 tyrosine phosphorylation coincide in primary human cells, the dependency of NLRP3 tyrosine phosphorylation on the presence of BTK and more specifically on BTK kinase activity was assessed. To this end, the same approach as described above was used, namely p-Y IP, this time, however, comparing the level of tyrosine phosphorylated NLRP3 between WT and *Btk* KO BMDMs, WT and XLA patient PMBCs, and non-treated and ibrutinib-treated PBMCs, to see an effect of the availability of an intact BTK on NLRP3 tyrosine phosphorylation.

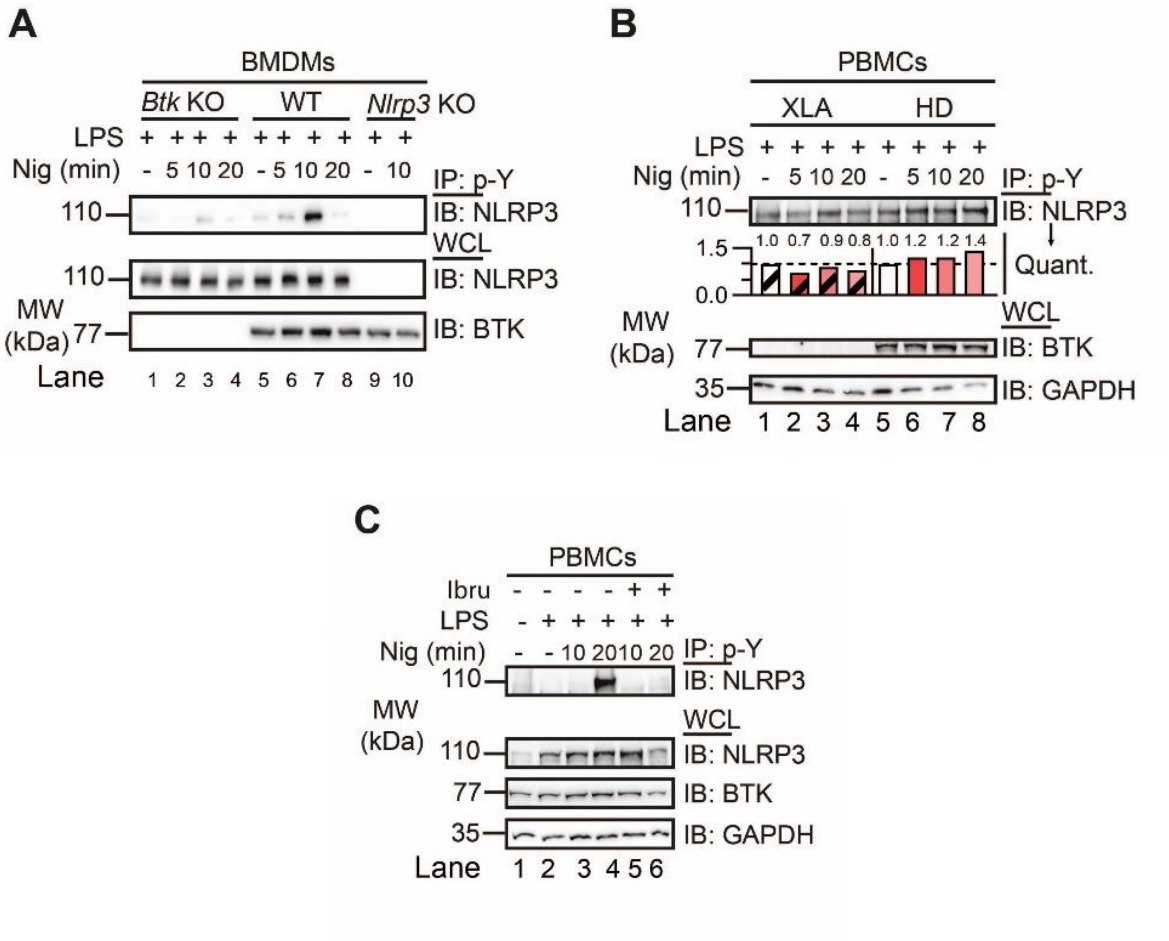

Figure 3.4. p-Y IP from murine BMDMs and human PBMCs.

A) p-Y IP from untreated, LPS-primed and for different time-points nigericin treated WT and *Btk* KO BMDMs (one representative of n=3). B) p-Y IP from LPS-primed and for different time-points stimulated healthy donor and XLA patient PBMCs (one representative of n=2). C) p-Y IP from LPS-primed, ibrutinib-treated and for different time-points nigericin stimulated PBMCs (one representative of n=2).

In both murine and human cells, NLRP3 tyrosine phosphorylation was shown to be dependent on the presence of an intact BTK (see figure 3.4. A) and B)), as less p-Y NLRP3 could be precipitated in *Btk* KO murine BMDMs and human XLA PBMCs compared to WT BMDMs and healthy donor PBMCs. Furthermore, although BTK was present, inhibition of its kinase activity with ibrutinib also abrogated NLRP3 tyrosine phosphorylation in human PBMCs (see figure 3.4.C)).

Next, NLRP3 tyrosine phosphorylation in HEK293T cells was measured upon co-transfection with WT BTK or BTK harboring distinct mutations; and upon BTK and NLRP3 inhibitor treatment. HEK293T cells do not express NLRP3 or BTK, thus co-

expression of intact and mutated proteins enabled studying the effect of the specific BTK mutation on NLRP3 tyrosine phosphorylation.

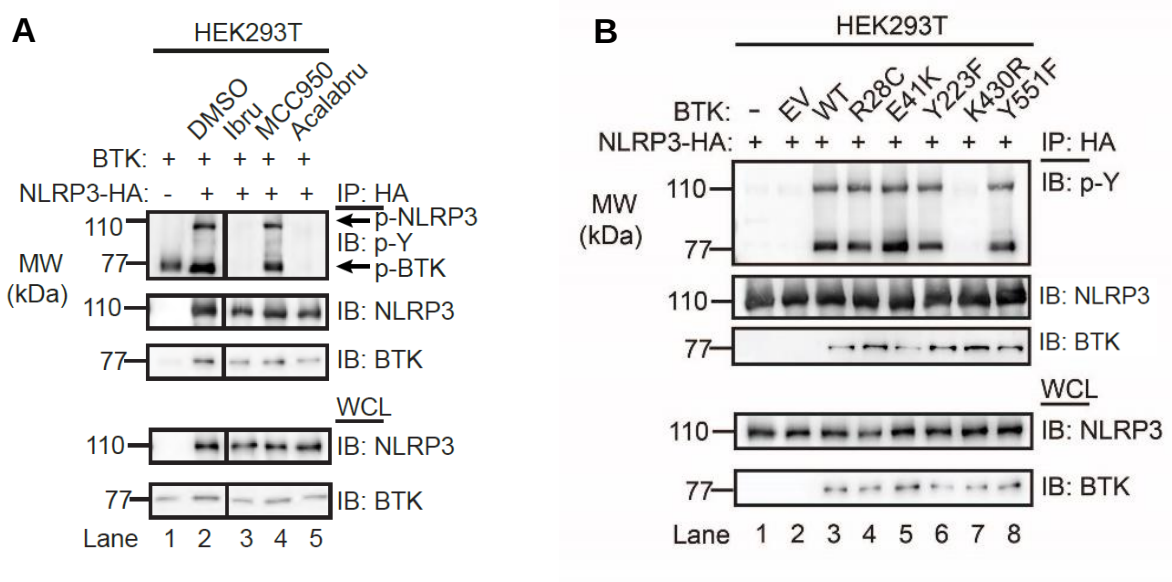

Figure 3.5. NLRP3 tyrosine phosphorylation is dependent on BTK in HEK293T cells.

A) HEK293T cells were co-transfected with NLRP3 and BTK and treated with ibrutinib, MCC950 and acalabrutinib for 4 h, 24 h before harvesting the cells, which was followed by NLRP3-HA IP and NLRRP3-HA, BTK-Flag and p-Y immunoblot (one representative of n=2). B) HEK293T cells were co-transfected with NLRP3-HA and WT or point-mutated BTK-Flag, then NLRP3-HA IP was performed, and NLRP3-HA, BTK-Flag and p-Y immunoblot was conducted (one representative of n=2). Experiments were performed by Xiao Liu.

In HEK293T cells, co-expression of NLRP3 with BTK resulted in NLRP3 activation independent tyrosine phosphorylation of BTK and NLRP3. NLRP3 and BTK tyrosine phosphorylation could be prohibited by treatment of the cells with the BTK kinase inhibitors ibrutinib and acalabrutinib. Nevertheless, the NLRP3 inhibitor MCC950 had no effect on the tyrosine phosphorylation of the expressed proteins (see figure 3.5.A)). When BTK mutants were co-expressed with NLRP3 (see figure 3.5.B)), solely the mutation that affected the integrity of BTK´s kinase domain (K430R, see introduction table 1.3.) abolished NLRP3 and BTK tyrosine phosphorylation. The conserved lysine in kinases´ catalytic domain has been shown to be critical for the kinases´ effector functions (Carrera, Alexandrov, and Roberts 1993). Thus, mutation of this lysine residue (in BTK´s case K430) to arginine leads to a "kinase dead" version of the protein.

As the other mutations affect phospho-addition-independent abilities of the kinase (membrane binding, upstream activation), and the model in HEK293T system functions without stimulation of the cells, it was expected that only the kinase-dead BTK mutant would show abrogated BTK and thus NLRP3 tyrosine phosphorylation, whereas the other mutants are still auto-phosphorylated and therefore capable of further phosphorylation of NLRP3.

3.2. BTK phosphorylates four tyrosine residues in the NLRP3 PYD-NACHT linker

Once the clear dependency of NLRP3 Y phosphorylation on BTK was established, the direct kinase-substrate relationship between BTK and NLRP3 was further analyzed, resulting in the identification of the NLRP3 Y residues phosphorylated by BTK.

3.2.1. NLRP3 is a direct substrate of BTK

Although NLRP3 Y phosphorylation was clearly dependent on BTK kinase activity in primary cells and HEK293T overexpression system, NLRP3 being a direct substrate could not be stated until a cell-free assay has been completed, containing solely recombinant NLRP3, BTK, the negative control protein PosiTag, kinase buffer, and ATP.

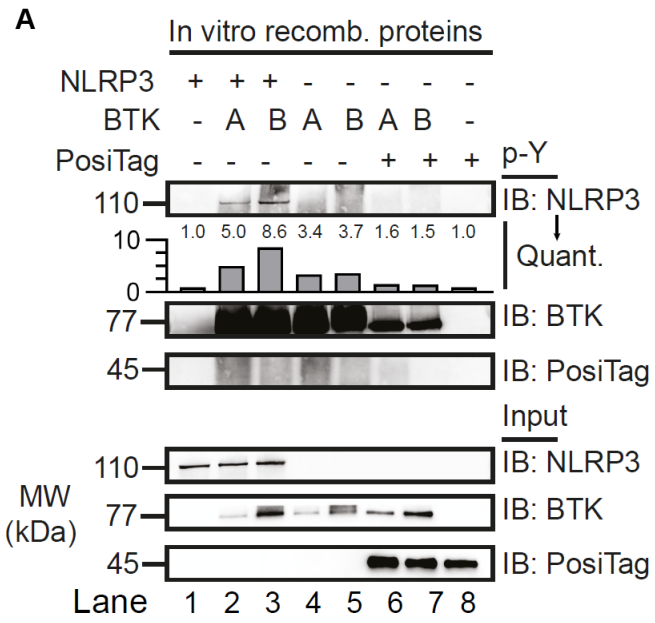

Figure 3.6. NLRP3 is a direct substrate of BTK.

A) *In vitro* kinase assay was performed with two distinct recombinant BTKs, recombinant NLRP3 and the negative control PosiTag (one representative of n=2). Protein content, as well as tyrosine phosphorylated proteins in the samples were visualized via immunoblot.

Having used two distinct recombinant BTKs, both specifically phosphorylated NLRP3 in a cell-free *in vitro* kinase set up (see figure 3.6.). As *in vitro* kinase assays often show false-positive results, we used the protein PosiTag (a fusion protein composed of several common tags, containing multiple tyrosine residues) as a negative control. The negative control PosiTag was not phosphorylated by BTK in our set-up, proving specificity of the assay.

These results display the direct kinase-substrate relationship between BTK and NLRP3.

3.2.2. BTK phosphorylates the PYD-NACHT linker

After NLRP3 has been proven to be directly phosphorylated by BTK, we next aimed to identify the target Y residue. To narrow down the Y residues, NLRP3 truncated versions, corresponding to NLRP3 single domains and linker regions (PYD; PYD/NACHT linker+NACHT domain, NACHT/LRR linker+LRR domain), were co-transfected with BTK in HEK293T cells to find the construct that is phosphorylated by BTK, containing the target Y residue.

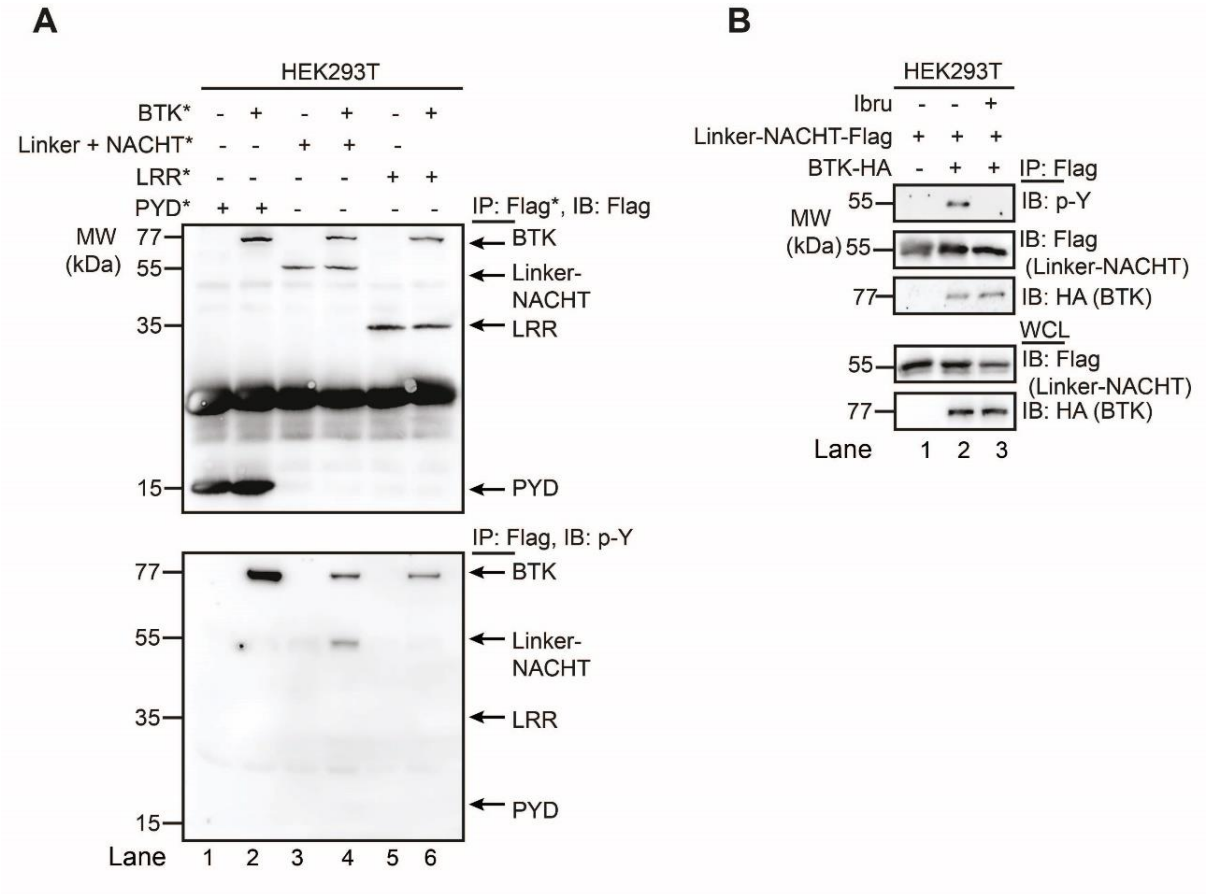

Figure 3.7. BTK phosphorylated the PYD-NACHT linker and NACHT containing construct.

A) HEK293T cells were co-transfected with BTK-Flag and NLRP3-Flag single domains. After Flag IP, p-Y immunoblot was performed (one representative of n=3). B) Ibrutinib-treatment of PYD-NACHT-Flag linker and BTK-HA co-transfected HEK293T cells followed by Flag IP, HA, Flag, and p-Y immunoblot (one representative of n=3).

Solely one out of the three transfected constructs was phosphorylated by BTK in HEK293T cells: the one containing the PYD-NACHT linker region and the NACHT domain (see figure 3.7.A). This result was confirmed by using ibrutinib in the same experimental setup, which indeed abolished Y phosphorylation of the linker-NACHT region (see figure 3.7.B).

3.2.3. BTK phosphorylates the PYD-NACHT linker residue Y168

Next, we aimed to identify the single NLRP3 Y residue that is phosphorylated by BTK. To this end, we purified NLRP3 expressed in HEK293T cells together with BTK and sent the sample for mass spectrometry analysis to a cooperation partner (Felix Meissner) to spot the

NLRP3 tyrosine residue that is phosphorylated by BTK. Unfortunately, the sequence coverage of NLRP3 was sparse, even using a combination of enzymes for NLRP3 cleavage (e.g. trypsin and glu-c, see Appendix 6.4.), therefore this approach was not fruitful.

Next, we generated single Y>F mutants of the Y residues that reside within the PYD-NACHT linker and the NACHT domain. The mutant where the phosphorylation is diminished would carry the Y residue that is phosphorylated by BTK.

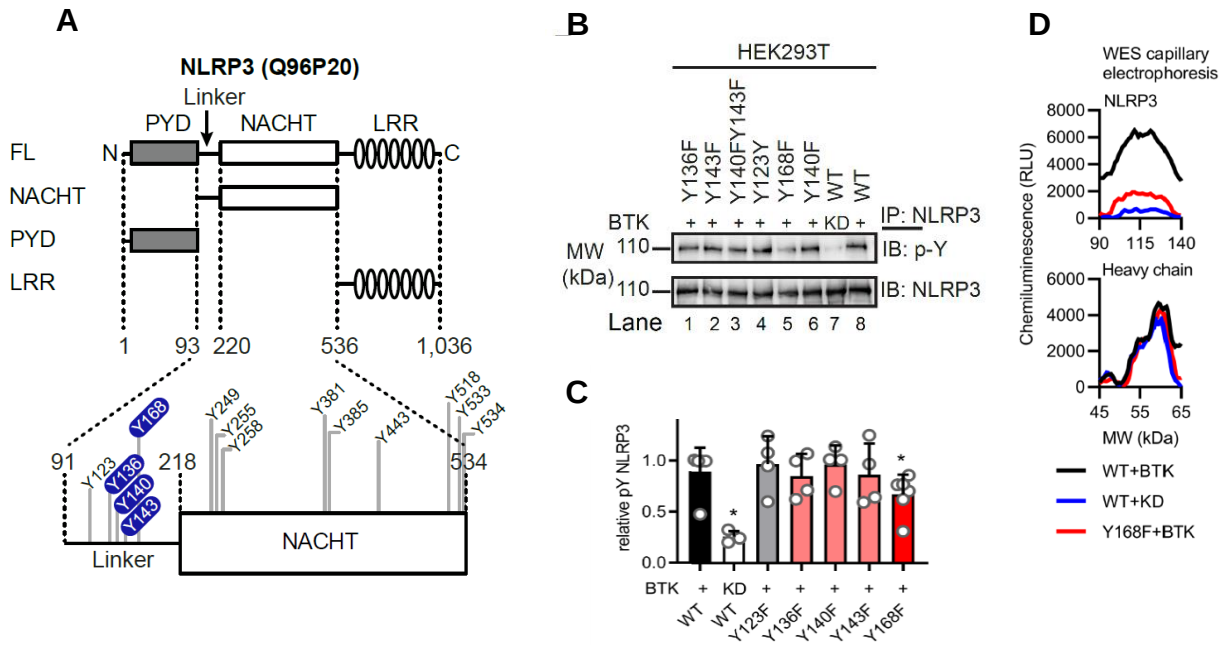

Figure 3.8. BTK phosphorylates NLRP3 Y168.

A) Schematic depiction of the NLRP3 domains. Highlighted are the PYD-NACHT linker and NACHT domain containing construct that was phosphorylated by BTK. Figure generated by Alexander Weber. B) Immunoblot analysis of p-Y NLRP3 mutants upon co-expression with BTK in HEK293T cells, NLRP3 IP and p-Y immunoblot. (one representative of n=3). C) Quantification of the phosphorylation ratio of total pulled-down NLRP3 vs. phosphorylated NLRP3 upon co-expression with BTK in HEK293T cells, NLRP3 IP and p-Y immunoblot (n=3, *:p<0.05 in one sample t-test). D) Samples from C) were run on ProteinSimple WES using p-Y antibody. Relative light unit (RLU) levels of the heavy chain serve as loading control (one representative of n=3).

Using the HEK293T co-transfection system, none of the mutations located in the NACHT domain resulted in a significant reduction in tyrosine phosphorylation levels (see Appendix 6.5.) Thus, Y>F mutations of the residues residing in the PYD-NACHT linker were generated and tested using the same approach. Even though double-mutations were also generated,

(e.g. Y140FY143F) these displayed no reduction in tyrosine phosphorylation. Nonetheless, the mutant Y168F showed significantly reduced tyrosine phosphorylation quantified upon immunoblot. Comparable to the conventional immunoblot results, the mutant Y168F showed reduced tyrosine phosphorylation in the WES analysis (see figure 3.8.). Still, however, significant, the reduction was not comparable to baseline levels. Thus, we hypothesized that more than a single NLRP3 Y residue is phosphorylated by BTK, and these would be very elaborate to find using the point-mutation methodology. Therefore, we realigned our approach to find all the NLRP3 tyrosine residues that are phosphorylated by BTK, see section 3.2.4.

3.2.4. BTK phosphorylates the NLRP3 PYD-NACHT linker residues Y136/Y140/Y143/Y168

To identify single Y residues that are phosphorylated by BTK, Xiaowu Zhang, a colleague of the company CST, suggested trying vitro kinase assay using recombinant BTK and NLRP3 sequence peptides instead of full-length NLRP3. Thus, we performed *in vitro* kinase assays using recombinant BTK mixed with equimolar NLRP3 15mer peptides, each of them holding a possible target tyrosine residue in the middle of the peptide. The peptides carrying Y>F modifications served as negative controls to show specificity of the assay to solely p-Y and not p-T/p-S. After the *in vitro* kinase assay, we purified the peptides from BTK-His using anti-His magnetic beads. This step was necessary, as BTK itself is strongly tyrosine phosphorylated and would have contaminated the peptide samples that were subjected to p-Y staining on a dot-blot membrane.

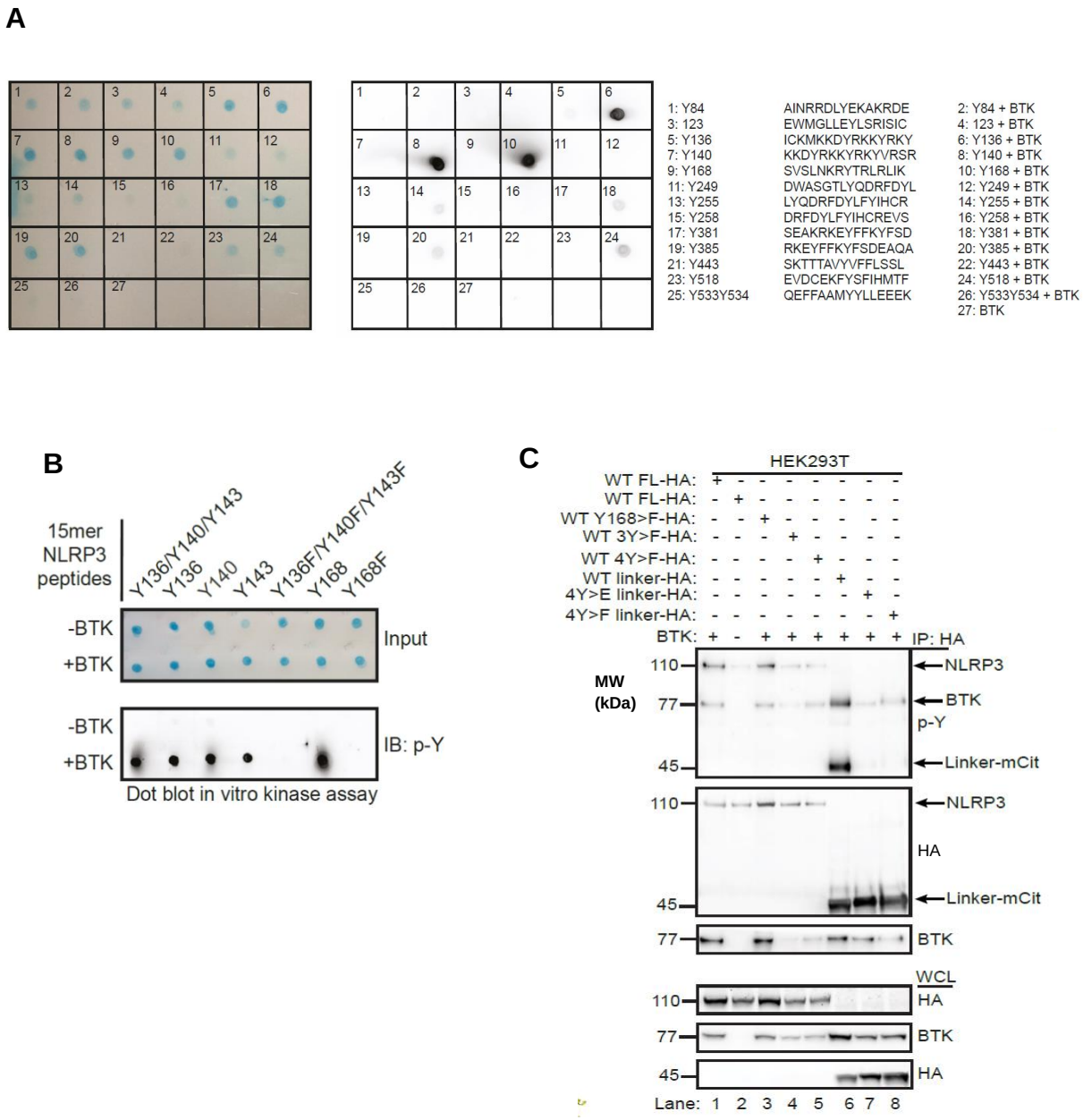

Figure 3.9. Y136/Y140/Y143/Y168 were phosphorylated by BTK *in vitro*.

A) *In vitro* kinase assay with 13 15mer peptides carrying Y residues of PYD/NACHT linker/NACHT domain region and recombinant BTK-His followed by BTK-His depletion using anti-His magnetic beads. Peptides holding Y136/Y140/Y143/Y168 were phosphorylated based on dot-blot analysis (one representative of n=2). B) *In vitro* kinase assay with single Y residue-carrying peptides (Y136/Y149/Y143/Y168) or negative controls Y>F (one representative of n=3). C) Co-expression of FL NLRP3-HA, 3Y>F (Y136/Y140/Y143) or 4Y>F (Y136/Y140/Y143/Y168) or PYD/NACHT linker-HA-mCit (WT, Y>F, Y>E) constructs with BTK in HEK293T cells followed by HA IP and p-Y immunoblot (one representative of n=3).

Most of the tested peptides were not modified by BTK (see figure 3.9.A). The peptide carrying Y168 was phosphorylated by BTK in the *in vitro* kinase set-up as well, thereby confirming the results obtained from the HEK293T co-expression system. Additionally, the residues Y136, Y140, and Y143 were phosphorylated in the *in vitro* peptide phosphorylation assay, as deduced from the peptides harboring single Y residues (as Y136/Y140/Y143 are closely in the sequence and overlap on the peptides, peptides with single Y variations were additionally used to be able to allocate the phosphorylated peptides to the phosphorylated residues). We tested phosphorylation of the analogue tyrosine residues in the murine sequence, and Y132, Y136, Y144 and very slightly Y164 were modified by human BTK (see Appendix 6.6.), indicating human-mouse transferability of the mechanism by which BTK modifies NLRP3. It was rather surprising to find not one or two, but four NLRP3 tyrosine residues that were phosphorylated by BTK. These results explained why not even the Y140FY143F double mutant showed a reduction in tyrosine phosphorylation by BTK in the HEK293T assay.

Thereupon, NLRP3 full-length human constructs carrying Y136F/Y140F/Y143F triple mutations or Y136F/Y140F/Y143F/Y168F quadruple mutations were generated and tested for Y phosphorylation by BTK in the HEK293T overexpression system. Both triple and quadruple mutants showed tyrosine phosphorylation levels similar to the background, showing that these residues are targeted by BTK also in the native form of NLRP3, and the residues are not only accessible to BTK in the short and linear peptide form. Additionally, WT, 4Y>F or 4Y>E mutant constructs based on the PYD-NACHT linker region were transfected together with BTK in HEK293T cells and Y phosphorylation of the truncated NLRP3 constructs was measured. In both 4Y>F and 4Y>E mutants the tyrosine phosphorylation was abolished, indicating that indeed these residues are targeted by BTK. The PYD/NACHT linker constructs were additionally fused to a C-terminal mCitrine protein. This design served the idea to use these constructs in the future in co-localization and oligomerization experiments assessed by microscopy analysis (plasmid maps in Appendix 6.2.).

3.3. Phosphorylation by BTK regulates NLRP3 Golgi binding via a charge switch

After having identified the four tyrosine residues of NLRP3 that are phosphorylated by BTK, we next sought to find out the mechanistic consequences of these phosphorylation events regarding NLRP3 inflammasome assembly and activation. We noticed that the residues reside in the recently identified and termed "polybasic region" of NLRP3 (J. Chen and Chen 2018). This region of NLRP3 is responsible for trans-Golgi network phospholipid (PI4P) binding of NLRP3, resulting in oligomerization of NLRP3 and in a pre-activated state on the Golgi membrane. We hypothesized that phosphorylation of the polybasic region, leading to neutralization of the polybasic region by introducing two minus charges per phospho-group, would weaken NLRP3 binding to the trans-Golgi membrane, facilitating the formation of the fully assembled NLRP3 inflammasome in the cytosol.

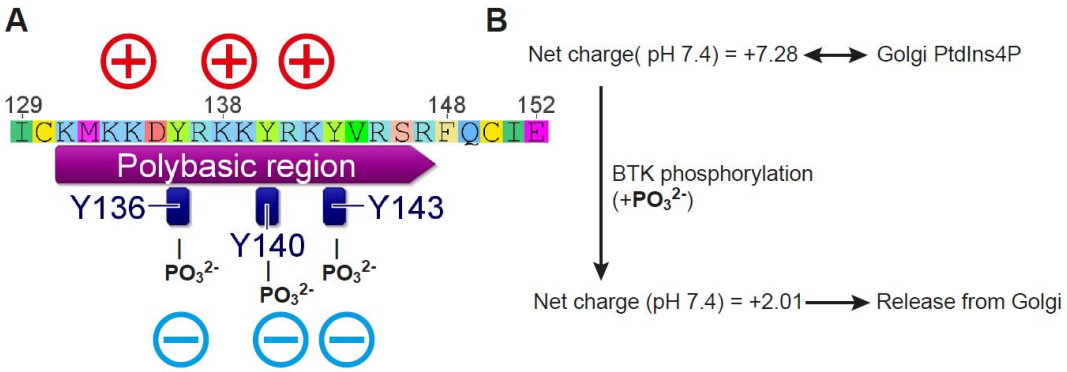

Figure 3.10. Phosphorylation of NLRP3 by BTK leads to a charge-switch of the modified area.

A) Schematic representation of the charges of the polybasic region without and with phosphorylation. B) Changes in the charge caused by phosphorylation of the polybasic area might lead to dissociation of NLRP3 from the phospholipids on the Golgi membrane. Figure generated by Alexander Weber.

Indeed, phosphorylation of the polybasic region is expected to shift the cytoplasmic charge of this area from +7.28 to +2.01, resulting in considerably reduced positive charge. As phosphorylated areas are facing outwards in the native NLRP3 structure (see Discussion 4.1.), this charge switch is probably also displayed on the surface of NLRP3. PI4Ps are negatively charged and the NLRP3/trans-Golgi network interaction would thus be weakened.

3.3.1. NLRP3 and BTK can be found in the heavy and light membrane fractions

After defining our hypothesis, that BTK mediated a charge-switch might facilitate the release of NLRP3 from the Golgi, we first aimed to replicate the results from the original publication (J. Chen and Chen 2018), stating that NLRP3 binds to the Golgi membrane in the first place. To this end, fractionation of primary BMDMs was performed upon NLRP3 inflammasome activation to obtain heavy membrane fractions, P5, (containing mitochondria, ER, and Golgi), light membrane fractions, P100, (containing ER and Golgi), and cytosolic, S100, fractions. The heavy and light membrane fragments were further fractionated using sucrose gradient ultracentrifugation, to additionally assess co-localization of NLRP3 with BTK.

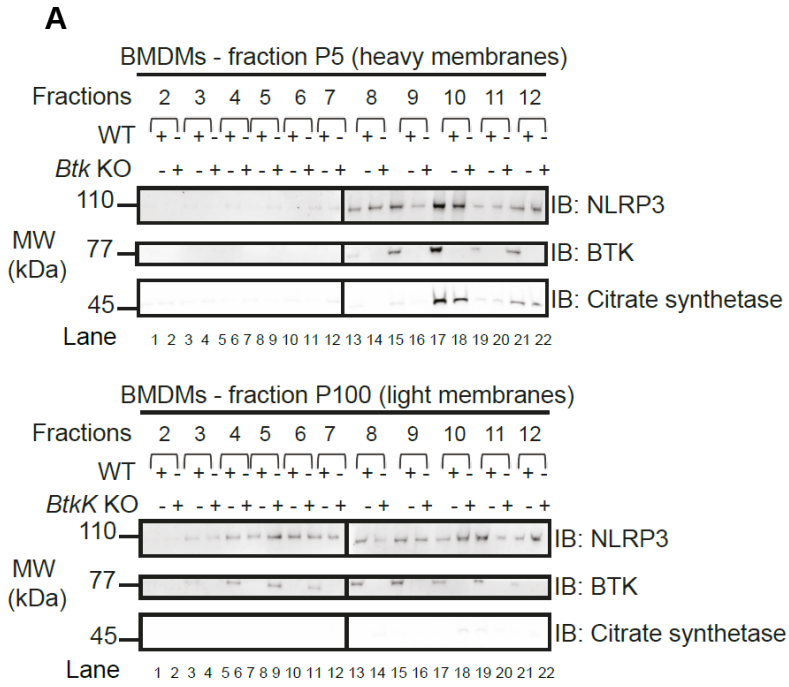

Figure 3.11. NLRP3 could be found in both heavy and light membrane fractions.

A) BMDMs were LPS-primed, nigericin stimulated, homogenized, and heavy (P5) as well as light (P100) membranes were isolated. P5 and P100 were further fractionated via sucrose gradient ultracentrifugation. Fractions were used for immunoblot analysis for NLRP3, BTK, and citrate synthetase (mitochondria) contents.

In line with the published results (J. Chen and Chen 2018) we found NLRP3 in both heavy and light membrane fractions. Interestingly, BTK followed the NLRP3 localization pattern. NLRP3 was present at the heavy and light membranes in *Btk* KO BMDMs as well, thus localization of NLRP3 to the Golgi is independent from BTK.

3.3.2. NLRP3 dissociation from the heavy membrane is BTK dependent

We next sought to test our "BTK-dependent NLRP3 Golgi-release" hypothesis using primary BMDMs by first mapping the kinetics of NLRP3 localization in the heavy and light membrane fractions upon inflammasome activation.

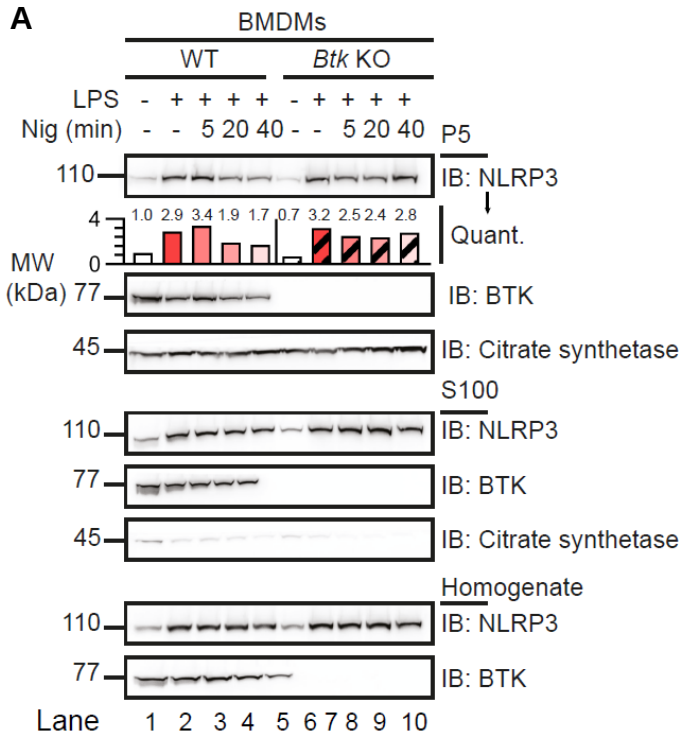

Figure 3.12. Kinetics of NLRP3 localization to heavy and light membranes in BMDMs upon inflammasome stimulation.

A) WT and *Btk* KO BMDMs were LPS-primed and nigericin stimulated. Cells were homogenized and P5 and S100 were separated. Immunoblot analysis followed to measure NLRP3 and BTK content of the membrane fractions (one representative of n=2).

LPS priming of the cells led to enrichment of NLRP3 to the heavy membrane in both WT and *Btk* KO BMDMs. Nonetheless, only in WT BMDMs led nigericin treatment to rapid dissociation of NLRP3 from the heavy membrane (and thus to a reduction of NLRP3 protein amounts in the P5 fraction); yet in *Btk* KO BMDMs NLRP3 levels in the P5 fractions stayed comparably similar in the course of nigericin treatment. BTK could be found at the heavy membrane in steady state already, and its amount in P5 reduced upon nigericin treatment, mirroring NLRP3´s kinetics in the WT cells. In the light membrane fractions, both NLRP3 and BTK could be measured in similar concentration upon stimulation. These results indicate that NLRP3 dissociates from P5 upon nigericin treatment when BTK is present, whereas it

stays on the heavy membrane in the absence of BTK, consistent with our hypothesis that BTK facilitates NLRP3´s release from the Golgi membrane. Further proof was, however, desired.

3.3.3. Charge-switch of the polybasic region leads to reduced PI4P binding

To tackle our hypothesis more mechanistically, we decided to challenge it by performing a PI4P binding assay using agarose beads covered with PI4P together with constructs of the PYD-NACHT linker (human) or the polybasic region only (murine). We expected binding of the WT constructs to the PI4P covered beads, whereas reduced binding of the phospho-mimetic Y>E construct, as well as the K>A mutants (loss of positive charge of the polybasic region).

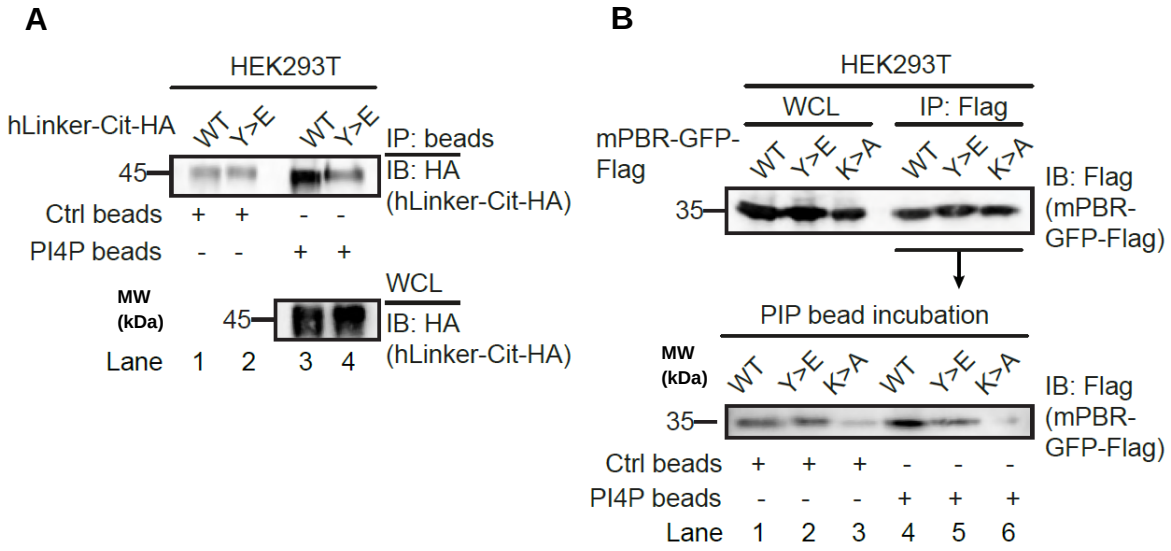

Figure 3.13. PI4P binding of NLRP3 PYD/NACHT linker polybasic region.

A) HEK293T cells were transfected with human WT or Y136E/Y140E/Y143E/Y168E (Y>E) PYD/NACHT linker construct and IP was conducted using agarose beads coated with PI4P, or control beads. Bead-bound protein was visualized using immunoblot (one representative of n=2). B) HEK293T cells were transfected with WT, all Y>E, or all K>A murine Flag-tagged polybasic region (AA127-146), the constructs were purified using anti-Flag magnetic beads and purified protein was incubated with Flag peptide-blocked agarose beads coated with PI4P, or control beads. Agarose bead-bound protein was analyzed using immunoblot (one representative of n=2).

As hoped, the phospho-mimetic Y>E version showed strongly reduced binding to phospholipids (see figure 3.13.A), comparable to that of the K>A neutralized polybasic region construct (see figure 3.13.B). These results demonstrate that solely the charge (not the amino-acid sequence) of the polybasic region is responsible for binding of NLRP3 to the phospholipids on the Golgi, and this binding can be reversed by either neutralizing the positivity (K>A) of the region, or by introducing negative charge in between the positive residues (Y>E, or p-Y). Although further experiments can be envisaged to prove this more unequivocally (see Discussion), these observations support the hypothesis that NLRP3 tyrosine phosphorylation by BTK might facilitate reduced binding of NLRP3 to the Golgi phospholipids, and that NLRP3 trafficking between P5 and the cytosol is BTK dependent.

3.4. BTK kinase activity affects NLRP3 oligomerization and inflammasome assembly in the cytosol

After having generated data that supports the hypothesis that phosphorylation of the polybasic region by BTK mediates charge-switch facilitated release of NLRP3 from the Golgi, we next wanted to follow the process of downstream inflammasome activation and assembly by measuring NLRP3 and ASC oligomerization in the cytosol in the presence and absence of BTK, or rather BTK kinase activity.

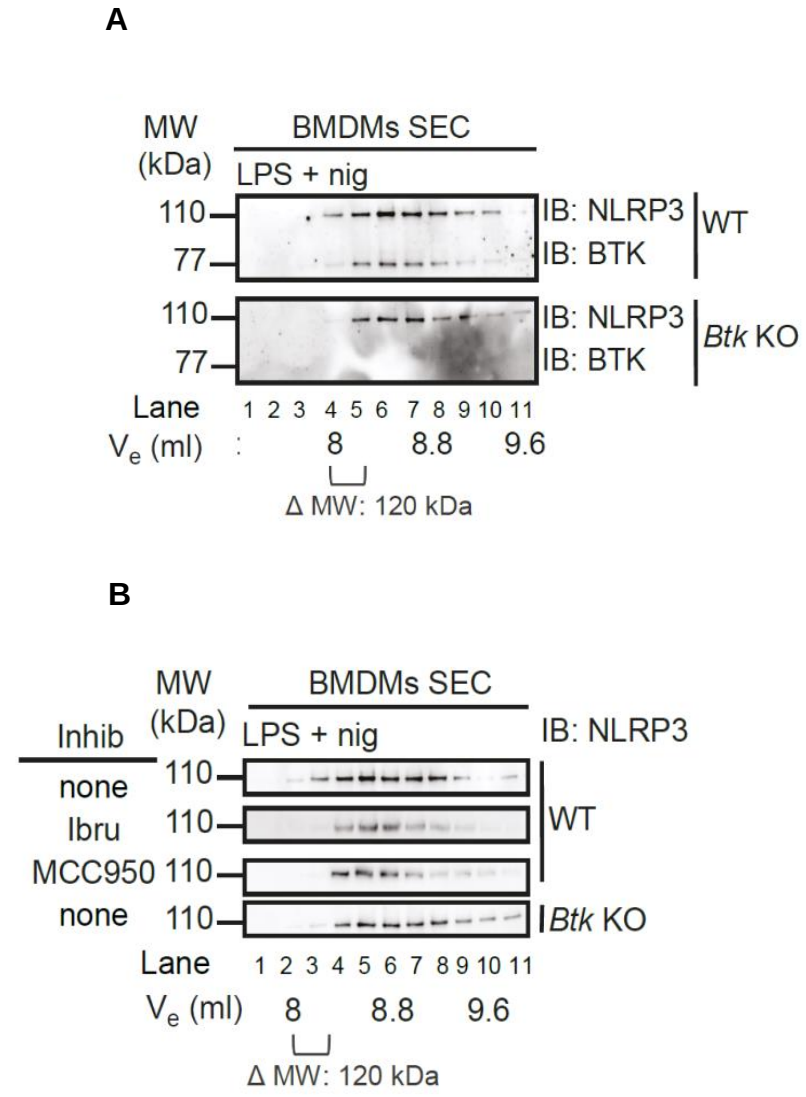

Figure 3.14. Size-exclusion chromatography of BMDMs.

A) LPS-primed and nigericin stimulated BMDM lysates were used for SEC. Fractions were used for immunoblot analysis to assess NLRP3 and BTK content (one representative of n=3). B) LPS-primed and nigericin and ibrutinib or MCC950 treated BMDM lysates were analyzed with SEC and immunoblot for NLRP3 content (one representative of n=3).

Size exclusion chromatography from primed and nigericin stimulated BMDMs lysates (samples generated as described in (N. Song et al. 2017)) revealed that BTK and NLRP3 stayed in complex also in later stages of inflammasome assembly, as they co-eluted from the column. Priming and stimulation of BMDMs led to the formation of high molecular weight NLRP3 complexes. Nonetheless, ibrutinib treatment as well as MCC950 treatment reduced NLRP3 oligomerization tendency to the level of oligomer size found in *Btk* KO BMDM lysates. These results show that inhibition the kinase activity of BTK reduces NLRP3

oligomerization to a similar level as the NLRP3 inhibitor MCC950 that again acts on NLRP3 oligomerization capability. Thus, BTK kinase activity, presumably by phosphorylation of NLRP3, strongly supports inflammasome assembly. These results were underpinned by the observation obtained from analyzing BMDM lysates using native PAGE.

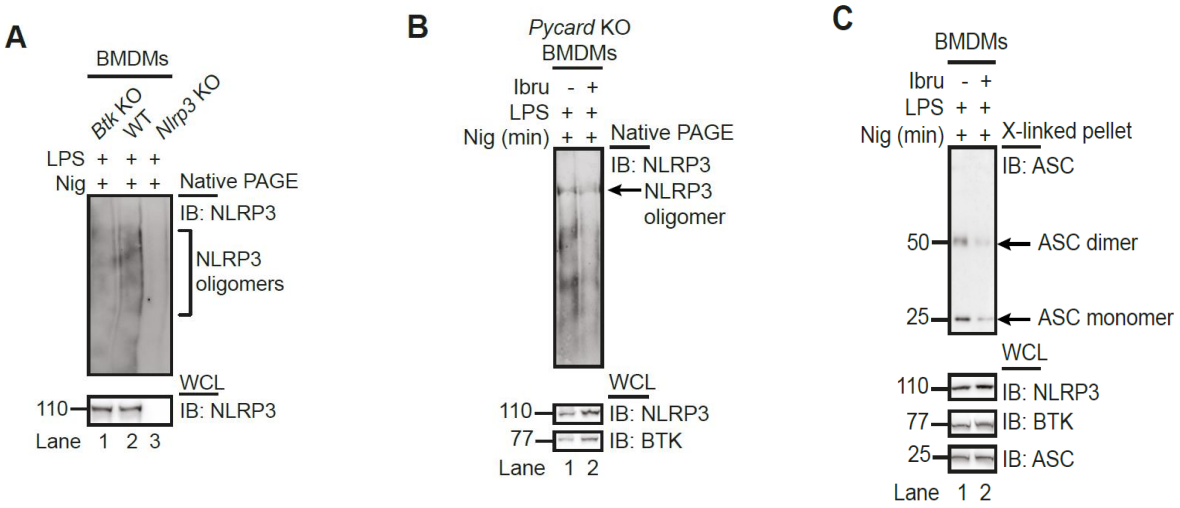

Figure 3.15. NLRP3 inflammasome assembly is reduced upon inhibition of BTK kinase activity.

A) Native PAGE analysis of NLRP3 oligomers in LPS-primed and nigericin stimulated *Btk* KO, WT and *Nlrp3* KO BMDMs (one representative of n=2). B) Native PAGE analysis of NLRP3 oligomers in LPS-primed and nigericin stimulated and ibrutinib-treated *Pycard* KO BMDMs (one representative of n=4). C) Immunoblot analysis for ASC oligomers of insoluble cross-linked pellets of LPS-primed, nigericin stimulated and ibrutinib treated BMDM lysates (one representative of n=4).

Cytosolic fractions of *Btk* KO BMDMs contained reduced amounts of oligomerized NLRP3, as shown in Figure 3.15.A. Furthermore, NLRP3 oligomers were diminished in *Pycard* KO BMDM lysate soluble fractions treated with ibrutinib compared to the untreated samples (see figure 3.15.B). The use of *Pycard* KO cells instead of WT will be discussed in the Discussion (4.5.). Additionally, ibrutinib treatment diminished ASC oligomers in the insoluble pellet after chemical cross-linking of the lysate (see figure 3.15C)). Taken together, these results show that kinase activity of BTK promotes NLRP3 inflammasome assembly in the cytosol.

3.5. Phosphorylation of the NLRP3 residues Y136/Y140/Y143 and Y168 by BTK is required for IL-1β release from murine macrophages

To test whether phosphorylation of the BTK target residues Y136/Y140/Y143 and Y168 is functionally relevant, Matthew Mangan (AG Latz) reconstituted *Nlrp3* KO immortalized macrophages (iMacs) using lentiviral transduction with WT human NLRP3 construct, Y136F/Y140F/Y143F/Y168F mutated human NLRP3 construct or with the empty backbone of the lentiviral vector. The reconstituted iMacs cells were then stimulated with diverse NLRP3 (nigericin and R837) or AIM2 (Poly(dA:dT), negative control) stimuli and released cytokines were measured via ELISA, as well as cell death via LDH release.

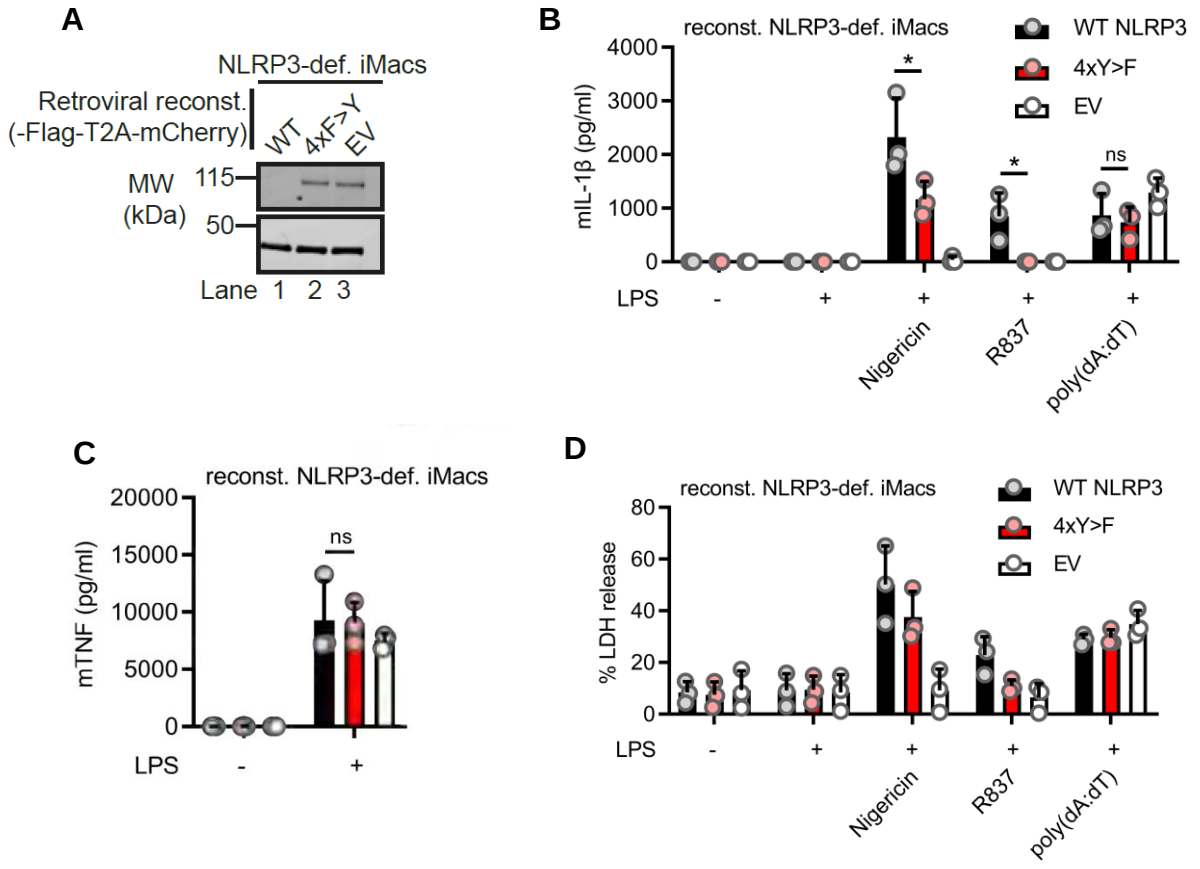

Figure 3.16. IL-1β production is reduced in 4Y>F reconstituted iMacs.

A) NLRP3 expression of the reconstituted iMacs was measured via immunoblot. B) IL-1β ELISA from the supernatant of reconstituted iMacs upon LPS-priming and nigericin, R837, and poly(dA:dT) treatment (n=3). C) TNFα ELISA from unprimed and primed iMac supernatant (n=3). D) LDH concentration measurement from the supernatant of reconstituted iMacs upon LPS-priming and nigericin, R837, and poly(dA:dT) treatment (n=3). Experiments were conducted by Matthew Mangan. * $p<0.05$ according to one-way ANOVA test with Sidak correction. Graphs and statistics were generated by Alexander Weber.

Expression of NLRP3 was similar in all reconstituted cell lines (see figure 3.16). Stimulation of the cells with LPS alone did not lead to IL-1β production, as expected, and the cell lines were capable of priming at same extent, as released TNFα concentrations were comparable. Stimulating the cells carrying Y>F mutant NLRP3 with nigericin led to the reduction of the produced IL-1β levels to approximately half of that of the WT NLRP3 iMacs. Even more striking was the effect of the Y>F mutations on the NLRP3 stimuli R837: iMacs carrying the Y>F mutations did not respond to R837 stimulation with IL-1β release, whereas WT cells produced significant amounts of IL-1β when stimulated with R837. There were no differences between the cell lines in IL-1β release when the AIM2 inflammasome was triggered with poly(dA:dT) (pathway independent of NLRP3). The pattern of LDH release followed that of IL-1β production: the more cytokine release, the more cell death via pyroptosis leading to LHD leakage.

These results clearly indicate that the possibility of the phosphorylation of the residues Y136/Y140/Y143/Y168 is required for fully NLRP3 inflammasome formation and IL-1β production.

3.6. CAPS mutations act independently of Golgi shuttling and downstream of BTK

While this work was performed, a study measuring the potency of novel NLRP3 inhibitors (produced by the company IFM) on PBMCs from patients carrying NLRP3 point mutations leading to CAPS was conducted. In parallel to the novel inhibitors, the cells were treated with ibrutinib to test whether ibrutinib was able to block spontaneous NLRP3 inflammasome assembly and IL-1β release. In parallel with the patients, PBMCs from healthy donors were also stimulated and treated with ibrutinib. Released IL-1β was measured in the supernatant.

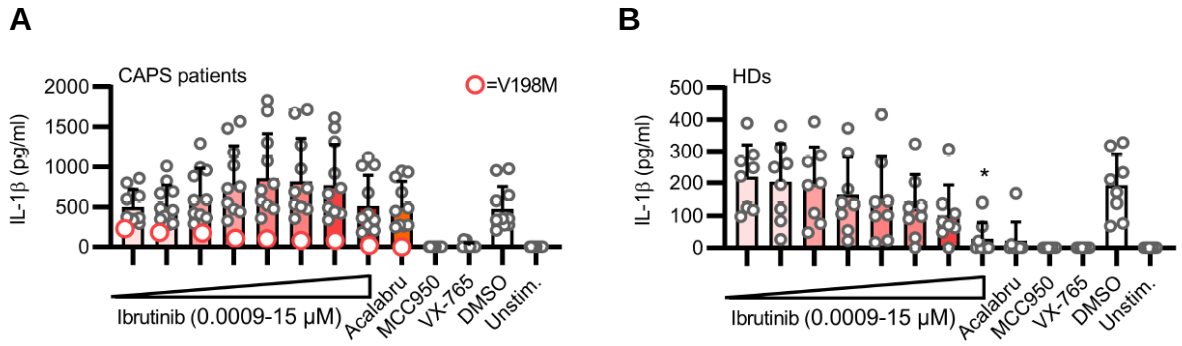

Figure 3.17. IL-1β release from CAPS and healthy PBMCs upon BTK kinase inhibition.

A)+B) PBMCs from CAPS (A) and healthy (B) donors were primed with LPS and treated with different concentrations of the BTK kinase inhibitors ibrutinib, acalabrutinib, the NLRP3 inhibitor MCC950, the caspase-1 inhibitor VX-765 or DMSO. IL-1β concentrations in the supernatant were measured by ELISA. IL-1β concentrations in the supernatant were measured by ELISA. Data generated by Sabine Dickhöfer.

Even though ibrutinib dose-dependently blocked IL-1β release from healthy PBMCs, it did not inhibit IL-1β production from CAPS patient PBMCs. Interestingly, the single patient alone carrying a mutation in the PYD/NACHT linker, namely V198M, showed a response to ibrutinib-treatment, similar to the healthy donors. These results indicate that BTK acts upstream of the CAPS mutations and the CAPS mutations lead to NLRP3 inflammasome assembly independent of BTK kinase activity, Golgi shuffling and release.

3.7. Summary of the results and graphical abstract

The presented results further describe the already observed relationship between BTK and NLRP3 during inflammasome activation: BTK not only increases IL-1β release by physical interaction but facilitates inflammasome formation by phosphorylating four tyrosine residues: Y136/Y140/Y143 and Y168. Y136/Y140/Y143 are located in the polybasic region, with which NLRP3 binds to negatively charged phospholipids on the trans-Golgi network. Phosphorylation of these residues presumably facilitates the release of NLRP3 from the trans-Golgi network by phosphorylation-mediated charge-switch of the polybasic region (positive to negative), which supports NLRP3 oligomerization, inflammasome formation and IL-1β release. This hypothesis is supported by the observations that NLRP3 in stimulated WT BMDMs shifts away from the heavy membrane P5, whereas in *Btk* KO BMDMs, NLRP3 stays on the P5 during the course of nigericin stimulation.

Furthermore, phosphomimetic Y>E mutated polybasic region shows reduced binding to PI4P coated beads *in vitro*. Finally, iMacs harboring Y136F/Y140F/Y143F/Y168F mutated human NLRP3 produce significantly reduced IL-1β compared to iMacs carrying WT human NLRP3.

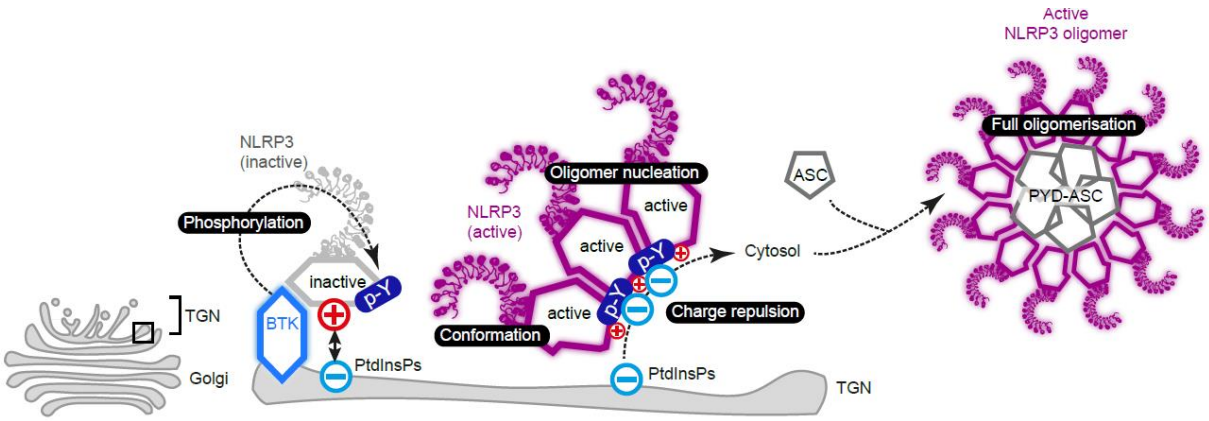

Figure 3.18. Graphical abstract of the mechanism by which BTK facilitates NLRP3 inflammasome formation.

BTK and NLRP3 interact on the P5 heavy membrane, where BTK presumably phosphorylates NLRP3 at four Y residues, thereby modifying the charge of the P5 membrane-binding polybasic region of NLRP3. NLRP3 P5 binding is thus weakened and NLRP3 oligomerization in the cytosol is facilitated, leading to increased IL-1β production. Figure generated by Alexander Weber.

4. DISCUSSION

4.1. BTK is a positive regulator of the NLRP3 inflammasome

BTK was identified as a positive regulator of the NLRP3 inflammasome in parallel in two independent studies: by Ito (Ito et al. 2015) and by our research group (Liu et al. 2017). These two studies used distinct approaches to study this topic: while Ito tested several different inhibitors in NLRP3 inflammasome activating set-ups in THP-1 cells and measured IL-1β release, our research group performed a phosphoproteomics screen in again THP-1 cells and compared phosphorylated peptide profile between resting and activated cells. Ito spotted that both the BTK inhibitor ibrutinib and a Syk inhibitor, (Syk is upstream of BTK in the signal cascade in B cells), blocked IL-1β processing in THP-1 cells. Our research group found a BTK peptide containing phosphorylated Y551 to be significantly upregulated in stimulated THP-1 cells. Y551 is phosphorylated by Syk promoting BTK activation. These results clearly indicated a role of BTK in NLRP3 inflammasome activation, and this activating function was verified by our team in primary human and murine immune cells using BTK inhibition and genetic BTK deletion. These conditions all showed a reduced NLRP3 inflammatory phenotype characterized by diminished ASC-speck formation, caspase-1 cleavage and IL-1β maturation.

These studies nicely complement each other. Given that BTK inhibitors, as described in section 1.5.4. are not exclusively targeting BTK, but some may target other Tec family kinases and additionally EGFR and JAK3 as well, it would thus be a hasty conclusion to focus solely on BTK as an NLRP3 regulator only based on BTK inhibitor application. The proteomics screen, nevertheless, unambiguously identified the phosphorylated BTK fragment, thereby ruling out other Tec family kinases as potential NLRP3 regulators. It is noteworthy that BTK inhibition by ibrutinib or genetical BTK ablation reduced IL-1β release however significantly, but not to baseline levels.

This effect could have multiple underlying reasons: it might be possible that once BTK is inactive, another Tec family kinase resumes BTK´s role in NLRP3 inflammasome regulation, given the structural and functional similarities between Tec family kinases. Even though inhibitors would block several Tec family kinases, the fact that BTK-specific genetic deficiency leads also to partial NLRP3 inflammasome inhibition underpins this theory. Another, probably more likely explanation to the phenotype elicited by BTK depletion is the

hypothesis that the regulatory effect that BTK carries can be compensated by other, Tec family kinase independent mechanisms or regulators, such as Nek7 for potential scaffold roles of BTK, or other kinases for phosphorylation of NLRP3 inflammasome components. BTK, even though a significant regulator of the NLRP3 inflammasome, is not an "all or nothing" component of the complex as e.g. ASC.

4.2. BTK and NLRP3 interact in primary cells

Ito et al. ruled out several mechanisms by which BTK could control the NLRP3 inflammasome: BTK did not act via upregulating intracellular Ca^{2+} concentrations similarly to its functions in B cells (as described in 1.5.2.), BTK could not be shown to be involved in phagocytosis or priming of the NLRP3 inflammasome, and lysosome rupture was also demonstrated to be independent of BTK (Ito et al. 2015).

Regulation of NLRP3 activity via interaction partners, such as Nek7, was previously proposed by multiple research groups (Y. He et al. 2016; Sharif et al. 2019) as described in the introduction 1.4.8. Nek7 is a mitotic kinase that facilitates NLRP3 oligomerization, nonetheless most probably only in interphase of the cell, via direct binding of NLRP3. NLRP3 was shown to interact via its LRR and NACHT domains with the C-terminal fold of Nek7 (Sharif et al. 2019). Active NLRP3 oligomer ring model shows further interaction between Nek7 and in the ring adjacent NLRP3 molecule.

Furthermore, SGT1, a ubiquitin ligase-associated protein, and HSP90, a heat shock protein, were also shown to convergently regulate NLRP3 inflammasome activation via interaction (Mayor et al. 2007). SGT1/HSP90 dimer binds and guards NLRP3 from lysosomal destruction.

Accordingly, Ito found that NLRP3 and BTK interacted in murine peritoneal macrophages, using in situ proximity ligation assay but not co-immunoprecipitation. Furthermore, they identified that overexpressed NLRP3 NACHT and LRR domains bound to BTK SH2, SH3 and TK domains using co-IPs from HEK293T cells. They, however, hypothesized primarily scaffold functions of BTK in NLRP3 inflammasome activation – despite the fact that the kinase inhibitor ibrutinib also showed significant effects in their studies.

In this study, we aimed to further clarify the connection between BTK and NLRP3 in primary cells. Therefore, co-immunoprecipitation experiments were conducted upon stimulation of the NLRP3 inflammasome to follow the kinetics of NLRP3 and BTK interaction, using primary NLRP3 antibody. As shown in figure 3.2., BTK and NLRP3 constitutively interacted in primary cells, even before priming of the cells. Furthermore, BTK and NLRP3 were found in the same P5 fractions in BMDMs (see figure 3.11.). BTK bound NLRP3 also *in vitro*, and HEK293T overexpression experiments from Ito could be successfully reproduced with similar results, showing stable binding of BTK and NLRP3. In HEK293T cells, as well as in primary cells, neither ibrutinib (3.2.) nor MCC950 influenced BTK-NLRP3 interaction.

These observations indicate fairly strong binding between the proteins as small molecules could penetrate the complex without disturbing the interaction. At least, the NLRP3/BTK interacting areas do not completely overlap with the binding sites of the inhibitors.

Even though in this study the kinase activity of BTK as the key event in NLRP3 regulation was concentrated on, scaffold functions of BTK for NLRP3 inflammasome assembly (e.g. via facilitating NLRP3 and ASC binding), as suggested by Ito, could still not be ruled out, given that NLRP3 and BTK interact already at steady state, and stay together during priming, activation, and assembly of the NLRP3 inflammasome complex, as found in the fractionation and SEC experiments conducted with LPS-primed and nigericin treated BMDMs (see figure 3.14.).

It would be interesting to investigate how the interaction between NLRP3 and BTK alters over time: why does BTK bind NLRP3 already before and during the priming phase? Does BTK stabilize monomeric NLRP3? Is the conformational change of NLRP3 upon stimulation and activation supported by BTK? Is there plasticity between the interacting domains? Nonetheless, one could argue that ibrutinib treatment (which only inhibits the kinase activity of BTK and does not disturb NLRP3/BTK interaction, thus hypothetical BTK scaffold functions would stay intact) reduced IL-1β production similarly to that of *Btk* KO cells (see figure 3.1.); whereas if a scaffold function would significantly contribute to NLRP3 activation additionally to BTK´s kinase activity, ibrutinib should have less of an effect than complete absence of BTK. It would be interesting to see, whether treatment of *Btk* KO BMDMs with ibrutinib would further block IL-1β release from the cells.

Nonetheless, the role of BTK/NLRP3 interaction in NLRP3 inflammasome activation and assembly still remains elusive and needs to be further explored. As a starting point, one could investigate which domains of NLRP3 and BTK interact before, and during priming, and upon nigericin stimulation (e.g. via co-expression of truncated proteins in HEK293T cells).

4.3. NLRP3 tyrosine phosphorylation is dependent on BTK

Based on the results that showed that inhibiting BTK´s kinase activity by the application of ibrutinib or other kinase inhibitors reduced IL-1β release from primary human immune cells to a similar extent as genetic BTK ablation (see figure 3.1.), we hypothesized that BTK´s kinase activity plays a major role in NLRP3 inflammasome regulation. This hypothesis was further supported by the findings of the phosphoproteomics screen, namely that BTK was rapidly tyrosine phosphorylated upon nigericin treatment, which is the upstream event before BTK becomes active as a kinase.

To test this hypothesis, we compared tyrosine phosphorylation of NLRP3 in *Btk* KO, ibrutinib treated WT with WT, LPS-primed and nigericin treated primary immune cells (see figure 3.4.). We observed reduced tyrosine phosphorylation of NLRP3 in conditions where BTK was inhibited or genetically deleted. Tyrosine phosphorylation was increasing with time upon nigericin treatment, peaking at 10 min in murine cells, and decreasing with further time elapse. In human cells, however, tyrosine phosphorylation increased until 20 min post nigericin addition. BTK tyrosine phosphorylation mirrored NLRP3 tyrosine phosphorylation, showing a continuous kinase activity of BTK (see 3.4.). We did not analyze tyrosine phosphorylation of NLRP3 at later time points than 20 min after nigericin application. It would be intriguing to measure the duration of NLRP3´s BTK-dependent tyrosine phosphorylation in human cells and determine the kinetics of tyrosine phosphorylation turnover, as observed in murine cells after 10 min. To this end, stimulating PBMCs with nigericin for longer time-periods (e.g.30 min, 45 min, 60 min) and p-Y IP followed by NLRP3 immunoblot could be conducted. Other studies (Spalinger et al. 2017), investigating effects of tyrosine phosphatases on NLRP3 activity, also analyzed longer time periods upon nigericin treatment (up until 60 min), so a protracted effect of NLRP3 phosphorylation by BTK might be possible.

The difference between murine and human tyrosine phosphorylation kinetics could be explained by the inhomogeneity of the human sample (PBMCs) comprising multiple cell types, whereas BMDMs in the murine system represent a more homogeneous cell population. Furthermore, the involvement and kinetics of a possible phosphatase (to date not identified), which might reverse the tyrosine modification applied to NLRP3 by BTK, might work on a different time scale between species, and, however unlikely, might involve distinct phosphatases. Furthermore, the kinetics of NLRP3 activation might also differ between murine and human cells. This might be reflected on the differences in the optimized stimulation protocol of murine and human cells: human cells are treated merely one hour with nigericin, longer times do not increase released IL-1β levels, as cell death at later times also becomes significant; whereas BMDMs are stimulated for two hours with nigericin for optimal cytokine release, implying slightly slower inflammasome assembly kinetics.

To test NLRP3 tyrosine phosphorylation in an easy-to-use manipulate and accessible system, HEK293T cells were co-transfected with NLRP3 and BTK, as HEK293T cells do not express these proteins endogenously. Solely the co-transfection was sufficient for phosphorylation of NLRP3 by BTK, LPS and nigericin treatment of the cells was not necessary to trigger BTK´s kinase activity, as in the primary cells. This might be explained by the high amounts of translated proteins upon transfection. The HEK293T system proved to be very advantageous in “yes or no” NLRP3 tyrosine phosphorylation questions, nonetheless, this model did not copy the situation in primary cells and fine dynamics of stimulus-dependent NLRP3 tyrosine phosphorylation by BTK could not be examined using this technique. To address the kinetics of NLRP3 Y phosphorylation by BTK, one could consider using BlaER1 cells, a human B cell line that can be transdifferentiated to macrophage-like cells via induction of the C/EBPα transcription factor (Rapino et al. 2013). These BlaER1 macrophages express NLRP3 and NLRP3 function is in many aspects comparable to human macrophage inflammasome (Gaidt et al. 2018). The BlaER1 cell line can be relatively easily modified via CRISPR/Cas9 gene editing. Thus, one could generate BlaER1 lineages harboring different BTK mutants, stimulate the NLRP3 inflammasome, perform co-IP (NLRP3/BTK) and measure NLRP3 tyrosine phosphorylation without any limitation of the conditions due to low cell numbers.

To show that NLRP3 tyrosine phosphorylation by BTK is a physiological event, in future work, NLRP3 tyrosine phosphorylation *in vivo* will be also assessed upon intraperitoneal LPS injection (4 h) followed by 15 min, 30 min, and 1 h ATP injection in WT and *Btk* KO mice.

NLRP3 tyrosine phosphorylation will be measured using p-Y IP conducted from infiltrated peritoneal cells, as well as splenocytes. Additionally, released cytokines will be measured from peritoneal lavage.

4.4. BTK phosphorylates four NLRP3 tyrosine residues

The above mentioned HEK293T co-expression system was essential in finding the tyrosine residues phosphorylated by BTK. The truncated NLRP3 versions (single domains together with linker regions) revealed that solely the construct containing the PYD/NACHT linker and the NACHT domain was phosphorylated by BTK in HEK293T cells. We aimed to identify the phosphorylated Y residues via mass-spectrometry. However, sequence coverage of human NLRP3 was low, and especially the PYD/NACHT linker region where the target residues are located was not available (see Appendix 6.4.).

Nonetheless, the *in vitro* kinase assay with 15mer NLRP3 Y peptides exposed all four tyrosine residues that were phosphorylated by BTK: Y136, Y140, Y143, Y168. The combination of these residues was confirmed in HEK293T cells using FL NLRP3 harboring Y>F mutations at the aforementioned residues, which displayed tyrosine phosphorylation comparable to the background signal.

Interestingly, when testing single Y>F mutants for phosphorylation by BTK in HEK293T cells, alone the Y168F mutant showed significantly reduced tyrosine phosphorylation, nonetheless still considerably higher than the background. It can be speculated that Y168 is phosphorylated first by BTK, and this event is upstream of the phosphorylation of the other three tyrosines (Y136, Y140, Y143). This would explain why the mutation of the single residue could show a significant effect: as Y168F could not be phosphorylated, Y136, Y140, and Y143 were less likely to be phosphorylated and the phosphorylation signal in total weakened.

This upstream impact could be carried out via a conformational change of NLRP3 triggered by phosphorylation of Y168. Nonetheless, the recent cryoEM structure (PDB 6NPY) of NLRP3 shows partial accessibility of Y136, Y140, and Y143 in the inactive conformation of NLRP3 (see figure 4.1.). However, how the PYD interferes with this region is still not solved. Furthermore, as phosphorylation of NLRP3 by BTK happens after the priming step, it is conceivable that NLRP3 holds an altered conformation at this stage compared to the inactive

form, hindering the accessibility of Y136, Y140, and Y143 to BTK.

Y168 lies closely to the suspected ADP binding site in the inactive conformation (see figure 4.1.). Thus a role in controlling ATP binding of NLRP3 could be hypothesized. ATP is needed for conformational change and activation of NLRP3 as its hydrolysis is thought to provide the activation energy for conformational change. It is conceivable that Y168 might stabilize the inactive conformation of NLRP3, until it is phosphorylated by BTK, which promotes the open or active NLRP3 conformation. To test whether phosphorylation of Y168 prompts a conformational change of NLRP3, a BRET assay (Compan, Baroja-Mazo, Bragg, et al. 2012) could be conducted, comparing the WT and Y168F construct in the presence or absence of BTK. In the BRET assay, cells (e.g. HEK293T), carrying NLRP3 with a donor and an acceptor molecule on one-one end are stimulated and the released bioluminescence that is generated by the donor activating the acceptor, if closely together, is measured. When NLRP3 is in a closed inactive conformation, released luminescence is high, whereas when it is activated and open, energy transfer between donor and acceptor molecules decreases and so does the generated luminescence.

Alternative to BRET, one could conduct limited proteolysis of recombinant WT and Y168F NLRP3. The digestion pattern of both proteins could be compared and analyzed via mass-spectrometry. Based on the regions that are accessible to the used enzyme the conformation of WT vs. Y168F NLRP3 could be deduced.

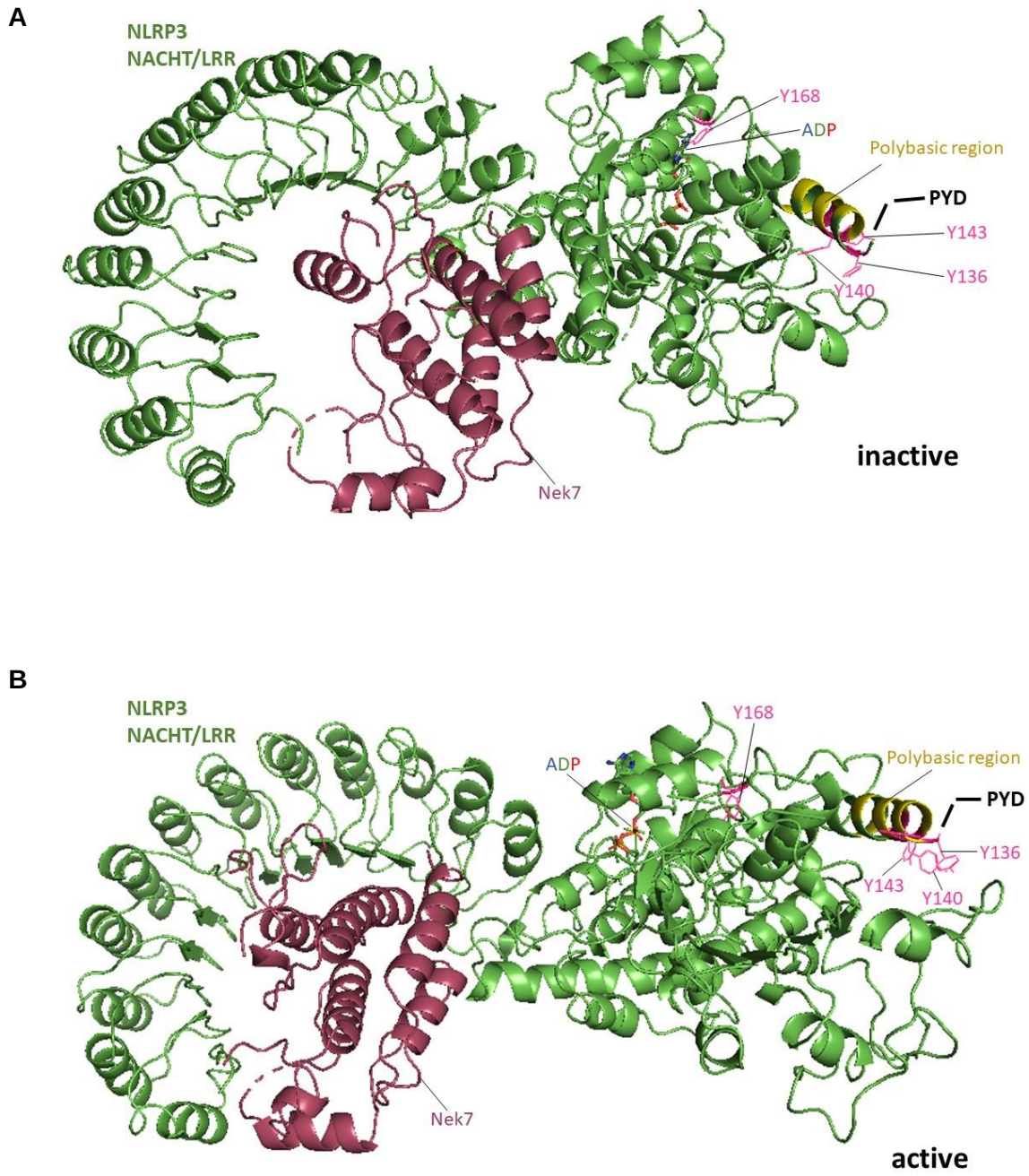

Figure 4.1. Visualization of the tyrosine residues in the polybasic region.

A) CryoEM structure PDB 6NPY was used to visualize the orientation of the polybasic tyrosine residues Y136, Y140 and Y143, as well as Y168 in the inactive conformation. Y168 lied closely to ADP, and the polybasic tyrosine residues are pointing to diverse directions. B) Analysis of the orientation of the tyrosine residues phosphorylated by BTK on the structure model of the hypothetical active conformation of NLRP3. Y168 moved away from ADP and the polybasic Y residues are now stacked. PDB files were kindly provided by Liudmila Andreeva (Sharif et al. 2019).

It was rather surprising to find no less than four tyrosine residues of NLRP3 that are modified by BTK. This explains why single mutations initially were not sufficient to identify all modified sites in the HEK293T assay. However, a previous study reported that BTK phosphorylates multiple (3) tyrosine residues of the adaptor molecule Mal (Gray et al. 2006). In the case of Mal, the phosphorylation events occur consequent to each other, with the first one leading to conformational change making the other residues accessible for further phosphorylation, similarly to the proposed mechanism in case of NLRP3 and BTK.

It would be compelling to use antibodies that are directed against single phospho-tyrosine residues of NLRP3 or the fully phosphorylated Y136/Y140/Y143 motif. These could be applied *in vitro* in parallel using the same sample for immunoprecipitation upon NLRP3 stimulation in primary cells or might even enable detection of phospho-NLRP3 in lysates without the need for IP. Alternative applications would be a phospho-specific ELISA or phospho-flow. The results of a time series involving such reagents could illuminate the sequence of tyrosine phosphorylation in time, as distinct antibodies would detect the abundant tyrosine phosphorylated NLRP3 possibly at different time-points upon nigericin treatment. Comparing the pattern of the immunoprecipitations or flow data from the same samples using separate p-Y specific antibodies would contribute to generating a complete temporal pattern of tyrosine phosphorylation of each single Y of NLRP3 by BTK. These p-Y specific antibodies could as well be applied with samples from *in vivo* experiments, after intraperitoneal LPS and ATP injection. Furthermore, the use of such reagents to monitor NLRP3 activity in clinical samples could be envisaged. Vaccinations to generate such reagents are already under way and initial sera will be tested soon. The point mutations generated here may be useful to demonstrate specificity of the antibodies.

4.5. BTK regulates NLRP3 organelle localization

It was interesting to notice that Y136, Y140, and Y143 reside within the polybasic region of NLRP3, with which NLRP3 locates to the negatively charged PI4P at the trans-Golgi network (J. Chen and Chen 2018). It was plausible to hypothesize that phosphorylation of these tyrosine residues serves a charge alteration of this region to separate NLRP3 from the Golgi, allowing full NLRP3 inflammasome assembly in the cytosol.

We used two slightly different approaches and angles to test and prove this hypothesis: an indirect approach, measuring the protein (NLRP3 and BTK) amount in distinct cell fractions corresponding to separate organelles upon NLRP3 stimulation in BMDMs, hoping to catch shifts of protein between fractions; and a more straightforward, charge-directed approach, testing the binding of WT polybasic region, or a phosphomimetic Y>E, or the positive to neutral K>A variant to PI4P lipid coated beads. If our hypothesis would hold true, we would expect to see a decrease of NLRP3 in the Golgi fraction over time upon stimulation of primary cells, and a less PI4P binding of expressed protein when the positivity of the polybasic region is disturbed either via E instead of Y (additional negative charge) or via A instead of K (loss of positive charge).

In fact, we could see the redistribution of NLRP3 between cell compartments in WT BMDMs upon NLRP3 stimulation, namely NLRP3 dissociated from the Golgi fraction, whereas in *Btk* KO cells NLRP3 concentrations in the Golgi fraction stayed nearly constant.

In case of the PI4P bead binding assay, we could detect reduced binding of the Y>E mutant or the K>A mutant to the beads. Repeating the experiment with full-length WT and Y>F or K>A NLRP3 instead of the shorter linker and polybasic region constructs would confirm that modifying the charge of the polybasic tyrosine residues affects PI4P binding of the native NLRP3.

Furthermore, it would be exceedingly valuable to establish the microscopy approach that Chen utilized in their publication: they measured co-localization of the trans-Golgi network and NLRP3 using HeLa cells stably expressing NLRP3-GFP (green fluorescent protein) and added the trans-Golgi network marker TGN38 (J. Chen and Chen 2018). They then quantified the overlapping spots, showing that the more K>A mutations in the polybasic region present, the less co-localization detected. Using the same principle, we could possibly show that instead of deleting positivity, introducing negativity via Y>E mutations thereby mimicking phosphorylated Y residues could also reduce NLRP3 localization to the trans-Golgi network.

Besides HeLa cells, Chen et al utilizes primary cells, interestingly ASC deficient primary BMDMs; and mentions that NLRP3 oligomers observed at the Golgi membrane in these cells were distinct from large oligomers in the cytosol when ASC was present. The reason why Chen preferred ASC deficient cells might be that ASC quickly “hijacks” NLRP3 from the Golgi membrane into larger complexes, and the relevance and effect of this pre-activation state at the Golgi membrane would submerge. For this reason, it would be appealing to repeat

the cell-fractionation NLRP3 localization experiment using *Pycard* KO instead of WT, and *Pycard/Btk* double KO BMDMs instead of *Btk* KO cells (the ASC in *Btk* single KO would falsify the results) for a stronger difference in NLRP3 re-distribution between the genotypes.

Furthermore, the PI change upon NLRP3 phosphorylation in this study is calculated and not measured. It would be informative to experimentally detect the difference of the PI between phosphorylated and non-phosphorylated polybasic region, e.g. via pH titration with NaOH either using phosphorylated and non-phosphorylated peptides of the polybasic region, or full-length NLRP3 before and after *in vitro* kinase assay with BTK.

Once the polybasic region of NLRP3 has bound to the Golgi membrane, this interaction might mask the polybasic tyrosine residues. Therefore, tyrosine phosphorylation of Y168 might be necessary for a conformational change that leaves the polybasic residues accessible for phosphorylation at the Golgi membrane. In this scenario phosphorylation of Y168 would solely control NLRP3 conformation and would serve no charge-altering functions. Consistent with this theory, we should find phosphorylation of Y168 to occur first, and phosphorylation of the polybasic tyrosine residues should take place consequent to Y168 phosphorylation, and probably simultaneously to most efficiently promote charge-switch of the polybasic region.

A principal similar to our hypothesis has been described by the Zhang et al. (Z. Zhang et al. 2017). They reported that NLRP3 inflammasome activation induced clustering of mitochondria-associated endoplasmic reticulum membranes (MAMs) and DAG, and it´s effector molecule PKD to the Golgi. They showed that NLRP3 formed oligomers on these Golgi-proximal membranes, where PKD phosphorylated NLRP3 at the residue S293 (murine). Association of NLRP3 with MAMs prior inflammasome assembly had been described before (Zhou et al. 2011; Missiroli et al. 2018). Zhang et al. elaborates these observations by showing that phosphorylation of S293 by PKD facilitates the release of NLRP3 from the MAMs and inflammasome assembly in the cytosol. These events proved to be upstream of NLRP3, as *Nlrp3* KO cells showed similar translocation phenotype to WT BMDMs. PKD was substantial for NLRP3 inflammasome activation, because PKD deficient cells produced reduced cleaved IL-1β. Phosphorylation of NLRP3 by PKD is downstream of CAPS mutations, because PKD deletion inhibited IL-1β release from cells carrying CAPS mutations.

Even though parallels with Zhou´s and Zhang´s observations and Chen´s and our work can be declared (release of NLRP3 from an organelle membrane upon phosphorylation), these two studies, nevertheless similar, describe NLRP3 inflammasome activating events that probably occur independently from each other, at distinct levels.

Zhang et al. was however looking for Golgi and NLRP3 co-localization, they could not detect such. In their system NLRP3 could be found solely at MAMs. Golgi was functioning as a DAG and PKD retaining organelle, but not as an NLRP3 organizing organelle. Interestingly, in B cells, BTK is upstream of DAG production upon BCR engagement. Thus, if the NLRP3 inflammasome assembly took place in B cells (similarly to macrophages), BCR activation might also lead to NLRP3 activation via BTK, DAG, and PKD signaling, as described by Zhang, and BTK and PKD NLRP3 activating signaling pathways would on multiple levels merge.

Nonetheless, in Chen´s publication, NLRP3 was solely found at the trans-Golgi network and not at mitochondrial membranes. Underlying reasons could be distinct cell types (both utilize BMDMs as well though), or differences in the handling and activation of the cells, and in microscopy markers and techniques. Zhang et al. do not propose a mechanism by which NLRP3 binds to MAMs, but only one how it is released from the MAMs upon phosphorylation by PKD. In the discussion they speculate that membrane binding of NLRP3 is dependent on the N terminal sequence of the PYD, and the phosphorylation of S293 leads to a conformational change of NLRP3 and thereby release from the MAMs, or alternatively the release of phosphorylated NLRP3 is supported by a chaperone. The work from Zhang et al. focuses more on a cellular than a molecular level, incorporates mouse models and does not offer further mechanistic details besides the phosphorylation into the regulatory process.

In contrast, Chen et al. concentrate solely on the mechanistic events of NLRP3 Golgi binding. They show that the polybasic region of the PYD/NACHT linker is responsible for binding to the specific phospholipid, PI4P at the trans-Golgi network, and that this sequence functions similarly to a PH domain. Nevertheless, they did not investigate the impact of the NLRP3-Golgi binding on cytokine release: K>A mutated NLRP3 formed indeed reduced puncta at the trans-Golgi membrane, however it would have been informative to measure IL-1β processing from the cells expressing this mutant instead of WT NLRP3.

As Zhang et al. continued the examination of the NLRP3 MAM-binding/activating pathway that Zhou et al. proposed, this work complements the NLRP3 activating model that Chen et al. described. Chen et al. does not engage with the mechanism by which NLRP3 is release from the pre-activated pre-oligomeric state at the trans-Golgi membrane to form full inflammasome complexes in the cytosol.

As BTK phosphorylates tyrosine residues in the polybasic region, we introduced the working model, which describes that charge switch of the polybasic region elicited by this phosphorylation event disturbs NLRP3 binding to the negatively charged PI4P and supports NLRP3 assembly in the cytosol.

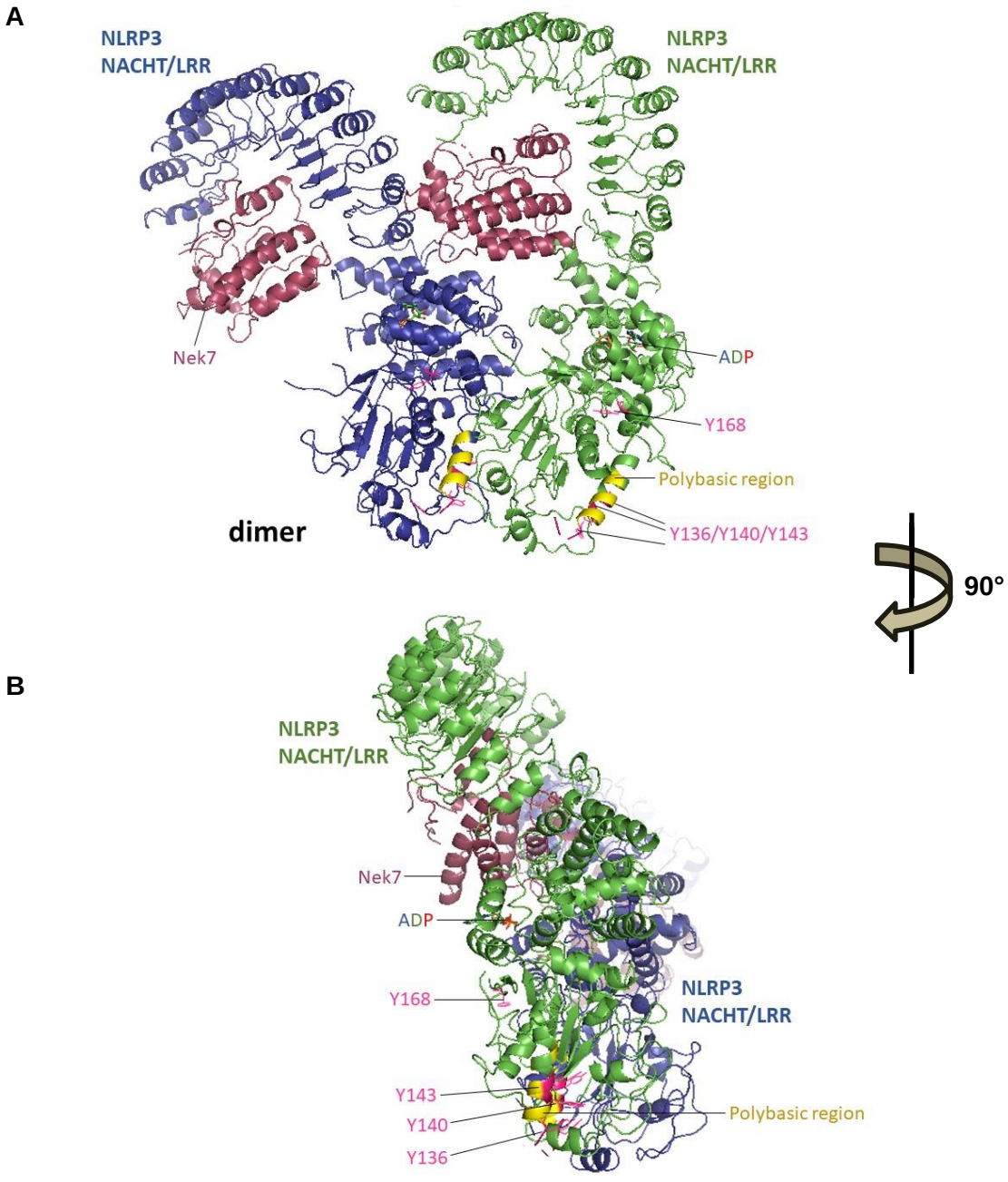

Figure 4.2. Structure of the hypothetical active NLRP3 dimer.

A) In the NLRP3 dimer, the polybasic region faces outwards together with Y168, whereas Y136, Y140, and Y143 face inwards, which is better distinguishable in B). Y168 lies accessible for phosphorylation and the polybasic region for binding to PI4P on the Golgi. PDB file of the model was provided by Liudmila Andreeva, Boston, USA from Sharif et al.

It can be noticed that in the hypothetical dimer of NLRP3 (see figure 4.2.), the polybasic region (yellow) is facing outwards, enabling the binding to PI4P at the trans-Golgi network. Furthermore, Y168 is located in a flexible loop, also pointing outwards and being accessible for phosphorylation by BTK. Nonetheless, the polybasic tyrosine residues are stacked and facing inwards, being less accessible for BTK phosphorylation. Based on this model, it is likely, as described above, that BTK first phosphorylates Y168, leading to a conformational change in NLRP3 that results in a slight rotation of the polybasic region, leaving the polybasic tyrosine residues available for phosphorylation by BTK, charge switch elicited by the negative phospho-groups and finally the release of NLRP3 from the trans- Golgi network.

The reconstitution NLRP3 deficient iMacs with Y136FY140FY143F mutant NLRP3 gave us a first insight that the phosphorylation of the polybasic region is functionally relevant (see figure 3.16.): if this region could not be phosphorylated (Y>F mutations) IL-1β processing upon stimulation was diminished. Nigericin treatment of the Y>F cells led to reduced IL-1β release to half compared to WT cells, indicating that the function was not completely compromised by the introduced mutations. Interestingly, treatment of the Y>F reconstituted cells with R837 led to no IL-1β production. These results indicate that nigericin and R837 trigger distinct NLRP3 inflammasome activation pathways and the extent of BTK-dependency between these pathways is different: while the pathway triggered by nigericin only partially relies on the phosphorylation of the polybasic region (IL-1β production is only reduced from the Y>F mutant cells), the pathway triggered by R837 treatment is entirely dependent on the phosphorylation of the polybasic region by BTK (Y>F cells produce no IL-1β). It would be intriguing to analyze how NLRP3 phosphorylation occurs upon R837 treatment in BMDMs and PBMCs and compare it with the results obtained upon nigericin activation.

Furthermore, using Y168F and an intact polybasic region variant would show, whether phosphorylation of Y168 is upstream of the phosphorylation of the polybasic region Y residues: if yes, IL-1β would be diminished in Y168F similarly to Y136FY140FY143F.

Zhang et al. hypothesize that phosphorylated-S293 would prevent NLRP3 binding to the MAMs, and cells carrying S293E mutated NLRP3 indeed produced reduced IL-1β. In line with this theory, polybasic region carrying K>A or Y>E mutations should act upstream of the Golgi and inhibit binding of NLRP3 to the trans-Golgi network, thereby resulting in reduced IL-1β production, as opposed to an increased dissociation of NLRP3 from the Golgi, leading to increased NLRP3 inflammasome assembly in the cytosol. Future work should investigate the above-mentioned situations and clarify the significance of NLRP3 Golgi binding for mature IL-1β release.

As described in the introduction (see section 1.4.) based on previous publications, NLRP3 activation is perplexing, highly complex, multilayered and manifold. I find it very plausible that the observations by Zhou and Zhang and Chen and myself are not conflicting, but instead both valid in certain NLRP3 activating situations, stimuli and cell types. To obtain unified concepts, research groups studying NLRP3 inflammasome signaling should test their hypothesis is several, standardized conditions and cells.

4.6. BTK deficiency leads to reduced cytosolic NLRP3 oligomerization

In line with the hypothesis that release of NLRP3 from the trans-Golgi network for full inflammasome assembly is BTK operated phosphorylation-dependent, we anticipated to find less NLRP3 oligomers in the cytosol in BTK kinase-inhibited or BTK deficient cells.

Interestingly, SEC experiments revealed that BTK inhibition by ibrutinib blocks NLRP3 oligomerization to a similar extent as MCC950, which is a potent NLRP3 inhibitor that was proven to constrain NLRP3 oligomerization. Even though the difference in oligomer size between WT and BTK deficient or MCC950-treated was not immense, the fact that BTK-deficiency was comparable to the negative control MCC950 proves reliability of the data. The minimal shifts in oligomerization state might be due to the limitations of the SEC assay, especially using the Superdex 200 increase 10/300 GL column that is not ideal for the separation in this high MW range. Repeating the experiments using a Superose 6 Increase column might show more precise differences in NLRP3 oligomerization between conditions.

It would be intriguing to visualize the direct effect of NLRP3 tyrosine phosphorylation by BTK on NLRP3 oligomerization. To this end, performing SEC experiments with samples before and after *in vitro* kinase assay using recombinant NLRP3 and BTK would be plausible.

One could test Y168F and polybasic Y>F mutant NLRP3 as well. These experiments would reveal whether BTK influences NLRP3 oligomerization directly via interaction or phosphorylation, or NLRP3 oligomerization and inflammasome assembly in the cytosol is only facilitated by BTK-mediated NLRP3 release from the Golgi.

4.7. NLRP3 tyrosine phosphorylation is upstream of CAPS mutations

In a previous study conducted by our research group (Liu et al. 2017) inhibition of IL-1β release by Muckle Well´s patients, a type of CAPS, using ibrutinib was successful. However, PBMCs from only three patients were analyzed. Parallel to my work, our research group was part of a bigger study that aimed measure how CAPS patients respond to novel NLRP3 inhibitor treatment (study together with the company IFM), and to ibrutinib.

Surprisingly, ibrutinib treatment did not decrease, but instead significantly increase IL-1β release from CAPS patients.

One single CAPS patient, carrying the V198M responded to ibrutinib treatment with reduced IL-1β release. It is quite intriguing that V198 is close to the polybasic region, yet solely this mutation did not lead to ibrutinib resistance. Mutation of V198 residue might stabilize NLRP3 in a position that is similar to WT NLRP3 and thus V198M NLRP3 still responds to ibrutinib treatment. On the other hand, the V198M donor had a generally rather low level of response. Responsiveness to ibrutinib of further patients carrying a mutation close to the polybasic region would be very informative. Furthermore, checking the genotype of the patients that were responsive to ibrutinib in course of the previous study would reveal which type of mutations still leave NLRP3 ibrutinib responsiveness intact.

CAPS mutations irresponsive to ibrutinib might change NLRP3 conformation in a way that their self-oligomerization becomes independent of pre-oligomerization on the Golgi and thereby of phosphorylation by BTK. To further assess this theory, it would be helpful to measure tyrosine phosphorylation of CAPS NLRP3 by BTK. Should CAPS NLRP3 oligomerization be independent of Golgi binding, the tyrosine phosphorylation by BTK might even be reduced compared to WT NLRP3 upon inflammasome stimulation. In a preliminary experiment, I indeed observed reduced NLRP3 tyrosine phosphorylation in PBMCs isolated from a CAPS patient upon inflammasome activation.

4.8. Upstream events of BTK in NLRP3 inflammasome signaling

It still remains elusive what the upstream events of BTK in the signal cascade are. In my hands NLRP3 stimulation was most successful using the common NLRP3 activator nigericin. Thus, for further analysis I used nigericin to trigger NLRP3 inflammasome assembly. Nonetheless, I had not tried R837, which might be even more relevant on BTK in NLRP3 inflammasome activation than nigericin, based on the results obtained from the iMac experiment (see figure 3.16.). Nigericin is a pore forming toxin that leads to potassium efflux from the cell, which is a common feature of many NLRP3 activators. It was speculated that potassium efflux is sensed by the LRR of NLRP3, leading to conformational change and downstream signaling. How NLRP3 senses potassium efflux is still elusive, it might be via the change in the membrane potential, via alteration of the cytosolic pH, or NLRP3 might bind potassium directly. Additionally, molecules might act upstream of NLRP3, thereby connecting potassium efflux with the NLRP3 reaction. One of these molecules might be BTK.

BTK was found to be phosphorylated at Y551 upon nigericin treatment. Thus, a kinase upstream of BTK (most likely Syk, as Syk inhibitors also led to reduced IL-1β release in macrophages (Ito et al. 2015)) has already have had reacted to nigericin and phosphorylated BTK. Nonetheless, it is not typical for kinases to sense and get activated via signals such as potassium efflux. A change in the pH of the cytosol might activate specific molecules, but this type of action would be more typical for PRRs such as NLRP3. NLRP3 could detect potassium efflux directly, e.g. NLRP3 could sense a drop in the membrane potential (upon priming NLRP3 might move closely to the cell membrane) and react via a small change e.g. in its conformation, which would activate upstream interaction partners and kinases (e.g. Syk) reinforcing a positive feedback loop ending in enhancement of NLRP3 activation e.g. via phosphorylation by BTK and release from the Golgi.

It is also not clear how NLRP3´s migration to the Golgi is guided. It might be similar to the published mechanism by which MARK4 guides NLRP3 to the mitochondria (X. Li et al. 2017). Chen observed that the trans-Golgi network is first formed upon destabilization of the cell by nigericin. This might restrict the binding of inactivated NLRP3 to PI4P at the Golgi membrane. Future work should also focus on the upstream events that link potassium efflux, kinases upstream of BTK, NLRP3, and NLRP3 migration.

Using inhibitors against molecules upstream of BTK in BCR signaling (e.g. in BMDMs against Syk) and measuring NLRP3 tyrosine phosphorylation would give us a first insight whether molecules upstream of BTK in B cells (BCR signaling) are also upstream of

BTK in macrophages (NLRP3 inflammasome signaling). This way one could slowly work the way up from BTK in NLRP3 inflammasome signaling, as BCR signaling is fairly well studied.

Furthermore, one could generate immortalized macrophages harboring fluorescently tagged NLRP3 and BTK, stain the Golgi and track NLRP3 and BTK cellular localization upon inflammasome stimulation, using *in vivo* confocal or fluorescence brightfield microscopy.

4.9. BTK in inflammasome regulation in other cell types

NLRP3 and BTK were shown to be expressed in other cell types besides macrophages and monocytes, such as neutrophils, DCs, B cells, and platelets. Therefore, it would be informative to test whether BTK also controls NLRP3 activity in these cells, and whether the control mechanism is analogue to that in macrophages.

Recently, NLRP3 inflammasome function was investigated in B cells. Ali et al. (Ali et al. 2017) found that upon TLR stimulation in B cells by fungal ligands or CpG, B cells produced NLRP3-dependent IL-1β mediated by Syk. As BTK is most likely downstream of Syk, also in NLRP3 inflammasome regulation in macrophages, it is plausible to speculate that BTK is involved in NLRP3 regulation in B cells as well.

Measuring IL-1β release upon ibrutinib treatment of the above-mentioned cells would give us a first insight, whether BTK operates similarly in those cells, as in macrophages. As the regulating mechanism was studied relatively cell-type independently, using HEK293T overexpression system and recombinant proteins, it is likely that on the level of BTK and NLRP3, the regulatory mechanism is analogous to that in macrophages. Should ibrutinib not block IL-1β release in other cell types, it might be because of distinct upstream events that regulate BTK in a distinct matter. Use of some of the methods employed here (IP of phospho-NLRP3, later use of phospho-specific antibodies) might be helpful in elucidating this intriguing result further.

4.10. Potential of ibrutinib for targeting the NLRP3 inflammasome

Ibrutinib is a drug that is applied in multiple B cell malignancies (see section 1.5.4.) to restraint cell growth and to make malignant B cells susceptible for combination chemotherapy. Nonetheless, several side effects of ibrutinib treatment regarding innate immunity are currently being neglected. Ibrutinib blocks BTK functions in innate immune cells as well that might be the underlying reason for several side effects that have been observed: susceptibility to infections, low white blood cell count, and fever.

In most non-CAPS individuals, ibrutinib might also block proper NLRP3 functions, as indicated from *in vitro* experiments with PBMCs (see figure 3.17.). This may lead to increased susceptibility to infections. Furthermore, analogue to the BTK mutated Xid mice that were more susceptible to infections via dysfunction in BTK-mediated TLR signaling, patients taking ibrutinib could also have defective TLR signaling and innate immune defense.

Nonetheless, and ideally, patients that have NLRP3 hyperactivation mediated diseases e.g. gout, Alzheimer´s disease, atherosclerosis, could take ibrutinib orally to restrict NLRP3 activity. As seen before (figure 3.1.), ibrutinib treatment does not block IL-1β release completely, a residual activity is preserved. Thus, ibrutinib might block the excess IL-1β that is generated due to the hyperactivation of NLRP3 and that is causing inflammatory symptoms but might still sustain physiological NLRP3 functions that protect the individual from infections. Measuring whether IL-1β release from PBMCs from individuals dealing with NLRP3 hyperactivation mediated diseases could be blocked by ibrutinib would give us a first insight into further application possibilities of ibrutinib. Nonetheless, one would have to find a therapeutic window that blocks NLRP3 activity but does not interfere with healthy B cell functions.

4.11. NLRP3 inhibitory strategies targeting BTK

Current NLRP3 inhibiting strategies are directed against IL-1β or IL-1R, are wearing for the patients due to regular injections and have several side-effects (see section 1.4.10). Having identified BTK as a novel positive regulator of the NLRP3 inflammasome, new potential therapy routs for autoinflammatory diseases open up. First of all, as an oral FDA-approved inhibitor is already applied in B cell malignancies to block BTK kinase activity, one could test

application of ibrutinib in NLRP3 dysfunction mediated diseases, as discussed above (see section 1.4.9).

On the other hand, if ibrutinib does not prove to be successful in the restraint of excess IL-1β, one could still develop NLRP3 inhibitors based on BTK´s NLRP3 activating functions. For instance, one could design small molecules that block BTK and NLRP3 interaction, this way prohibiting both scaffold and kinase functions of BTK regarding NLRP3 specifically whilst leaving the roles of BCR and other innate pathways (e.g. TLR signaling, phagocytosis, see section 1.5.3.) intact. Furthermore, having identified the NLRP3 Y residues that are phosphorylated by BTK, one could formulate small molecules, or nanobodies that inhibit phosphorylation of these key NLRP3 residues or block PI4P binding. As the NLRP3 Y residues that are phosphorylated by BTK reside in the polybasic region of NLRP3 that is responsible for the phosphorylation upstream event NLRP3-Golgi binding, the nanobodies might even hinder this event as well and thus inhibit NLRP3 activation on two levels: Golgi binding and phosphorylation by BTK. Moreover, if cells carrying the phosphomimetic polybasic region showed reduced IL-1β processing and release that would prove that shift of the polybasic region into negative charge is sufficient for NLRP3 inhibition. Therefore, a specific molecule that has a high affinity towards the polybasic region and is negatively charged might act as a phosphomimetic polybasic region "mask" and therefore inhibit NLRP3 Golgi translocation and activation.

There are several novel potential possibilities how NLRP3 could be restraint based on the gained knowledge on the mechanism by which BTK regulates the NLRP3 inflammasome. Nonetheless, further confirmation of the mechanism and its relevance *in vivo* has to be studied before trying innovative NLRP3 blocking strategies based on BTK.

4.12. Summary and Outlook

In this study, we aimed to clarify the molecular mechanisms by which BTK acts on NLRP3 and the NLRP3 inflammasome. It could be shown that BTK rapidly phosphorylated NLRP3 upon nigericin treatment in primary cells. Furthermore, the tyrosine residues that BTK modified could be identified: Y136, Y140, Y143, and Y168 in the PYD/NACHT linker region of NLRP3. The phosphorylation of these residues was functionally relevant, as Y>F NLRP3 carrying iMacs produced reduced IL-1β.

Interestingly, the tyrosine residues that are modified by BTK reside in the recently identified polybasic region of NLRP3: the positivity of the polybasic region targets NLRP3 to the negatively charged PI4Ps at the trans-Golgi network membrane that forms upon nigericin stimulation. Having phosphorylated the polybasic tyrosine residues, BTK would shift the positivity of this region to negative charge, provoking release of NLRP3 from the negative PI4Ps on the membrane. BTK would thereby facilitate the formation of the NLRP3 inflammasome in the cytosol.

Nonetheless, several aspects of the regulatory mechanism still remain to be elucidated: Even though we could show that Y>E polybasic region holds reduced PI4P binding capacities, the BTK/NLRP3 phosphorylation event happening on the trans-Golgi network and the release thereupon of NLRP3 from the membrane still has to be demonstrated. To this end, (live) confocal microscopy using fluorescently labeled NLRP3, BTK, trans-Golgi network, and p-Y NLRP3 specific antibodies could be considered. Additionally, using fluorescent microscopy, one could track BTK´s and NLRP3´s cellular localization upon priming and activation of the cell (e.g. transfected HEK293T, BMDMs using antibodies against primary sequences, or iMacs reconstituted with fluorescently tagged BTK and NLRP3).

Furthermore, the role of the phosphorylation of Y168 has not completely been clarified yet. We hypothesized that phosphorylation of Y168 is upstream of the phosphorylation of the polybasic region and serves a structure alteration step which leaves the polybasic tyrosine residues available for phosphorylation by BTK. Additionally, Y168 lies closely to the ATP binding site, thus non-phosphorylated Y168 might act as a gatekeeper of the closed, inactive NLRP3 conformation. To prove this hypothesis, conducting BRET using WT and Y168F mutated NLRP3 co-expressed with BTK in HEK293T cells and measuring the conformational change (closed-inactive vs. open-active) of NLRP3 would give us a first insight into the structure-modifying role of the phosphorylation of Y168 by BTK. In addition, macrophages expressing Y168F mutated NLRP3 should again produce reduced amounts of

IL-1β, as the phosphorylation of Y168 by BTK, and thus downstream the phosphorylation of the polybasic region would be precluded. Therefore NLRP3 charge switch, release from the Golgi, and cytosolic inflammasome assembly would be hindered.

It would be very important to verify that the NLRP3 phosphorylation events also occur *in vivo*. Activation of the NLRP3 inflammasome *in vivo* via intraperitoneal LPS and ATP injection for different time points and analyzing NLRP3 phosphorylation in peritoneal macrophages and splenocytes (p-Y IP) would authenticate the results from the *in vitro* experiments that showed NLRP3 tyrosine phosphorylation upon nigericin treatment. Comparing tyrosine phosphorylation of NLRP3 upon *in vivo* stimulation between WT and *Btk* KO mice would reveal BTK-dependency of NLRP3 tyrosine phosphorylation *in vivo* as well. Using antibodies upon *in vivo* or *in vitro* stimulation of the NLRP3 inflammasome, directed against single phosphorylated residues, or at least against p-Y168 and phosphorylated polybasic tyrosine residues would also give us further insight into the sequence of these phosphorylation events.

To find out how nigericin treatment leads to BTK phosphorylation, upstream events of BTK activation in NLRP3 inflammasome signaling could also be mapped, e.g. via application of inhibitors of known BTK-upstream kinases (e.g. Syk) before nigericin-treatment of the cells (e.g. BMDMs) and measuring p-BTK and p-NLRP3 levels using the methods established in this study (e.g. p-Y IP).

Besides CAPS, NLRP3 is linked to several inflammatory diseases, such as Alzheimer´s disease, gout, diabetes (Mangan et al. 2018), see section 1.4.9. To date, the NLRP3 inhibiting strategies comprise targeting the very end of the NLRP3 signal cascade, namely IL-1β and IL-1R. Having identified BTK as a positive regulator of NLRP3, application of the FDA-approved BTK kinase inhibitor ibrutinib could be further exploited besides B cell malignancies, also in NLRP3 dysfunction or hyperactivation associated diseases. Furthermore, knowing the tyrosine residues that BTK acts on, small molecules hindering the binding of BTK to NLRP3 or the phosphorylation of BTK´s target NLRP3 residues could also be an optional therapeutic route.

Therefore, the results of the current study take us one step further to the application of BTK kinase activity- or BTK/NLRP3 interaction-inhibition based therapeutic options in NLRP3-associated inflammatory diseases.

5. REFERENCES

"A Current View on Inflammation." 2017. *Nature Immunology*. https://doi.org/10.1038/ni.3798.

Abdulkhaleq, L. A., M. A. Assi, Rasedee Abdullah, M. Zamri-Saad, Y. H. Taufiq-Yap, and M. N.M. Hezmee. 2018. "The Crucial Roles of Inflammatory Mediators in Inflammation: A Review." *Veterinary World*. https://doi.org/10.14202/vetworld.2018.627-635.

Aderem, Alan, and David M. Underhill. 1999. "MECHANISMS OF PHAGOCYTOSIS IN MACROPHAGES." *Annual Review of Immunology*. https://doi.org/10.1146/annurev.immunol.17.1.593.

Advani, Ranjana H., Joseph J. Buggy, Jeff P. Sharman, Sonali M. Smith, Thomas E. Boyd, Barbara Grant, Kathryn S. Kolibaba, et al. 2013. "Bruton Tyrosine Kinase Inhibitor Ibrutinib (PCI-32765) Has Significant Activity in Patients with Relapsed/Refractory B-Cell Malignancies." *Journal of Clinical Oncology*. https://doi.org/10.1200/JCO.2012.42.7906.

Akira, Shizuo, Satoshi Uematsu, and Osamu Takeuchi. 2006. "Pathogen Recognition and Innate Immunity." *Cell*. https://doi.org/10.1016/j.cell.2006.02.015.

Ali, Mohamed F., Harika Dasari, Virginia P. Van Keulen, and Eva M. Carmona. 2017. "Canonical Stimulation of the NLRP3 Inflammasome by Fungal Antigens Links Innate and Adaptive B-Lymphocyte Responses by Modulating IL-1β and IgM Production." *Frontiers in Immunology*. https://doi.org/10.3389/fimmu.2017.01504.

Altan-Bonnet, Grégoire, and Ratnadeep Mukherjee. 2019. "Cytokine-Mediated Communication: A Quantitative Appraisal of Immune Complexity." *Nature Reviews Immunology*. https://doi.org/10.1038/s41577-019-0131-x.

Anderson, Kathryn V., Liselotte Bokla, and Christiane Nüsslein-Volhard. 1985. "Establishment of Dorsal-Ventral Polarity in the Drosophila Embryo: The Induction of Polarity by the Toll Gene Product." *Cell*. https://doi.org/10.1016/0092-8674(85)90275-2.

Anderson, Kathryn V., Gerd Jürgens, and Christiane Nüsslein-Volhard. 1985. "Establishment of Dorsal-Ventral Polarity in the Drosophila Embryo: Genetic Studies on the Role of the Toll Gene Product." *Cell*. https://doi.org/10.1016/0092-8674(85)90274-0.

Bae, Ju Young, and Hyun Ho Park. 2011. "Crystal Structure of NALP3 Protein Pyrin Domain (PYD) and Its Implications in Inflammasome Assembly." *Journal of Biological Chemistry*. https://doi.org/10.1074/jbc.M111.278812.

Baker, Paul J., Dave Boucher, Damien Bierschenk, Christina Tebartz, Paul G. Whitney, Damian B. D'Silva, Maria C. Tanzer, et al. 2015. "NLRP3 Inflammasome Activation Downstream of Cytoplasmic LPS Recognition by Both Caspase-4 and Caspase-5." *European Journal of Immunology*. https://doi.org/10.1002/eji.201545655.

Barry, Rachael, Sidonie Wicky John, Gianmaria Liccardi, Tencho Tenev, Isabel Jaco, Chih Hong Chen, Justin Choi, et al. 2018. "SUMO-Mediated Regulation of NLRP3 Modulates Inflammasome Activity." *Nature Communications*. https://doi.org/10.1038/s41467-018-05321-2.

Barton, Gregory M., and Ruslan Medzhitov. 2003. "Toll-like Receptor Signaling Pathways." *Science*. https://doi.org/10.1126/science.1085536.

Bauernfeind, Franz, Eva Bartok, Anna Rieger, Luigi Franchi, Gabriel Núñez, and Veit Hornung. 2011. "Cutting Edge: Reactive Oxygen Species Inhibitors Block Priming, but Not Activation, of the NLRP3 Inflammasome." *The Journal of Immunology*. https://doi.org/10.4049/jimmunol.1100613.

Booshehri, Laela M., and Hal M. Hoffman. 2019. "CAPS and NLRP3." *Journal of Clinical Immunology*. https://doi.org/10.1007/s10875-019-00638-z.

Broek, Theo Van Den, José A.M. Borghans, and Femke Van Wijk. 2018. "The Full Spectrum of Human Naive T Cells." *Nature Reviews Immunology*. https://doi.org/10.1038/s41577-018-0001-y.

Bronner, Denise N., Basel H. Abuaita, Xiaoyun Chen, Katherine A. Fitzgerald, Gabriel Nuñez, Yongqun He, Xiao Ming Yin, and Mary X.D. O'Riordan. 2015. "Endoplasmic Reticulum Stress Activates the Inflammasome via NLRP3- and Caspase-2-Driven Mitochondrial Damage." *Immunity*. https://doi.org/10.1016/j.immuni.2015.08.008.

Broz, Petr, and Vishva M. Dixit. 2016. "Inflammasomes: Mechanism of Assembly, Regulation and Signalling." *Nature Reviews Immunology*. https://doi.org/10.1038/nri.2016.58.

Bruchard, Mélanie, Cédric Rebé, Valentin Derangère, Dieudonnée Togbé, Bernhard Ryffel, Romain Boidot, Etienne Humblin, et al. 2015. "The Receptor NLRP3 Is a Transcriptional Regulator of TH2 Differentiation." *Nature Immunology*. https://doi.org/10.1038/ni.3202.

BRUTON, O. C. 1952. "Agammaglobulinemia." *Pediatrics*.

Burger, Jan A., and Adrian Wiestner. 2018. "Targeting B Cell Receptor Signalling in Cancer: Preclinical and Clinical Advances." *Nature Reviews Cancer*. https://doi.org/10.1038/nrc.2017.121.

Carrera, A. C., K. Alexandrov, and T. M. Roberts. 1993. "The Conserved Lysine of the Catalytic Domain of Protein Kinases Is Actively Involved in the Phosphotransfer Reaction and Not Required for Anchoring ATP." *Proceedings of the National Academy of Sciences of the United States of America*. https://doi.org/10.1073/pnas.90.2.442.

Cavalli, Giulio, and Charles A. Dinarello. 2018. "Anakinra Therapy for Non-Cancer Inflammatory Diseases." *Frontiers in Pharmacology*. https://doi.org/10.3389/fphar.2018.01157.

Chaplin, David D. 2010. "Overview of the Immune Response." *Journal of Allergy and Clinical Immunology*. https://doi.org/10.1016/j.jaci.2009.12.980.

Chavarría-Smith, Joseph, and Russell E. Vance. 2015. "The NLRP1 Inflammasomes." *Immunological Reviews*. https://doi.org/10.1111/imr.12283.

Chen, Jueqi, and Zhijian J. Chen. 2018. "PtdIns4P on Dispersed Trans-Golgi Network Mediates NLRP3 Inflammasome Activation." *Nature*. https://doi.org/10.1038/s41586-018-0761-3.

Chen, Linlin, Huidan Deng, Hengmin Cui, Jing Fang, Zhicai Zuo, Junliang Deng, Yinglun Li, Xun Wang, and Ling Zhao. 2018. "Inflammatory Responses and Inflammation-Associated Diseases in Organs." *Oncotarget*. https://doi.org/10.18632/oncotarget.23208.

Christ, Anette, Patrick Günther, Mario A.R. Lauterbach, Peter Duewell, Debjani Biswas, Karin Pelka, Claus J. Scholz, et al. 2018. "Western Diet Triggers NLRP3-Dependent Innate Immune Reprogramming." *Cell*. https://doi.org/10.1016/j.cell.2017.12.013.

Cinar, Munevver, Farid Saei Hamedani, Zhicheng Mo, Bekir Cinar, Hesham M. Amin, and Serhan Alkan. 2013. "Bruton Tyrosine Kinase Is Commonly Overexpressed in Mantle Cell Lymphoma and Its Attenuation by Ibrutinib Induces Apoptosis." *Leukemia Research*. https://doi.org/10.1016/j.leukres.2013.07.028.

Coll, Rebecca C., James R. Hill, Christopher J. Day, Alina Zamoshnikova, Dave Boucher, Nicholas L. Massey, Jessica L. Chitty, et al. 2019. "MCC950 Directly Targets the NLRP3 ATP-Hydrolysis Motif for Inflammasome Inhibition." *Nature Chemical Biology*. https://doi.org/10.1038/s41589-019-0277-7.

Coll, Rebecca C., and Luke A.J. O'Neill. 2011. "The Cytokine Release Inhibitory Drug CRID3 Targets ASC Oligomerisation in the NLRP3 and AIM2 Inflammasomes." *PLoS ONE*. https://doi.org/10.1371/journal.pone.0029539.

Coll, Rebecca C., Avril A.B. Robertson, Jae Jin Chae, Sarah C. Higgins, Raúl Muñoz-Planillo, Marco C. Inserra, Irina Vetter, et al. 2015. "A Small-Molecule Inhibitor of the NLRP3 Inflammasome for the Treatment of Inflammatory Diseases." *Nature Medicine*. https://doi.org/10.1038/nm.3806.

Compan, Vincent, Alberto Baroja-Mazo, Laricia Bragg, Alexei Verkhratsky, Julie Perroy, and Pablo Pelegrin. 2012. "A Genetically Encoded IL-1β Bioluminescence Resonance Energy Transfer Sensor To Monitor Inflammasome Activity." *The Journal of Immunology*. https://doi.org/10.4049/jimmunol.1201349.

Compan, Vincent, Alberto Baroja-Mazo, Gloria López-Castejón, Ana I. Gomez, Carlos M. Martínez, Diego

Angosto, María T. Montero, et al. 2012. “Cell Volume Regulation Modulates NLRP3 Inflammasome Activation.” *Immunity*. https://doi.org/10.1016/j.immuni.2012.06.013.

Davids, Matthew S., and Jennifer R. Brown. 2014. “Ibrutinib: A First in Class Covalent Inhibitor of Bruton’s Tyrosine Kinase.” *Future Oncology*. https://doi.org/10.2217/fon.14.51.

Diebolder, Christoph A., Els F. Halff, Abraham J. Koster, Eric G. Huizinga, and Roman I. Koning. 2015. “Cryoelectron Tomography of the NAIP5/NLRC4 Inflammasome: Implications for NLR Activation.” *Structure*. https://doi.org/10.1016/j.str.2015.10.001.

Dolgin, Elie. 2019. “Parkinson’s Drug Makers Target Inflammasome.” *Nature Biotechnology*. https://doi.org/10.1038/d41587-019-00005-8.

Dreyling, Martin, Wojciech Jurczak, Mats Jerkeman, Rodrigo Santucci Silva, Chiara Rusconi, Marek Trneny, Fritz Offner, et al. 2016. “Ibrutinib versus Temsirolimus in Patients with Relapsed or Refractory Mantle-Cell Lymphoma: An International, Randomised, Open-Label, Phase 3 Study.” *The Lancet*. https://doi.org/10.1016/S0140-6736(15)00667-4.

Elliott, Eric I., and Fayyaz S. Sutterwala. 2015. “Initiation and Perpetuation of NLRP3 Inflammasome Activation and Assembly.” *Immunological Reviews*. https://doi.org/10.1111/imr.12286.

Faustin, Benjamin, Lydia Lartigue, Jean Marie Bruey, Frederic Luciano, Eduard Sergienko, Beatrice Bailly-Maitre, Niels Volkmann, Dorit Hanein, Isabelle Rouiller, and John C. Reed. 2007. “Reconstituted NALP1 Inflammasome Reveals Two-Step Mechanism of Caspase-1 Activation.” *Molecular Cell*. https://doi.org/10.1016/j.molcel.2007.01.032.

Fiedler, Katja, Anca Sindrilaru, Grzegorz Terszowski, Enikö Kokai, Thorsten B. Feyerabend, Lars Bullinger, Hans Reimer Rodewald, and Cornelia Brunner. 2011. “Neutrophil Development and Function Critically Depend on Bruton Tyrosine Kinase in a Mouse Model of X-Linked Agammaglobulinemia.” *Blood*. https://doi.org/10.1182/blood-2010-04-281170.

Fresno, Carlos del, Salvador Iborra, Paula Saz-Leal, María Martínez-López, and David Sancho. 2018. “Flexible Signaling of Myeloid C-Type Lectin Receptors in Immunity and Inflammation.” *Frontiers in Immunology*. https://doi.org/10.3389/fimmu.2018.00804.

Fujita, Teizo, Misao Matsushita, and Yuichi Endo. 2004. “The Lectin-Complement Pathway - Its Role in Innate Immunity and Evolution.” *Immunological Reviews*. https://doi.org/10.1111/j.0105-2896.2004.0123.x.

Gaidt, Moritz M., Thomas S. Ebert, Dhruv Chauhan, Tobias Schmidt, Jonathan L. Schmid-Burgk, Francesca Rapino, Avril A.B. Robertson, Matthew A. Cooper, Thomas Graf, and Veit Hornung. 2016. “Human Monocytes Engage an Alternative Inflammasome Pathway.” *Immunity*. https://doi.org/10.1016/j.immuni.2016.01.012.

Gaidt, Moritz M., Francesca Rapino, Thomas Graf, and Veit Hornung. 2018. “Modeling Primary Human Monocytes with the Trans–Differentiation Cell Line BLaER1.” In *Methods in Molecular Biology*. https://doi.org/10.1007/978-1-4939-7519-8_4.

Gieseck, Richard L., Mark S. Wilson, and Thomas A. Wynn. 2018. “Type 2 Immunity in Tissue Repair and Fibrosis.” *Nature Reviews Immunology*. https://doi.org/10.1038/nri.2017.90.

Goldbach-Mansky, Raphaela. 2011. “Current Status of Understanding the Pathogenesis and Management of Patients with NOMID/CINCA.” *Current Rheumatology Reports*. https://doi.org/10.1007/s11926-011-0165-y.

Gordon, Richard, Eduardo A. Albornoz, Daniel C. Christie, Monica R. Langley, Vinod Kumar, Susanna Mantovani, Avril A.B. Robertson, et al. 2018. “Inflammasome Inhibition Prevents -Synuclein Pathology and Dopaminergic Neurodegeneration in Mice.” *Science Translational Medicine*. https://doi.org/10.1126/scitranslmed.aah4066.

Gray, Pearl, Aisling Dunne, Constantinos Brikos, Caroline A. Jefferies, Sarah L. Doyle, and Luke A.J. O’Neill. 2006. “MyD88 Adapter-like (Mal) Is Phosphorylated by Bruton’s Tyrosine Kinase during TLR2 and TLR4 Signal Transduction.” *Journal of Biological Chemistry*. https://doi.org/10.1074/jbc.M508892200.

Guo, Chuansheng, Zhexu Chi, Danlu Jiang, Ting Xu, Weiwei Yu, Zhen Wang, Sheng Chen, et al. 2018. "Cholesterol Homeostatic Regulator SCAP-SREBP2 Integrates NLRP3 Inflammasome Activation and Cholesterol Biosynthetic Signaling in Macrophages." *Immunity*. https://doi.org/10.1016/j.immuni.2018.08.021.

Guo, Chuansheng, Shujun Xie, Zhexu Chi, Jinhua Zhang, Yangyang Liu, Li Zhang, Mingzhu Zheng, et al. 2016. "Bile Acids Control Inflammation and Metabolic Disorder through Inhibition of NLRP3 Inflammasome." *Immunity*. https://doi.org/10.1016/j.immuni.2016.09.008.

Hafner-Bratkovič, Iva, Petra Sušjan, Duško Lainšček, Ana Tapia-Abellán, Kosta Cerović, Lucija Kadunc, Diego Angosto-Bazarra, Pablo Pelegrín, and Roman Jerala. 2018. "NLRP3 Lacking the Leucine-Rich Repeat Domain Can Be Fully Activated via the Canonical Inflammasome Pathway." *Nature Communications*. https://doi.org/10.1038/s41467-018-07573-4.

Halle, Annett, Veit Hornung, Gabor C. Petzold, Cameron R. Stewart, Brian G. Monks, Thomas Reinheckel, Katherine A. Fitzgerald, Eicke Latz, Kathryn J. Moore, and Douglas T. Golenbock. 2008. "The NALP3 Inflammasome Is Involved in the Innate Immune Response to Amyloid-β." *Nature Immunology*. https://doi.org/10.1038/ni.1636.

Hamilton, Claire, and Paras K. Anand. 2019. "Right Place, Right Time: Localisation and Assembly of the NLRP3 Inflammasome." *F1000Research*. https://doi.org/10.12688/f1000research.18557.1.

Han, Seung Hye, Travis B. Lear, Jacob A. Jerome, Shristi Rajbhandari, Courtney A. Snavely, Dexter L. Gulick, Kevin F. Gibson, Chunbin Zou, Bill B. Chen, and Rama K. Mallampalli. 2015. "Lipopolysaccharide Primes the NALP3 Inflammasome by Inhibiting Its Ubiquitination and Degradation Mediated by the SCFFBXL2 E3 Ligase." *Journal of Biological Chemistry*. https://doi.org/10.1074/jbc.M115.645549.

Hara, Hideki, Sergey S. Seregin, Dahai Yang, Koichi Fukase, Mathias Chamaillard, Emad S. Alnemri, Naohiro Inohara, Grace Y. Chen, and Gabriel Núñez. 2018. "The NLRP6 Inflammasome Recognizes Lipoteichoic Acid and Regulates Gram-Positive Pathogen Infection." *Cell*. https://doi.org/10.1016/j.cell.2018.09.047.

He, Hongbin, Hua Jiang, Yun Chen, Jin Ye, Aoli Wang, Chao Wang, Qingsong Liu, et al. 2018. "Oridonin Is a Covalent NLRP3 Inhibitor with Strong Anti-Inflammasome Activity." *Nature Communications*. https://doi.org/10.1038/s41467-018-04947-6.

He, Yuan, Hideki Hara, and Gabriel Núñez. 2016. "Mechanism and Regulation of NLRP3 Inflammasome Activation." *Trends in Biochemical Sciences*. https://doi.org/10.1016/j.tibs.2016.09.002.

He, Yuan, Melody Y. Zeng, Dahai Yang, Benny Motro, and Gabriel Núñez. 2016. "NEK7 Is an Essential Mediator of NLRP3 Activation Downstream of Potassium Efflux." *Nature*. https://doi.org/10.1038/nature16959.

Heilig, Rosalie, and Petr Broz. 2018. "Function and Mechanism of the Pyrin Inflammasome." *European Journal of Immunology*. https://doi.org/10.1002/eji.201746947.

Hemmer, Bernhard, Clemencia Pinilla, Bruno Gran, Marco Vergelli, Nick Ling, Paul Conlon, Henry F. McFarland, Richard Houghten, and Roland Martin. 2000. "Contribution of Individual Amino Acids Within MHC Molecule or Antigenic Peptide to TCR Ligand Potency." *The Journal of Immunology*. https://doi.org/10.4049/jimmunol.164.2.861.

Heneka, Michael T., Markus P. Kummer, Andrea Stutz, Andrea Delekate, Stephanie Schwartz, Ana Vieira-Saecker, Angelika Griep, et al. 2013. "NLRP3 Is Activated in Alzheimer's Disease and Contributes to Pathology in APP/PS1 Mice." *Nature*. https://doi.org/10.1038/nature11729.

Hoffman, Hal M., Uma Yasothan, and Peter Kirkpatrick. 2008. "Rilonacept." *Nature Reviews Drug Discovery*. https://doi.org/10.1038/nrd2579.

Honda, Fumiko, Hirotsugu Kano, Hirokazu Kanegane, Shigeaki Nonoyama, Eun Sung Kim, Sang Kyou Lee, Masatoshi Takagi, Shuki Mizutani, and Tomohiro Morio. 2012. "The Kinase Btk Negatively Regulates the Production of Reactive Oxygen Species and Stimulation-Induced Apoptosis in Human Neutrophils." *Nature Immunology*. https://doi.org/10.1038/ni.2234.

Honigberg, Lee A., Ashley M. Smith, Mint Sirisawad, Erik Verner, David Loury, Betty Chang, Shyr Li, et al.

2010. “The Bruton Tyrosine Kinase Inhibitor PCI-32765 Blocks B-Cell Activation and Is Efficacious in Models of Autoimmune Disease and B-Cell Malignancy.” *Proceedings of the National Academy of Sciences of the United States of America*. https://doi.org/10.1073/pnas.1004594107.

Hornung, Veit, Franz Bauernfeind, Annett Halle, Eivind O. Samstad, Hajime Kono, Kenneth L. Rock, Katherine A. Fitzgerald, and Eicke Latz. 2008. “Silica Crystals and Aluminum Salts Activate the NALP3 Inflammasome through Phagosomal Destabilization.” *Nature Immunology*. https://doi.org/10.1038/ni.1631.

Hoving, J. Claire, Gillian J. Wilson, and Gordon D. Brown. 2014. “Signalling C-Type Lectin Receptors, Microbial Recognition and Immunity.” *Cellular Microbiology*. https://doi.org/10.1111/cmi.12249.

Hoy, Sheridan M. 2015. “Canakinumab: A Review of Its Use in the Management of Systemic Juvenile Idiopathic Arthritis.” *BioDrugs*. https://doi.org/10.1007/s40259-015-0123-8.

Huang, Yi, Hua Jiang, Yun Chen, Xiaqiong Wang, Yanqing Yang, Jinhui Tao, Xianming Deng, et al. 2018. “ Tranilast Directly Targets NLRP 3 to Treat Inflammasome-driven Diseases .” *EMBO Molecular Medicine*. https://doi.org/10.15252/emmm.201708689.

Humphries, Fiachra, Ronan Bergin, Ruaidhri Jackson, Nezira Delagic, Bingwei Wang, Shuo Yang, Alice V. Dubois, Rebecca J. Ingram, and Paul N. Moynagh. 2018. “The E3 Ubiquitin Ligase Pellino2 Mediates Priming of the NLRP3 Inflammasome.” *Nature Communications*. https://doi.org/10.1038/s41467-018-03669-z.

Ito, Minako, Takashi Shichita, Masahiro Okada, Ritsuko Komine, Yoshiko Noguchi, Akihiko Yoshimura, and Rimpei Morita. 2015. “Bruton’s Tyrosine Kinase Is Essential for NLRP3 Inflammasome Activation and Contributes to Ischaemic Brain Injury.” *Nature Communications*. https://doi.org/10.1038/ncomms8360.

Iyer, Shankar S., Qiong He, John R. Janczy, Eric I. Elliott, Zhenyu Zhong, Alicia K. Olivier, Jeffrey J. Sadler, et al. 2013. “Mitochondrial Cardiolipin Is Required for Nlrp3 Inflammasome Activation.” *Immunity*. https://doi.org/10.1016/j.immuni.2013.08.001.

Jager, Jennifer, Thierry Grémeaux, Mireille Cormont, Yannick Le Marchand-Brustel, and J. F. Tanti. 2007. “Interleukin-1β-Induced Insulin Resistance in Adipocytes through down-Regulation of Insulin Receptor Substrate-1 Expression.” *Endocrinology*. https://doi.org/10.1210/en.2006-0692.

Janeway, C. A. 1989. “Approaching the Asymptote? Evolution and Revolution in Immunology.” In *Cold Spring Harbor Symposia on Quantitative Biology*. https://doi.org/10.1101/sqb.1989.054.01.003.

Janeway, Charles Alderson, Paul Travers, Mark Walport, and Et Al. 2001. “Principles of Innate and Adaptive Immunity.” *Immunobiology: The Immune System in Health and Disease. 5th Edition.*

Jang, Jiho, Sangjun Park, Hye Jin Hur, Hyun Ju Cho, Inhwa Hwang, Yun Pyo Kang, Isak Im, et al. 2016. “25-Hydroxycholesterol Contributes to Cerebral Inflammation of X-Linked Adrenoleukodystrophy through Activation of the NLRP3 Inflammasome.” *Nature Communications*. https://doi.org/10.1038/ncomms13129.

Jiang, Hua, Hongbin He, Yun Chen, Wei Huang, Jinbo Cheng, Jin Ye, Aoli Wang, et al. 2017. “Identification of a Selective and Direct NLRP3 Inhibitor to Treat Inflammatory Disorders.” *Journal of Experimental Medicine*. https://doi.org/10.1084/jem.20171419.

Jongstra-Bilen, Jenny, Adrianet Puig Cano, Manvi Hasija, Haiyan Xiao, C. I. Edvard Smith, and Myron I. Cybulsky. 2008. “Dual Functions of Bruton’s Tyrosine Kinase and Tec Kinase during Fcγ Receptor-Induced Signaling and Phagocytosis.” *The Journal of Immunology*. https://doi.org/10.4049/jimmunol.181.1.288.

Karasawa, Tadayoshi, and Masafumi Takahashi. 2017. “Role of NLRP3 Inflammasomes in Atherosclerosis.” *Journal of Atherosclerosis and Thrombosis*. https://doi.org/10.5551/jat.RV17001.

Kawai, Taro, and Shizuo Akira. 2008. “Toll-like Receptor and RIG-1-like Receptor Signaling.” *Annals of the New York Academy of Sciences*. https://doi.org/10.1196/annals.1443.020.

Kawai, T, Akira, S. 2011. “Toll-like Receptors and Their Crosstalk with Other Innate Receptors in Infection and Immunity.” *Immunity*. https://doi.org/10.1016/j.immuni.2011.05.006.

Kawashima, Akira, Tadayoshi Karasawa, Kenji Tago, Hiroaki Kimura, Ryo Kamata, Fumitake Usui-Kawanishi, Sachiko Watanabe, et al. 2017. “ARIH2 Ubiquitinates NLRP3 and Negatively Regulates NLRP3 Inflammasome Activation in Macrophages.” *The Journal of Immunology*. https://doi.org/10.4049/jimmunol.1700184.

Kayagaki, Nobuhiko, Irma B. Stowe, Bettina L. Lee, Karen O’Rourke, Keith Anderson, Søren Warming, Trinna Cuellar, et al. 2015. “Caspase-11 Cleaves Gasdermin D for Non-Canonical Inflammasome Signalling.” *Nature*. https://doi.org/10.1038/nature15541.

Kayagaki, Nobuhiko, Michael T. Wong, Irma B. Stowe, Sree Ranjani Ramani, Lino C. Gonzalez, Sachiko Akashi-Takamura, Kensuke Miyake, et al. 2013. “Noncanonical Inflammasome Activation by Intracellular LPS Independent of TLR4.” *Science*. https://doi.org/10.1126/science.1240248.

Kelley, Nathan, Devon Jeltema, Yanhui Duan, and Yuan He. 2019. “The NLRP3 Inflammasome: An Overview of Mechanisms of Activation and Regulation.” *International Journal of Molecular Sciences*. https://doi.org/10.3390/ijms20133328.

Khare, Sonal, Alexander D. Radian, Andrea Dorfleutner, and Christian Stehlik. 2016. “Measuring NLR Oligomerization I: Size Exclusion Chromatography, Co-Immunoprecipitation, and Cross-Linking.” In *Methods in Molecular Biology*. https://doi.org/10.1007/978-1-4939-3566-6_8.

Khor, Bernard, Agnès Gardet, and Ramnik J. Xavier. 2011. “Genetics and Pathogenesis of Inflammatory Bowel Disease.” *Nature*. https://doi.org/10.1038/nature10209.

Kitamura, Akiko, Yuki Sasaki, Takaya Abe, Hirotsugu Kano, and Koji Yasutomo. 2014. “An Inherited Mutation in NLRC4 Causes Autoinflammation in Human and Mice.” *Journal of Experimental Medicine*. https://doi.org/10.1084/jem.20141091.

Klein, Ludger, Bruno Kyewski, Paul M. Allen, and Kristin A. Hogquist. 2014. “Positive and Negative Selection of the T Cell Repertoire: What Thymocytes See (and Don’t See).” *Nature Reviews Immunology*. https://doi.org/10.1038/nri3667.

Klimpel, Gary R. 1996. *Immune Defenses. Medical Microbiology*.

Kuo, Hsu Ping, Scott A. Ezell, Karl J. Schweighofer, Leo W.K. Cheung, Sidney Hsieh, Mutiah Apatira, Mint Sirisawad, et al. 2017. “Combination of Ibrutinib and ABT-199 in Diffuse Large B-Cell Lymphoma and Follicular Lymphoma.” *Molecular Cancer Therapeutics*. https://doi.org/10.1158/1535-7163.MCT-16-0555.

la Roche, Marianne de, Claire Hamilton, Rebecca Mortensen, A. Arockia Jeyaprakash, Sanjay Ghosh, and Paras K. Anand. 2018. “Trafficking of Cholesterol to the ER Is Required for NLRP3 Inflammasome Activation.” *The Journal of Cell Biology*. https://doi.org/10.1083/jcb.201709057.

Laman, Alexander G., Richard Lathe, Anna O. Shepelyakovskaya, Alexandra Gartseva, Feodor A. Brovko, Svetlana Guryanova, Ludmila Alekseeva, Elena A. Meshcheryakova, and Vadim T. Ivanov. 2016. “Muramyl Peptides Activate Innate Immunity Conjointly via YB1 and NOD2.” *Innate Immunity*. https://doi.org/10.1177/1753425916668982.

Latz, Eicke, T. Sam Xiao, and Andrea Stutz. 2013. “Activation and Regulation of the Inflammasomes.” *Nature Reviews Immunology*. https://doi.org/10.1038/nri3452.

Lee, Geun Shik, Naeha Subramanian, Andrew I. Kim, Ivona Aksentijevich, Raphaela Goldbach-Mansky, David B. Sacks, Ronald N. Germain, Daniel L. Kastner, and Jae Jin Chae. 2012. “The Calcium-Sensing Receptor Regulates the NLRP3 Inflammasome through Ca2+ and CAMP.” *Nature*. https://doi.org/10.1038/nature11588.

Lemaitre, Bruno, Emmanuelle Nicolas, Lydia Michaut, Jean Marc Reichhart, and Jules A. Hoffmann. 1996. “The Dorsoventral Regulatory Gene Cassette Spatzle/Toll/Cactus Controls the Potent Antifungal Response in Drosophila Adults.” *Cell*. https://doi.org/10.1016/S0092-8674(00)80172-5.

Levy, Maayan, Hagit Shapiro, Christoph A. Thaiss, and Eran Elinav. 2017. "NLRP6: A Multifaceted Innate Immune Sensor." *Trends in Immunology*. https://doi.org/10.1016/j.it.2017.01.001.

Li, Lexiao, Saifudeen Ismael, Sanaz Nasoohi, Kazuko Sakata, Francesca Fang Liao, Michael P. McDonald, and Tauheed Ishrat. 2019. "Thioredoxin-Interacting Protein (TXNIP) Associated NLRP3 Inflammasome Activation in Human Alzheimer's Disease Brain." *Journal of Alzheimer's Disease*. https://doi.org/10.3233/JAD-180814.

Li, Xuan, Sarah Thome, Xiaodan Ma, Mamta Amrute-Nayak, Alison Finigan, Lauren Kitt, Leanne Masters, et al. 2017. "MARK4 Regulates NLRP3 Positioning and Inflammasome Activation through a Microtubule-Dependent Mechanism." *Nature Communications*. https://doi.org/10.1038/ncomms15986.

Li, Yang, Tian Min Fu, Alvin Lu, Kristen Witt, Jianbin Ruan, Chen Shen, and Hao Wu. 2018. "Cryo-EM Structures of ASC and NLRC4 CARD Filaments Reveal a Unified Mechanism of Nucleation and Activation of Caspase-1." *Proceedings of the National Academy of Sciences of the United States of America*. https://doi.org/10.1073/pnas.1810524115.

Li, Zuomei, Matthew I. Wahl, Alicia Eguinoa, Leonard R. Stephens, Phillip T. Hawkins, and Owen N. Witte. 1997. "Phosphatidylinositol 3-Kinase-γ Activates Bruton's Tyrosine Kinase in Concert with Src Family Kinases." *Proceedings of the National Academy of Sciences of the United States of America*. https://doi.org/10.1073/pnas.94.25.13820.

Liu, Xiao, Tica Pichulik, Olaf-Oliver Wolz, Truong-Minh Dang, Andrea Stutz, Carly Dillen, Magno Delmiro Garcia, et al. 2017. "Human NLRP3 Inflammasome Activity Is Regulated by and Potentially Targetable via BTK." *Journal of Allergy and Clinical Immunology*. https://doi.org/10.1016/j.jaci.2017.01.017.

Loo, Yueh Ming, and Michael Gale. 2011. "Immune Signaling by RIG-I-like Receptors." *Immunity*. https://doi.org/10.1016/j.immuni.2011.05.003.

Lu, Alvin, and Hao Wu. 2015. "Structural Mechanisms of Inflammasome Assembly." *FEBS Journal*. https://doi.org/10.1111/febs.13133.

Lu, Lenette L., Todd J. Suscovich, Sarah M. Fortune, and Galit Alter. 2018. "Beyond Binding: Antibody Effector Functions in Infectious Diseases." *Nature Reviews Immunology*. https://doi.org/10.1038/nri.2017.106.

M, Houde, Mathieu Houde, Sylvie Bertholet, Etienne Gagnon, Sylvain Brunet, Guillaume Goyette, Annie Laplante, et al. 2003. "Phagosomes Are Competent Organelles for Antigen Cross-Presentation." *Nature*. https://doi.org/10.1038/nature01911.1.

Maekawa, Sakiko, Umeharu Ohto, Takuma Shibata, Kensuke Miyake, and Toshiyuki Shimizu. 2016. "Crystal Structure of NOD2 and Its Implications in Human Disease." *Nature Communications*. https://doi.org/10.1038/ncomms11813.

Man, Si Ming, Rajendra Karki, and Thirumala Devi Kanneganti. 2016. "AIM2 Inflammasome in Infection, Cancer, and Autoimmunity: Role in DNA Sensing, Inflammation, and Innate Immunity." *European Journal of Immunology*. https://doi.org/10.1002/eji.201545839.

Man, SM, Karki, R, Kanneganti, TD. 2017. "Molecular Mechanisms and Functions of Pyroptosis, Inflammatory Caspases and Inflammasomes in Infectious Diseases." *Immunological Reviews*. https://doi.org/10.1111/imr.12534.

Mangan, Matthew S.J., Edward J. Olhava, William R. Roush, H. Martin Seidel, Gary D. Glick, and Eicke Latz. 2018. "Targeting the NLRP3 Inflammasome in Inflammatory Diseases." *Nature Reviews Drug Discovery*. https://doi.org/10.1038/nrd.2018.97.

Mano, Hiroyuki. 1999. "Tec Family of Protein-Tyrosine Kinases: An Overview of Their Structure and Function." *Cytokine and Growth Factor Reviews*. https://doi.org/10.1016/S1359-6101(99)00019-2.

Mao, Kairui, Shuzhen Chen, Mingkuan Chen, Yonglei Ma, Yan Wang, Bo Huang, Zhengyu He, et al. 2013. "Nitric Oxide Suppresses NLRP3 Inflammasome Activation and Protects against LPS-Induced Septic Shock." *Cell Research*. https://doi.org/10.1038/cr.2013.6.

Marchetti, C, B Swartzwelter, MI Koenders, CA Dinarello, and LA Joosten. 2017. “OP0090 The Human Safe NLRP3 Inflammasome Inhibitor OLT1177 Suppresses Joint Inflammation in Murine Models of Experimental Arthritis.” In . https://doi.org/10.1136/annrheumdis-2017-eular.2775.

Martinon, Fabio, Kimberly Burns, and Jürg Tschopp. 2002. “The Inflammasome: A Molecular Platform Triggering Activation of Inflammatory Caspases and Processing of ProIL-β.” *Molecular Cell*. https://doi.org/10.1016/S1097-2765(02)00599-3.

Mayilyan, K. R., Y. H. Kang, A. W. Dodds, and R. B. Sim. 2008. “The Complement System in Innate Immunity.” In . https://doi.org/10.1007/978-3-540-73930-2_10.

Mayor, Annick, Fabio Martinon, Thibaut De Smedt, Virginie Pétrilli, and Jürg Tschopp. 2007. “A Crucial Function of SGT1 and HSP90 in Inflammasome Activity Links Mammalian and Plant Innate Immune Responses.” *Nature Immunology*. https://doi.org/10.1038/ni1459.

Melcher, Martin, Bernd Unger, Uwe Schmidt, Iiro A. Rajantie, Kari Alitalo, and Wilfried Ellmeier. 2008. “Essential Roles for the Tec Family Kinases Tec and Btk in M-CSF Receptor Signaling Pathways That Regulate Macrophage Survival.” *The Journal of Immunology*. https://doi.org/10.4049/jimmunol.180.12.8048.

Menu, P., A. Mayor, R. Zhou, A. Tardivel, H. Ichijo, K. Mori, and J. Tschopp. 2012. “ER Stress Activates the NLRP3 Inflammasome via an UPR-Independent Pathway.” *Cell Death and Disease*. https://doi.org/10.1038/cddis.2011.132.

Merolle, Maria I., Makhdum Ahmed, Krystle Nomie, and Michael L. Wang. 2018. “The B Cell Receptor Signaling Pathway in Mantle Cell Lymphoma.” *Oncotarget*. https://doi.org/10.18632/oncotarget.25011.

Miklos, David, Corey S. Cutler, Mukta Arora, Edmund K. Waller, Madan Jagasia, Iskra Pusic, Mary E. Flowers, et al. 2017. “Ibrutinib for Chronic Graft-versus-Host Disease after Failure of Prior Therapy.” *Blood*. https://doi.org/10.1182/blood-2017-07-793786.

Mishra, Bibhuti B., Vijay A.K. Rathinam, Gregory W. Martens, Amanda J. Martinot, Hardy Kornfeld, Katherine A. Fitzgerald, and Christopher M. Sassetti. 2013. “Nitric Oxide Controls the Immunopathology of Tuberculosis by Inhibiting NLRP3 Inflammasome-Dependent Processing of IL-1β.” *Nature Immunology*. https://doi.org/10.1038/ni.2474.

Missiroli, Sonia, Simone Patergnani, Natascia Caroccia, Gaia Pedriali, Mariasole Perrone, Maurizio Previati, Mariusz R. Wieckowski, and Carlotta Giorgi. 2018. “Mitochondria-Associated Membranes (MAMs) and Inflammation.” *Cell Death and Disease*. https://doi.org/10.1038/s41419-017-0027-2.

Moayeri, Mahtab, Inka Sastalla, and Stephen H. Leppla. 2012. “Anthrax and the Inflammasome.” *Microbes and Infection*. https://doi.org/10.1016/j.micinf.2011.12.005.

Mócsai, Attila. 2013. “Diverse Novel Functions of Neutrophils in Immunity, Infammation, and Beyond.” *Journal of Experimental Medicine*. https://doi.org/10.1084/jem.20122220.

Murakami, Tomohiko, Johan Ockinger, Jiujiu Yu, Vanessa Byles, Aisleen McColl, Aldebaran M. Hofer, and Tiffany Horng. 2012. “Critical Role for Calcium Mobilization in Activation of the NLRP3 Inflammasome.” *Proceedings of the National Academy of Sciences of the United States of America*. https://doi.org/10.1073/pnas.1117765109.

Negroni, Anna, Maria Pierdomenico, Salvatore Cucchiara, and Laura Stronati. 2018. “NOD2 and Inflammation: Current Insights.” *Journal of Inflammation Research*. https://doi.org/10.2147/JIR.S137606.

Ormsby, Tereza, Eva Schlecker, Janina Ferdin, Anja Sibylle Tessarz, Pavla Angelisová, Afitap Derya Köprülü, Michael Borte, et al. 2011. “Btk Is a Positive Regulator in the TREM-1/DAP12 Signaling Pathway.” *Blood*. https://doi.org/10.1182/blood-2010-11-317016.

Oroz, Javier, Susana Barrera-Vilarmau, Carlos Alfonso, Germán Rivas, and Eva De Alba. 2016. “ASC Pyrin Domain Self-Associates and Binds NLRP3 Protein Using Equivalent Binding Interfaces∗.” *Journal of Biological Chemistry*. https://doi.org/10.1074/jbc.M116.741082.

Pal Singh, Simar, Floris Dammeijer, and Rudi W. Hendriks. 2018. “Role of Bruton’s Tyrosine Kinase in B Cells

and Malignancies." *Molecular Cancer*. https://doi.org/10.1186/s12943-018-0779-z.

Panicker, Nikhil, Souvarish Sarkar, Dilshan S. Harischandra, Matthew Neal, Tae In Kam, Huajun Jin, Hariharan Saminathan, et al. 2019. "Fyn Kinase Regulates Misfolded α-Synuclein Uptake and NLRP3 Inflammasome Activation in Microglia." *The Journal of Experimental Medicine*. https://doi.org/10.1084/jem.20182191.

Ping, Lingyan, Ning Ding, Yunfei Shi, Lixia Feng, Jiao Li, Yalu Liu, Yufu Lin, et al. 2017. "The Bruton's Tyrosine Kinase Inhibitor Ibrutinib Exerts Immunomodulatory Effects through Regulation of Tumorinfiltrating Macrophages." *Oncotarget*. https://doi.org/10.18632/oncotarget.16836.

Poeck, Hendrik, Michael Bscheider, Olaf Gross, Katrin Finger, Susanne Roth, Manuele Rebsamen, Nicole Hannesschläger, et al. 2010. "Recognition of RNA Virus by RIG-I Results in Activation of CARD9 and Inflammasome Signaling for Interleukin 1B Production." *Nature Immunology*. https://doi.org/10.1038/ni.1824.

Ponader, Sabine, and Jan A. Burger. 2014. "Bruton's Tyrosine Kinase: From X-Linked Agammaglobulinemia toward Targeted Therapy for B-Cell Malignancies." *Journal of Clinical Oncology*. https://doi.org/10.1200/JCO.2013.53.1046.

Py, Bénédicte F., Mi Sung Kim, Helin Vakifahmetoglu-Norberg, and Junying Yuan. 2013. "Deubiquitination of NLRP3 by BRCC3 Critically Regulates Inflammasome Activity." *Molecular Cell*. https://doi.org/10.1016/j.molcel.2012.11.009.

Qiao, Qi, Chenghua Yang, Chao Zheng, Lorena Fontán, Liron David, Xiong Yu, Clay Bracken, et al. 2013. "Structural Architecture of the CARMA1/Bcl10/MALT1 Signalosome: Nucleation-Induced Filamentous Assembly." *Molecular Cell*. https://doi.org/10.1016/j.molcel.2013.08.032.

Ragland, Stephanie A., and Alison K. Criss. 2017. "From Bacterial Killing to Immune Modulation: Recent Insights into the Functions of Lysozyme." *PLoS Pathogens*. https://doi.org/10.1371/journal.ppat.1006512.

Rapino, Francesca, Eloy F. Robles, Jose A. Richter-Larrea, Eric M. Kallin, Jose A. Martinez-Climent, and Thomas Graf. 2013. "C/EBPα Induces Highly Efficient Macrophage Transdifferentiation of B Lymphoma and Leukemia Cell Lines and Impairs Their Tumorigenicity." *Cell Reports*. https://doi.org/10.1016/j.celrep.2013.03.003.

Rigg, Rachel A., Joseph E. Aslan, Laura D. Healy, Michael Wallisch, Marisa L.D. Thierheimer, Cassandra P. Loren, Jiaqing Pang, Monica T. Hinds, András Gruber, and Owen J.T. McCarty. 2016. "Oral Administration of Bruton's Tyrosine Kinase Inhibitors Impairs GPVI-Mediated Platelet Function." *American Journal of Physiology - Cell Physiology*. https://doi.org/10.1152/ajpcell.00325.2015.

Roche, Paul A., and Kazuyuki Furuta. 2015. "The Ins and Outs of MHC Class II-Mediated Antigen Processing and Presentation." *Nature Reviews Immunology*. https://doi.org/10.1038/nri3818.

Rogers, Corey, Teresa Fernandes-Alnemri, Lindsey Mayes, Diana Alnemri, Gino Cingolani, and Emad S. Alnemri. 2017. "Cleavage of DFNA5 by Caspase-3 during Apoptosis Mediates Progression to Secondary Necrotic/Pyroptotic Cell Death." *Nature Communications*. https://doi.org/10.1038/ncomms14128.

Roh, Jong Seong, and Dong Hyun Sohn. 2018. "Damage-Associated Molecular Patterns in Inflammatory Diseases." *Immune Network*. https://doi.org/10.4110/in.2018.18.e27.

Romagnani, S. 2000. "T-Cell Subsets (Th1 versus Th2)." *Annals of Allergy, Asthma and Immunology*. https://doi.org/10.1016/S1081-1206(10)62426-X.

Schorn, Christine, Benjamin Frey, Kirsten Lauber, Christina Janko, Moritz Strysio, Hildegard Keppeler, Udo S. Gaipl, et al. 2011. "Sodium Overload and Water Influx Activate the NALP3 Inflammasome." *Journal of Biological Chemistry*. https://doi.org/10.1074/jbc.M110.139048.

Sharif, Humayun, Li Wang, Wei Li Wang, Venkat Giri Magupalli, Liudmila Andreeva, Qi Qiao, Arthur V. Hauenstein, et al. 2019. "Structural Mechanism for NEK7-Licensed Activation of NLRP3 Inflammasome." *Nature*. https://doi.org/10.1038/s41586-019-1295-z.

Shenoy, Avinash R., David A. Wellington, Pradeep Kumar, Hilina Kassa, Carmen J. Booth, Peter Cresswell, and

John D. MacMicking. 2012. “GBP5 Promotes NLRP3 Inflammasome Assembly and Immunity in Mammals.” *Science*. https://doi.org/10.1126/science.1217141.

Shi, Hexin, Ying Wang, Xiaohong Li, Xiaoming Zhan, Miao Tang, Maggy Fina, Lijing Su, et al. 2016. “NLRP3 Activation and Mitosis Are Mutually Exclusive Events Coordinated by NEK7, a New Inflammasome Component.” *Nature Immunology*. https://doi.org/10.1038/ni.3333.

Shi, Jianjin, Wenqing Gao, and Feng Shao. 2017. “Pyroptosis: Gasdermin-Mediated Programmed Necrotic Cell Death.” *Trends in Biochemical Sciences*. https://doi.org/10.1016/j.tibs.2016.10.004.

Shim, Do Wan, Woo Young Shin, Sang Hyeun Yu, Byung Hak Kim, Sang Kyu Ye, Sushruta Koppula, Hyung Sik Won, Tae Bong Kang, and Kwang Ho Lee. 2017. “BOT-4-One Attenuates NLRP3 Inflammasome Activation: NLRP3 Alkylation Leading to the Regulation of Its ATPase Activity and Ubiquitination.” *Scientific Reports*. https://doi.org/10.1038/s41598-017-15314-8.

Shishido, Stephanie N., Sriram Varahan, Kai Yuan, Xiangdong Li, and Sherry D. Fleming. 2012. “Humoral Innate Immune Response and Disease.” *Clinical Immunology*. https://doi.org/10.1016/j.clim.2012.06.002.

Song, Hui, Bingyu Liu, Wanwan Huai, Zhongxia Yu, Wenwen Wang, Jing Zhao, Lihui Han, et al. 2016. “The E3 Ubiquitin Ligase TRIM31 Attenuates NLRP3 Inflammasome Activation by Promoting Proteasomal Degradation of NLRP3.” *Nature Communications*. https://doi.org/10.1038/ncomms13727.

Song, Nan, Zhao Shan Liu, Wen Xue, Zhao Fang Bai, Qian Yi Wang, Jiang Dai, Xin Liu, et al. 2017. “NLRP3 Phosphorylation Is an Essential Priming Event for Inflammasome Activation.” *Molecular Cell*. https://doi.org/10.1016/j.molcel.2017.08.017.

Spalinger, Marianne R., Silvia Lang, Claudia Gottier, Xuezhi Dai, David J. Rawlings, Andrew C. Chan, Gerhard Rogler, and Michael Scharl. 2017. “PTPN22 Regulates NLRP3-Mediated IL1B Secretion in an Autophagy-Dependent Manner.” *Autophagy*. https://doi.org/10.1080/15548627.2017.1341453.

Stadler, Nicole, Astrid Hasibeder, Pamela Aranda Lopez, Daniel Teschner, Alexander Desuki, Oliver Kriege, Alexander N.R. Weber, et al. 2017. “The Bruton Tyrosine Kinase Inhibitor Ibrutinib Abrogates Triggering Receptor on Myeloid Cells 1-Mediated Neutrophil Activation.” *Haematologica*. https://doi.org/10.3324/haematol.2016.152017.

Stavnezer, Janet, Jeroen E.J. Guikema, and Carol E. Schrader. 2008. “Mechanism and Regulation of Class Switch Recombination.” *Annual Review of Immunology*. https://doi.org/10.1146/annurev.immunol.26.021607.090248.

Steinberg, Gregory R., and Jonathan D. Schertzer. 2014. “AMPK Promotes Macrophage Fatty Acid Oxidative Metabolism to Mitigate Inflammation: Implications for Diabetes and Cardiovascular Disease.” *Immunology and Cell Biology*. https://doi.org/10.1038/icb.2014.11.

Stutz, Andrea, Carl Christian Kolbe, Rainer Stahl, Gabor L. Horvath, Bernardo S. Franklin, Olivia van Ray, Rebecca Brinkschulte, Matthias Geyer, Felix Meissner, and Eicke Latz. 2017. “NLRP3 Inflammasome Assembly Is Regulated by Phosphorylation of the Pyrin Domain.” *Journal of Experimental Medicine*. https://doi.org/10.1084/jem.20160933.

Takeuchi, Osamu, and Shizuo Akira. 2010. “Pattern Recognition Receptors and Inflammation.” *Cell*. https://doi.org/10.1016/j.cell.2010.01.022.

Tapia-Abellán, Ana, Diego Angosto-Bazarra, Helios Martínez-Banaclocha, Carlos de Torre-Minguela, Jose P. Cerón-Carrasco, Horacio Pérez-Sánchez, Juan I. Arostegui, and Pablo Pelegrin. 2019. “MCC950 Closes the Active Conformation of NLRP3 to an Inactive State.” *Nature Chemical Biology*. https://doi.org/10.1038/s41589-019-0278-6.

Trapani, Joseph A., and Mark J. Smyth. 2002. “Functional Significance of the Perforin/Granzyme Cell Death Pathway.” *Nature Reviews Immunology*. https://doi.org/10.1038/nri911.

Unamuno, Xabier, Javier Gómez-Ambrosi, Beatriz Ramírez, Amaia Rodríguez, Sara Becerril, Víctor Valentí, Rafael Moncada, et al. 2019. “NLRP3 Inflammasome Blockade Reduces Adipose Tissue Inflammation and Extracellular Matrix Remodeling.” *Cellular and Molecular Immunology*. https://doi.org/10.1038/s41423-019-0296-z.

Vetrie, David, Igor Vořechovský, Paschalis Sideras, Jill Holland, Angela Davies, Frances Flinter, Lennart Hammarström, et al. 1993. "The Gene Involved in X-Linked Agammaglobulinaemia Is a Member of the Src Family of Protein-Tyrosine Kinases." *Nature*. https://doi.org/10.1038/361226a0.

Vivier, Eric, and Bernard Malissen. 2005. "Innate and Adaptive Immunity: Specificities and Signaling Hierarchies Revisited." *Nature Immunology*. https://doi.org/10.1038/ni1153.

Wang, Yan, Chen Yang, Kairui Mao, Shuzhen Chen, Guangxun Meng, and Bing Sun. 2013. "Cellular Localization of NLRP3 Inflammasome." *Protein and Cell*. https://doi.org/10.1007/s13238-013-2113-2.

Weber, Alexander N.R., Zsofia Bittner, Xiao Liu, Truong Minh Dang, Markus Philipp Radsak, and Cornelia Brunner. 2017. "Bruton's Tyrosine Kinase: An Emerging Key Player in Innate Immunity." *Frontiers in Immunology*. https://doi.org/10.3389/fimmu.2017.01454.

Wen, Haitao, Denis Gris, Yu Lei, Sushmita Jha, Lu Zhang, Max Tze Han Huang, Willie June Brickey, and Jenny P.Y. Ting. 2011. "Fatty Acid-Induced NLRP3-ASC Inflammasome Activation Interferes with Insulin Signaling." *Nature Immunology*. https://doi.org/10.1038/ni.2022.

Woyach, Jennifer A., Richard R. Furman, Ta Ming Liu, Hatice Gulcin Ozer, Marc Zapatka, Amy S. Ruppert, Ling Xue, et al. 2014. "Resistance Mechanisms for the Bruton's Tyrosine Kinase Inhibitor Ibrutinib." *New England Journal of Medicine*. https://doi.org/10.1056/NEJMoa1400029.

Woyach, Jennifer A., Amy J. Johnson, and John C. Byrd. 2012. "The B-Cell Receptor Signaling Pathway as a Therapeutic Target in CLL." *Blood*. https://doi.org/10.1182/blood-2012-02-362624.

Xhindoli, Daniela, Sabrina Pacor, Monica Benincasa, Marco Scocchi, Renato Gennaro, and Alessandro Tossi. 2016. "The Human Cathelicidin LL-37 - A Pore-Forming Antibacterial Peptide and Host-Cell Modulator." *Biochimica et Biophysica Acta - Biomembranes*. https://doi.org/10.1016/j.bbamem.2015.11.003.

Yan, Yiqing, Wei Jiang, Lei Liu, Xiaqiong Wang, Chen Ding, Zhigang Tian, and Rongbin Zhou. 2015. "Dopamine Controls Systemic Inflammation through Inhibition of NLRP3 Inflammasome." *Cell*. https://doi.org/10.1016/j.cell.2014.11.047.

Yang, Chul Su, Jwa Jin Kim, Tae Sung Kim, Phil Young Lee, Soo Yeon Kim, Hye Mi Lee, Dong Min Shin, et al. 2015. "Small Heterodimer Partner Interacts with NLRP3 and Negatively Regulates Activation of the NLRP3 Inflammasome." *Nature Communications*. https://doi.org/10.1038/ncomms7115.

Yang, Guang, Yangsheng Zhou, Xia Liu, Lian Xu, Yang Cao, Robert J. Manning, Christopher J. Patterson, et al. 2013. "A Mutation in MYD88 (L265P) Supports the Survival of Lymphoplasmacytic Cells by Activation of Bruton Tyrosine Kinase in Waldenström Macroglobulinemia." *Blood*. https://doi.org/10.1182/blood-2012-12-475111.

Yang, Yang, Huanan Wang, Mohammed Kouadir, Houhui Song, and Fushan Shi. 2019. "Recent Advances in the Mechanisms of NLRP3 Inflammasome Activation and Its Inhibitors." *Cell Death and Disease*. https://doi.org/10.1038/s41419-019-1413-8.

Ye, Bingjue, Cheng Zhou, Huiting Guo, and Min Zheng. 2019. "Effects of BTK Signalling in Pathogenic Microorganism Infections." *Journal of Cellular and Molecular Medicine*. https://doi.org/10.1111/jcmm.14548.

Ye, Xinchun, Dandan Zuo, Lu Yu, Liang Zhang, Jiao Tang, Chengcheng Cui, Lei Bao, et al. 2017. "ROS/TXNIP Pathway Contributes to Thrombin Induced NLRP3 Inflammasome Activation and Cell Apoptosis in Microglia." *Biochemical and Biophysical Research Communications*. https://doi.org/10.1016/j.bbrc.2017.02.019.

Yeretssian, Garabet. 2012. "Effector Functions of NLRs in the Intestine: Innate Sensing, Cell Death, and Disease." *Immunologic Research*. https://doi.org/10.1007/s12026-012-8317-3.

Zhang, Jun Ming, and Jianxiong An. 2007. "Cytokines, Inflammation, and Pain." *International Anesthesiology Clinics*. https://doi.org/10.1097/AIA.0b013e318034194e.

Zhang, Zhirong, Gergö Meszaros, Wan Ting He, Yanfang Xu, Helena de Fatima Magliarelli, Laurent Mailly, Michael Mihlan, et al. 2017. "Protein Kinase D at the Golgi Controls NLRP3 Inflammasome Activation."

Journal of Experimental Medicine. https://doi.org/10.1084/jem.20162040.

Zhao, Yue, Jieling Yang, Jianjin Shi, Yi Nan Gong, Qiuhe Lu, Hao Xu, Liping Liu, and Feng Shao. 2011. "The NLRC4 Inflammasome Receptors for Bacterial Flagellin and Type III Secretion Apparatus." *Nature*. https://doi.org/10.1038/nature10510.

Zhou, Rongbin, Amir S. Yazdi, Philippe Menu, and Jürg Tschopp. 2011. "A Role for Mitochondria in NLRP3 Inflammasome Activation." *Nature*. https://doi.org/10.1038/nature09663.

Zou, Hua, Yuchen Li, Xuesong Liu, and Xiaodong Wang. 1999. "An APAf-1 · Cytochrome C Multimeric Complex Is a Functional Apoptosome That Activates Procaspase-9." *Journal of Biological Chemistry*. https://doi.org/10.1074/jbc.274.17.11549.

6. APPENDIX

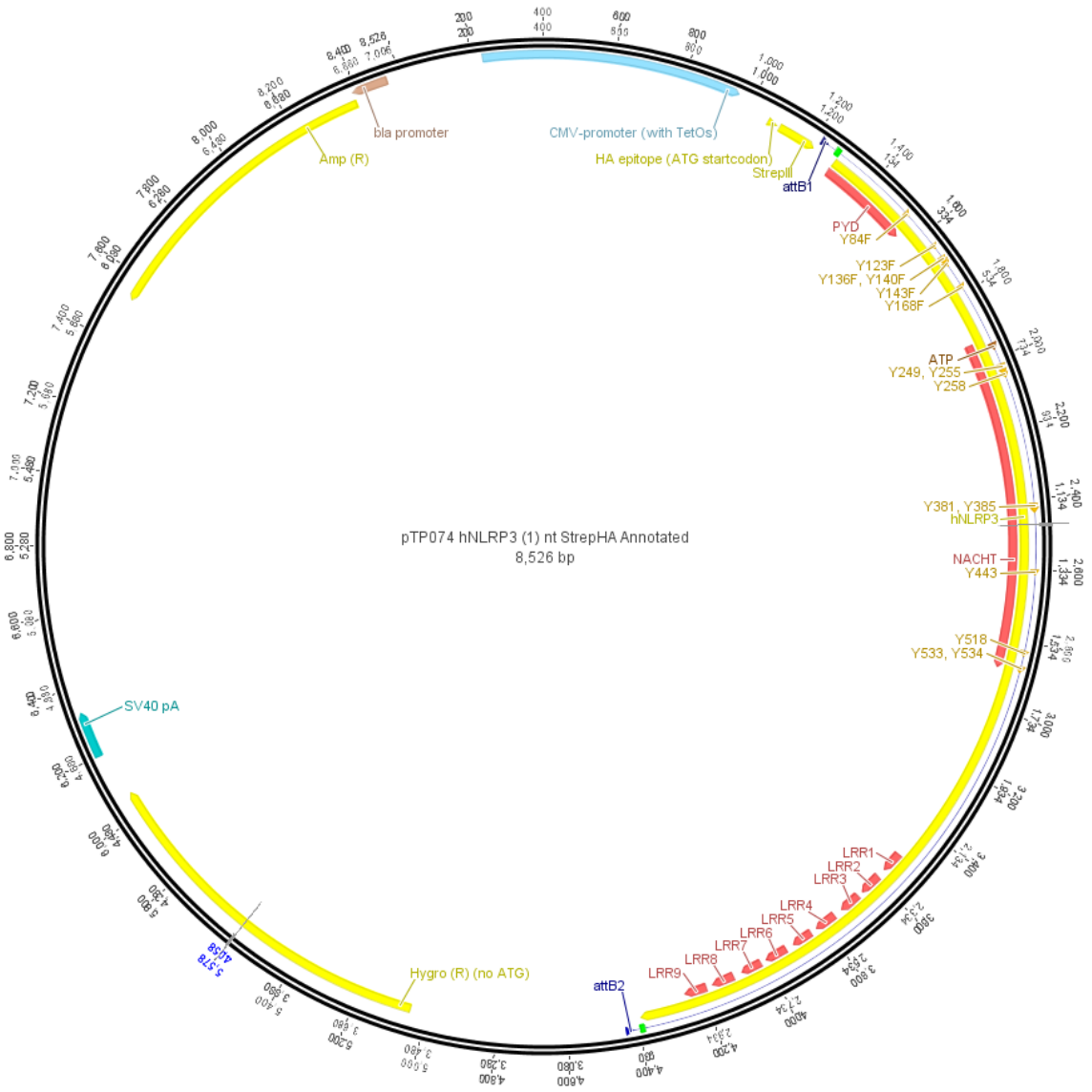

Figure 6.1. Plasmid map of the full-length WT NLRP3 construct (pTP074).

The NLRP3 domains as well as the tyrosine residues that were mutated to F are annotated.

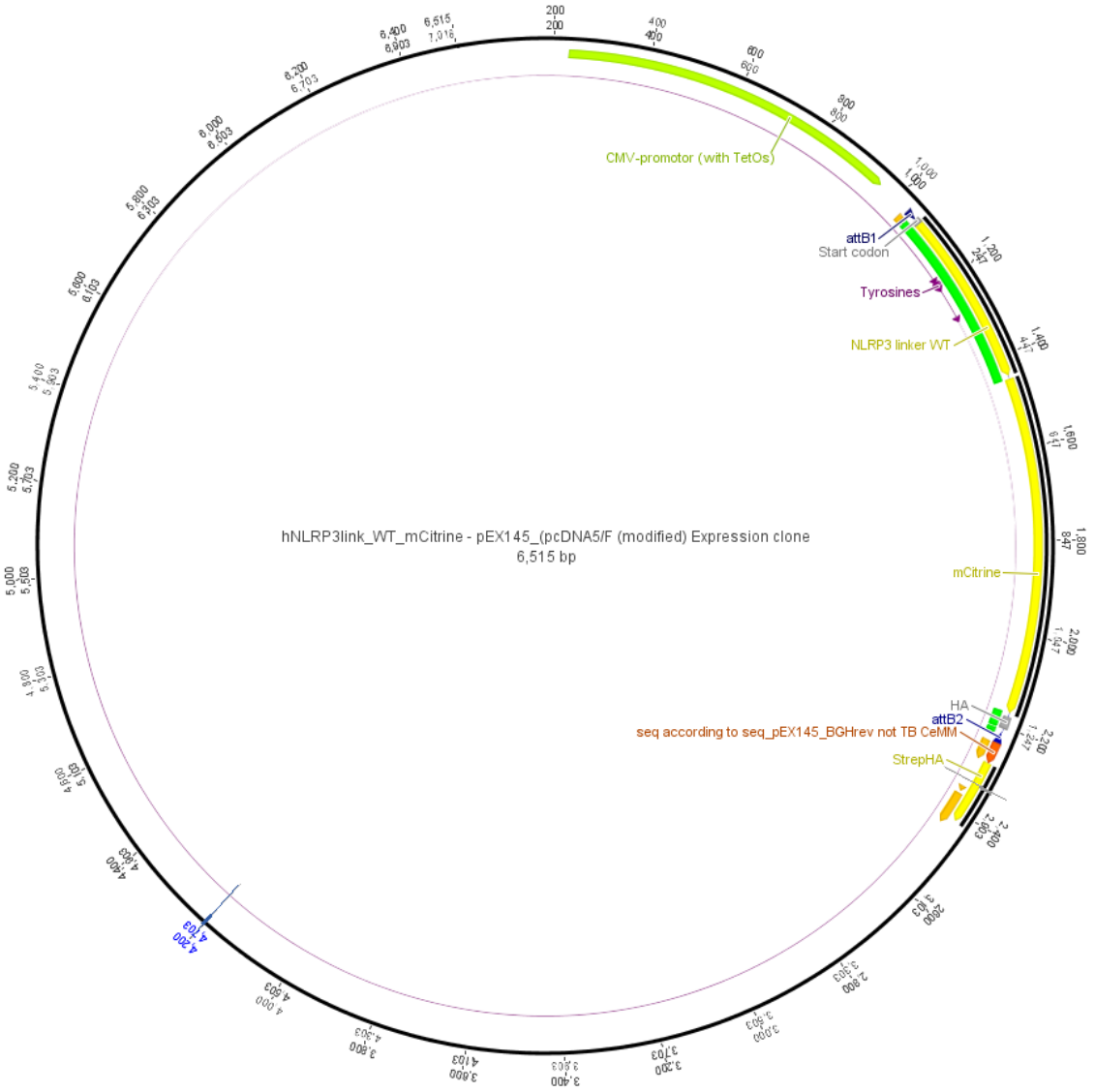

Figure 6.2. Plasmid map of the PYD/NACHT linker/NACHT-HA-mCitrine construct (pZsB048).

The Y>F mutations (pZsB049 and pZsB050) were generated on this backbone.

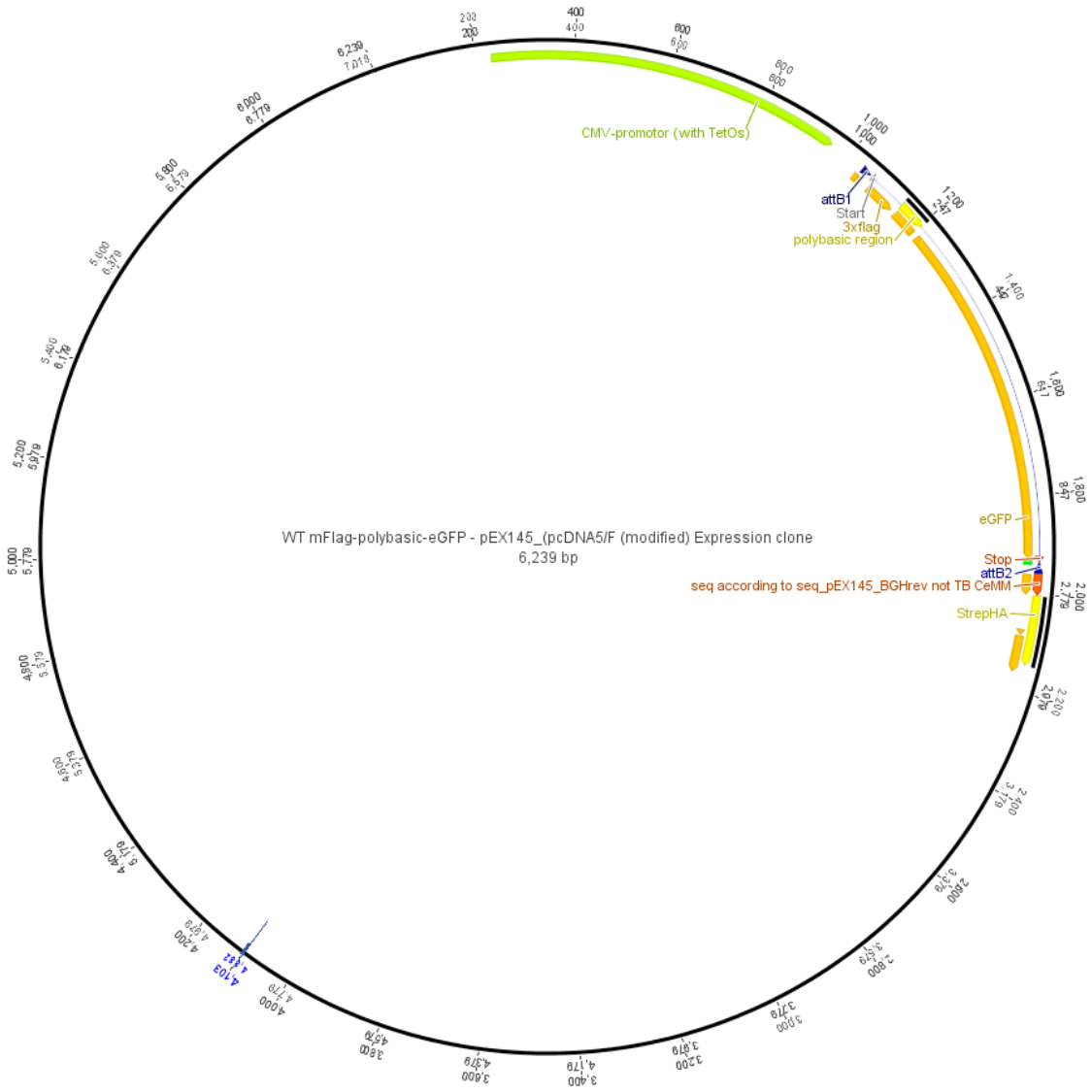

Figure 6.3. Plasmid map of the Flag-mPolybasic region-GFP construct (pZsB074).

Mutations (Y>F, Y>E, and K>A) were generated on the same backbone.

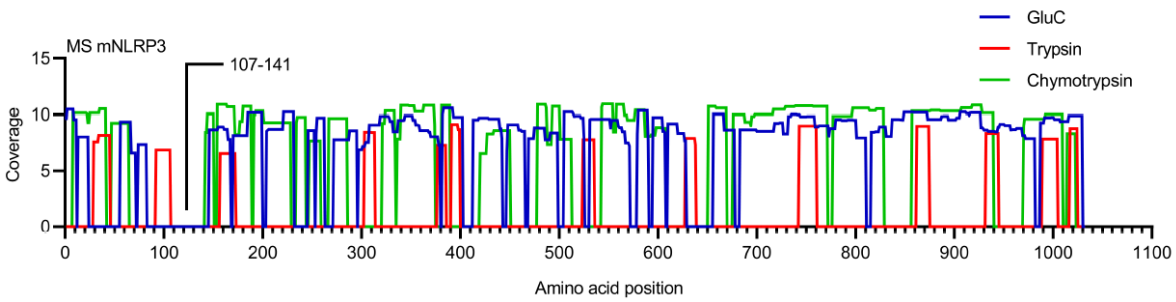

Figure 6.4. Sequence coverage of murine NLRP3 upon mass spectrometry analysis using GluC, trypsin, and chymotrypsin. Data provided by Felix Meissner.

The sequence between AA107 and 141, where two of the four phosphorylated tyrosine residues reside, could not be detected via mass spectrometry.

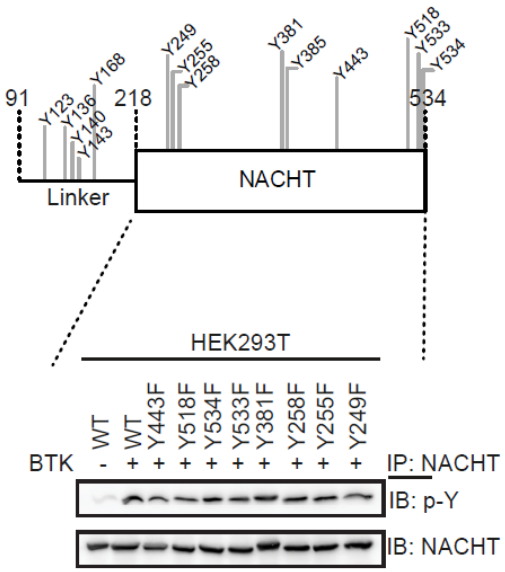

Figure 6.5. Phosphorylation of NLRP3 NACHT Y>F mutants by BTK in HEK293T cells.

None of the tyrosine residues in the NACHT domain were phosphorylated by BTK.

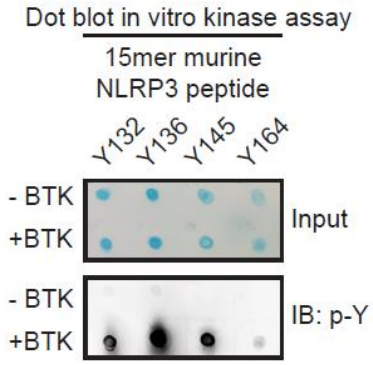

Figure 6.6. *In vitro* kinase assay with murine NLRP3 peptides and human recombinant BTK.

Human BTK phosphorylates the murine equivalent of the human NLRP3 sequences.